Studies on homotypic and heterotypic communications in chaperone protein ClpB from *T. thermophilus*

Dissertation

Submitted to the

Combined Faculties for the Natural Sciences and for Mathematics

of the Ruperto-Carola University of Heidelberg, Germany

for the degree of

Doctor of Natural Sciences

Presented by

Rajeswari Auvula

Born in Tenali/ India

Oral Examination:……..

Referees: PD. Dr. Jochen Reinstein

Prof. Dr. Ilme Schlichting

INDEX

SUMMARY

ClpB$_{Tth}$ is a molecular motor, which exerts an ATP hydrolysis driven mechanical force, resulting in disaggregation of aggregated proteins. ClpB$_{Tth}$ belonging to the AAA family of ATPases carries the signature AAA module, which comprises of a large nucleotide binding domain (NBD) and an α-helical small domain (SD). The two tandem AAA modules present per subunit of ClpB$_{Tth}$ interact with each other and the neighboring AAA modules in the hexameric ring-like structure. The current study focuses on inter-subunit (homotypic) and intra-subunit (heterotypic) communications between the AAA modules in ClpB$_{Tth}$ oligomer, in respect to nucleotide binding and hydrolysis.

The two tandem AAA modules of ClpB$_{Tth}$ upon isolation exhibit unique properties. The isolated AAA2 module more or less represents a building block for the full-length hexameric protein. It appears to have retained most of the key characteristics, exhibited by full-length ClpB$_{Tth}$, as evident by sigmoidal kinetics in ATP hydrolysis and nucleotide binding-related conformational changes. So, nucleotide binding in the isolated AAA modules was investigated using fluorescently labeled proteins to gain insights into the nucleotide-mediated oligomer dissociation. Experiments were performed using the isolated AAA modules to reduce the complexity which comes with studying full-length hexamer. Experiments provided hints for involvement of the α-helical small domain 2 in nucleotide-dependent oligomer formation. Importance of the presence of SD2 has been demonstrated; upon its deletion, isolated AAA2 domain lost nucleotide binding and hydrolysis. Studies using a mutant carrying proline mutation in a loop connecting SD2 to NBD2 in the AAA2 module revealed loss of chaperone and ATPase activity. This study pointed out at the importance of flexibility and motion in SD2 of the AAA2 module. Nucleotide binding studies hinted at a possible biphasic nature and inter-subunit communication. ADP binding in one AAA2 module appeared to have triggered a conformational change in SD2 of the neighboring AAA2 module. These results gave insights into the conformational changes involved in ADP-mediated oligomer dissociation in ClpB$_{Tth}$. Although oligomer dissociation has been linked to ADP binding/formation in several instances, the inter-subunit communications pattern has never been clearly discerned. This work provides a platform for further studies to investigate conformational changes that result in oligomer formation and dissociation.

Summary

The isolated AAA modules of $ClpB_{Tth}$ upon reconstitution exhibit functional higher order oligomer formation. This reconstituted complex resembles wild type $ClpB_{Tth}$ hexamer in all aspects related to oligomerization, chaperone activity and ATP hydrolysis. So, complex formation between the isolated AAA modules was studied to understand the thermodynamics behind the communication between them. Isothermal titration calorimetry measurements were performed to study binding between the isolated AAA modules. Experiments provided hints at temperature dependency in binding between the AAA modules in $ClpB_{Tth}$.

Allostery in ATP hydrolysis is central to the function of $ClpB_{Tth}$, which represents both homotypic and heterotypic communications between the AAA modules. Absence of heterotypic allostery always resulted in a loss of function in $ClpB_{Tth}$. Importance of heterotypic allosteric communications between the AAA modules within each subunit and their role in chaperone activity of $ClpB_{Tth}$ was investigated in this work. This was done by alteration of the related interface by mutating amino acids involved in interface interactions. Most of the mutants resulted in subtle changes in nucleotide hydrolysis properties and heterotypic allostery. Changes in allosteric behavior did not translate into a loss in chaperone activity, as evident by no loss of function in mutants exhibiting altered allostery. Experiments in the presence of GdmCl, which acts as an uncompetitive inhibitor for ATP binding, additionally revealed interesting insights to the allostery-defective situation in $ClpB_{Tth}$. Furthermore, this study has shed some light on possible mechanisms involved for attaining catalytic effectiveness in $ClpB_{Tth}$.

ZUSAMMENFASSUNG

ClpB$_{TTh}$ ist ein molekularer Motor, welcher eine durch ATP-Hydrolyse getriebene mechanische Kraft ausübt, die zur Disaggregation von Proteinaggregaten führt. ClpB gehört zur Familie der AAA-ATPasen und besteht aus AAA-Modulen, die sich aus einer Nukleotidbindedomäne (NBD) und einer kleinen a-helicalen Domäne (SD) zusammensetzen. Zwei AAA-Module auf einer Untereinheit interagieren sowohl untereinander als auch mit anderen AAA-Modulen auf benachbarten Untereinheiten innerhalb eines ringförmigen hexameren Komplexes. Die vorliegende Arbeit beschäftigt sich mit der Kommunikation innerhalb und zwischen den Untereinheiten des oligomeren ClpB$_{TTh}$ Komplexes hinsichtlich der Nukleotidbindung und Hydrolyse.

In Isolation zeigen die zwei AAA-Module jeder Untereinheit einzigartige Charakteristika. Das isolierte AAA2 Modul repräsentiert in gewisser Hinsicht einen Baustein für den hexameren Komplex aus voll-längen ClpB. Es scheint die meiste Schlüsseleigenschaftern des voll-längen ClpB beibehalten zu haben, ersichtlich durch die sigmoidale steady-state ATPase Kurve sowie nukleotidabhängige Konformationsänderungen. Um Einblicke in die nukleotidabhängige Dissoziation der Untereinheiten zu gewinnen, wurde die Nukleotidbindung an die isolierten AAA-Module mittels fluoreszenzmarkierter Proteine gemessen. Die isolierten Module wurden verwendet, um die Komplexität der voll-längen Konstrukte zu reduzieren. Die durchgeführten Experimente ergaben hinweise auf einer Rolle der kleinen a-helikalen Domäne in nukleotidabhängiger Oligomerisierung. Weiterhin konnte gezeigt werden, dass die Anwesenheit der kleinen a-helikalen Domäne sehr wichtig ist, da das Entfernen dieser Domäne im isolierten AAA2-Modul zum Verlust von Nulkleotidbindung und ATP-Hydrolyse führt. Untersuchungen an einer AAA2 Variante, die eine Prolin-Mutation innherhalb einer Loop-Region enthält, welche die SD2-Domäne mit der NBD2-Domäne verbindet, zeigten, dass diese Variante weder Chaperon- noch ATPase-Aktivität zeigt. Dies deutet darauf hin, dass die Flexibilität dieser Region eine wichtige Rolle spielt. Untersuchungen der Nukleotidbindung deuten auf eine mögliche zwei-phasige Bindung hin sowie auf Kommunikation zwischen benachbarten Untereinheiten. ADP Bindung in einer Untereinheit könnte demnach eine Konformationsänderung in der SD2 einer benachbarten Untereinheit auslösen. Diese Resultate geben Hinweise auf Konformationsänderungen, die einer ADP-induzierte Auflösung von

$ClpB_{TTh}$- Oligomeren zugrunde liegen. Obwohl ADP-Bindung und Oligomer-Dissoziation schon in einigen Fällen miteinander in Verbindung gebracht werden konnte, konnte das Muster der Kommunikation zwischen den Untereinheiten nicht eindeutig aufgeklärt werden. Die vorliegende Arbeit stellt eine Plattform für zukünftige Arbeiten dar, welche Konformationsänderungen untersuchen, die zur Auflösung und Assemblierung von Oligomeren führen.

Die zwei isolierten AAA-Module (AAA1 und AAA2) rekonstituieren, wenn sie gemischt werden, zu funktionellen Oligomeren. Dieser rekonstituierte Komplex ähnelt den Eigenschaften vom voll-längen wildtyp $ClpB_{TTh}$ in allen Apekten bezüglich der Oligomerisierung, der Chaperon-Aktivität und der ATP-Hydrolyse. Deshalb wurde die Bildung von Komplexen zwischen den isolierten AAA-Modulen untersucht mit dem Ziel die Thermodynamik der Kommunikation zwischen diesen zu verstehen. Um dies zu erreichen wurden Messungen mittels Isothermer Titrationskalorimetrie durchgeführt. Diese Experimente legen eine Temperaturabhängigkeit der Bindung der AAA-Module von $ClpB_{TTh}$ nahe.

Allosterie in der ATP-Hydrolyse ist Zentral für die Funktion von $ClpB_{TTh}$, welches sowohl homotypische Kommunikation – d.h. Kommunikation zwischen gleichen AAA-Modulen – als auch heterotypische Kommunikation - d.h. Kommunikation zwischen verschiedenen AAA-Modulen – aufzeigt. Die Abwesenheit heterotypischer Allosterie hatte immer den Verlust der Funktion zur Folge. Die Bedeutung der heterotypischen allosterischen Kommunikation zwischen den AAA-Modulen einer Untereinheit und die Auswirkung dieser auf die Chaperonaktivität wurde in dieser Arbeit untersucht. Dies wurde erreicht durch Mutation von Aminosäuren, welche Interaktionen innerhalb der Grenzfläche zwischen den AAA-Modulen bilden. Die meisten Mutationen zeigten feine Unterschiede in ATP-Hydrolyse und heterotypischer Allosterie. Die veränderte Allosterie übertrug sich jedoch nicht auf eine veränderte Chaperonaktiviät, da Varianten mit veränderter Allosterie keinen Verlust der Chaperonaktivität zeigten. Experimente in Anwesenheit von GdmCl, welches ein unkompetetiver Inhibitor für die Bindung von ATP ist, erbrachten weitere Einblicke in die Störung der Allosterie von $ClpB_{TTh}$. Weiterhin beleuchtete diese Arbeit einen möglichen Mechanismus zur Erlangung von katalytischer Effektivität in $ClpB_{TTh}$.

1. INTRODUCTION

Specific interactions between bio-molecules are an integral part of numerous aspects of a living cell. Specificity plays a significant role in fidelity of DNA replication, transcription, translation, enzymatic reactions, ligand binding and several other processes. Specificity in a bio-molecular interaction is obtained by complementarity between the involved partners (Fersht 1984). This is achieved by precise three-dimensional structures of the biological macromolecules. Hence the production and maintenance of biological macromolecules, especially proteins, in thermodynamically and functionally viable form is vital for life. As per the central dogma of life, genetic information encoded in DNA is transcribed to a messenger RNA; which, in turn on a ribosome, gets translated to build a polypeptide chain. Nascent polypeptide chains get folded into a three-dimensional structure prior to getting dispatched to their site of action. Although it is known that the primary sequence determines a protein's ability to fold and the shape it should acquire, there are several factors that affect the folding process and its stability. Less influential factors, like macromolecular crowding, to more significant aspects like aggregation have their definite role (Minton et al., 2000; Ellis et al., 2001). Protein folding is affected due to environment-induced stress factors and in certain disease conditions. Several disorders like bovine spongiform encephalopathy (Dobson 1999), prion-related diseases, and Alzheimer's disease are protein folding anomaly related. Hence, a cell makes use of a variety of processes to ensure the quality of its protein content; these fall into three categories: prevention, restoration and termination.

Phenomenal accuracy is maintained during the process of translation by close monitoring of the maturation of mRNA and tRNA, selection of the right amino acids and correct base pairing between the tRNA and the mRNA (Ibba et al., 1999). This is done to ensure the quality of outgoing polypeptide chains, because misincorporation of unwanted amino acids affects protein folding and stability. Protein folding is a spontaneous process involving the formation of ionic, hydrogen and disulfide bonds and van der Waals's interactions. Secondary structural elements, like α-helices and β-sheets, are formed with less difficulty. Once formed, they are stable owing to their inherent framework of hydrogen bonds. Formation of the final tertiary structure, with all the structural elements intact, occurs for different proteins on varying time scales. Some proteins (around 100 amino acids) fold spontaneously (Dobson et al., 1999); whereas, some others (larger

and multi-domain proteins) tend to fold incorrectly (Goldberg et al., 1991), hence require assistance.

1.1 Assisted folding and Chaperones

Most proteins fold to their correct three-dimensional structures post-translationally (Agashe et al., 2004; Netzer et al., 1997), whereas, some fold in a co-translational mode (Nicola et al., 1999). Co-translational folding involves risks like misfolding of a partially emerged polypeptide chain, before the translation process is finished completely. Proteins like trigger factor provide a protected space for the emerging polypeptide chain to fold by shielding it from the surrounding cytoplasm and proteases (Ferbitz et al., 2004) (Fig 1.1).

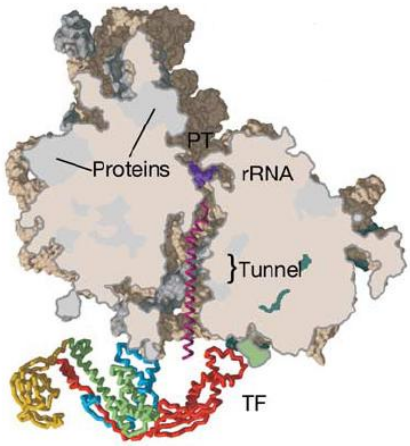

Fig 1.1: Trigger Factor. Cross sectioned grey part of the figure features a ribosome in action. In pink is the polypeptide chain emerging out of the exit tunnel of the ribosome. Trigger factor (in trace representation) binds to the ribosome by providing a 'hydrophobic cradle to the emerging polypeptide chain to fold' (Obtained from Ferbitz et al., 2004).

Assisted folding involves chaperone proteins that help polypeptide chains to attain correct conformation by providing a platform to fold. Although, discovered and described like heat shock proteins, most chaperones are also involved in *de novo* protein folding. Almost all of them are both constitutively expressed and stress-induced. Proteins that fall in this category are Trigger factor, the Hsp70/DnaK system, the Hsp60/GroEL-GroES system, Hsp90, Small Heat Shock proteins, etc. Most of these proteins are protein-remodeling molecular machines, fueled by energy released from ATP hydrolysis. Nucleotide binding and hydrolysis play a central role in the mechanism of action of many proteins that are outlined below.

The GroEL-GroES system is probably the best studied chaperone system to date. It helps nascent polypeptide chains to fold, by spatially separating them from the surrounding cytoplasm. The GroEL-GroES system comprises of the GroEL tetra-decamer and the GroES heptamer stacked onto each other in a ring-like fashion. This provides an encapsulated environment for the polypeptide chains to fold (Mayhew et al., 1996; Hartl et al., 2002).

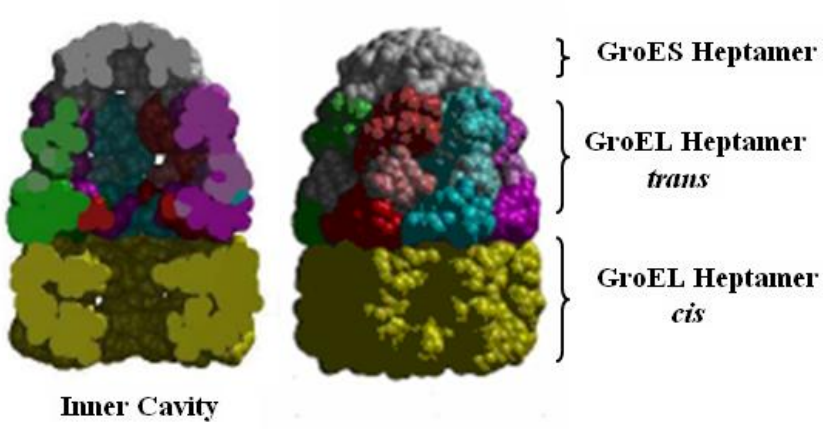

Fig 1.2: GroEL-GroES System. Right side of the figure shows a GroEL-GroES oligomer (space-fill representation) with 14 GroEL subunits arranged in 2 rings. The GroES heptamer sits on the *trans*-ring of the GroEL heptamer. Left side shows a vertical section of the GroEL-GroES oligomer which visualizes the central cavity, where polypeptide chains are folded. The colored part of the *trans*-ring depicts each subunit in one color, and the shading represents the apical (medium), intermediate (light) and equatorial (dark) domains of each monomer. (Obtained from Ellis 2006)

ATP hydrolysis-mediated conformational changes inside the GroEL cavity result in folding of unfolded or partially folded polypeptide chains (Mayhew et al., 1996; Hartl et al., 2002). Both rings of the GroEL system (*trans* and *cis*) exhibit negative allosteric behavior in nucleotide binding and hydrolysis, which is the key for their mechanism of action. Unfolded or partially folded polypeptide chains with exposed hydrophobic surfaces are taken into the cavity of GroEL. This occurs by interaction with exposed hydrophobic residues of the apical domains on the *trans*-ring (Fenton et al., 1997). Nascent polypeptide chain binding to the apical domain of the *trans*-GroEL ring results in binding of ATP and GroES (Xu et al 1997; Hartl et al., 2002). Upon ATP hydrolysis and subsequent conformational changes, folding intermediates move into the *cis*-ring. There they are allowed to fold for ~10s. ATP binding at the *trans*-ring results in the opening of the cage to release folded polypeptide chains, and the GroEL-GroES system is ready for the next round of action (Hartl et al., 2002). Evidence from Hydrogen-Deuterium exchange studies

suggested that GroEL-GroES system also probably acts as a passive unfoldase which unfolds misfolded proteins (Zahn et al., 1996).

Hsp70 proteins are versatile, and constitutively expressed in almost all organisms studied, except for *Methanococus janischii* (Bult et al., 1999). Sub-cellular location includes cytosol of prokaryotes and eukaryotes, chloroplasts, mitochondria and lumen of ER in eukaryotes. Hsp70 proteins are involved in transport across membranes (Hermann and Neuport et al., 2000, Pfanner et al., 2000, Schatz and Dobberstein 1996), disassembly of clathrin-coated vesicles (Schmid et al., 1985, Schmid and Rothmann 1985) and regulation of heat shock response (Abravaya et al., 1992; Yura et al., 1993). However, their main role in the cell is to assist nascent polypeptide chains to fold into proper three-dimensional structures. Both in eukaryotes and prokaryotes, several co-chaperones assist the DnaK protein in its primary function of *de novo* protein folding.

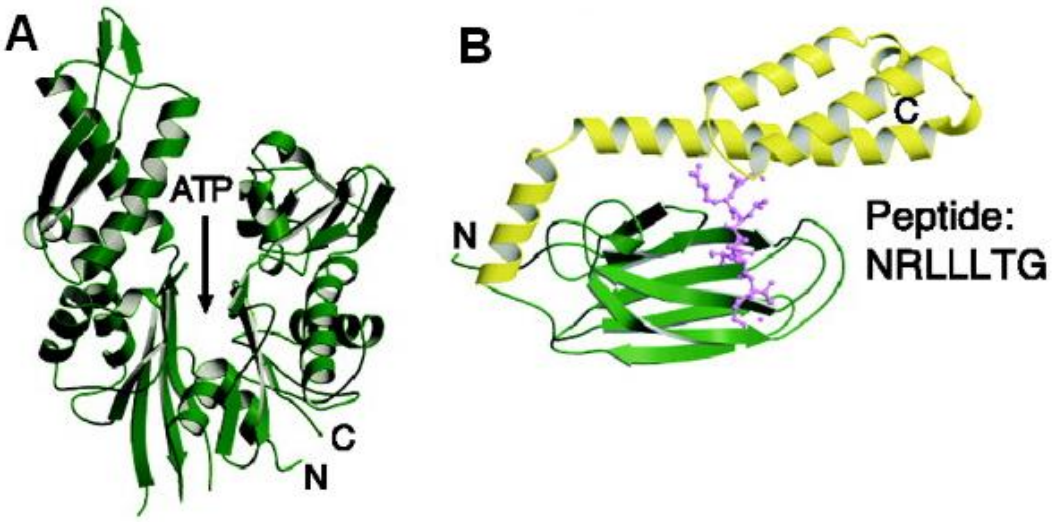

Fig 1.3: Structure of ATPase and Peptide binding domains of DnaK$_{E\ coli}$. (A) The ATPase domain of the DnaK protein shows an actin like fold, where ATP binds at the cleft formed between the two distinct sub domains (Obtained from Hartl et al., 2002). **(B)** The structure of the peptide binding domain (PBD) of the DnaK protein in complex with the peptide NRLLLTG revealed two distinct domains. The N-terminal part of the PBD forms an anti-parallel β-sandwich and the C-terminal end forms an α-helical domain. The loops connecting the β-sheet form a hydrophobic peptide binding groove, which is closed and opened by closing and opening of the long α-helical domain. The peptide bound at the peptide binding domain of Hsp70/DnaK is shown in a ball and stick representation. (Mayer et al., 2000) (Obtained from Hartl et al., 2002).

Hsp70/DnaK proteins interact with a variety of substrates, which are unrelated in sequence, structure and conformation. The binding affinities range between 5 nm-5 µM (Bukau and Horwich 1998). A typical binding site in a substrate protein consists of a hydrophobic amino acid

patch flanked by basic amino acid-rich sequences. DnaK/Hsp70 proteins consist of an N-terminal ATPase domain, a central peptide binding domain and a C-terminal glycine-rich domain (Flaherty et al., 1990) (Fig 1.3). Hsp70/DnaK system along with its co-chaperones Hsp40/DnaJ and GrpE help nascent polypeptide chains to fold by merely functioning as a holdase (Schlee et al., 2002). Holding and release of polypeptide chains by the Hsp70/DnaK system is determined by the bound nucleotide (Buchberger et al., 1995; McCarty et al., 1995). ATP-bound Hsp70/DnaK binds polypeptide chains with less affinity and releases rapidly, whereas the ADP-bound form holds them with high affinity. ATP hydrolysis in $DnaK_{E.coli}$ is enhanced by the DnaJ co-chaperone (Mayer et al., 2000; Pellecchia et al., 2000), and nucleotide exchange from ADP to ATP is facilitated by nucleotide exchange factor, GrpE (Harrison et al., 1997).

1.2 Protein Degradation

Another quality control mechanism employed by a cell is the termination strategy; where, unwanted, aggregated and misfolded proteins are degraded by proteases. The most studied and better understood protein degradation pathway inside a cell is ubiquitin-mediated protein degradation. Apart from proteins that are involved in regulatory pathways that needed to be rapidly synthesized and degraded in accordance with stimuli, proteins that are misfolded or malformed are also tagged with poly-ubiquitin side chains. Poly-ubiquitination targets these proteins to the 26S protease assembly, where they are degraded to amino acids. Protein degradation is not only essential for the maintenance of a cell but also for diverse signal transduction mechanisms. For example, proteolysis-dependent CDK activity directly triggers the entry of a cell from metaphase to anaphase (King et al., 1996).

1.3 ClpB/Hsp104: A Protein Disaggregating Molecular Motor

A cell employs several restoration strategies to maintain the integrity of its protein content. A central player in the restoration mechanisms of a cell is the Hsp104/ClpB protein, which disaggregates aggregated proteins. It was first discovered in *S. cerevisia* where deletion of the Hsp104 gene resulted in loss of tolerance to heat, ethanol, arsenate and long term cold storage (Sanchez et al., 1992). ClpB/Hsp104 homologues are present in many organisms and are vital for cell survival under stress conditions, by conferring thermotolerance and rescuing aggregated proteins (Mogk et al., 1999; Schmitt et al., 1996; Quietsch et al., 2000). In human cells, Hsp104 from *S. cerevisia* has been shown to inhibit stress-induced apoptotic signaling (Mosser et al., 2004). Therapeutic role of Hsp104 is recently discovered in mice carrying mutations for Huntington's disease (Vacher et al., 2005; Perrin et al., 2007). Its importance in prion propagation is also, one of the well-known examples (Chernoff et al., 1995). Specific *in vitro* reactivation of heat-denatured substrate proteins has also been reported for ClpB from *T. thermophilus* (HB8 cells) (Motohashi et al., 1999) along with the DnaK/Hsp70 system.

ClpB/Hsp104 proteins belong to the AAA family of ATPases (ATPases Associated with various cellular Activities) (Lee et al., 2004; Dougan et. al 2002; Neuwald et al., 1999; Schirmer et al., 1996). Members of this widely occurring family include proteins involved in proteolysis (ClpA, ClpX, HslU and FtsH), intra-cellular transport (p97, NSF and Dynein), transcriptional activators (NtrC1), DNA binding proteins (RuvB and Helicases), proteins involved in membrane transport (ABC transporters) and many more (Neuwald et al., 1999, Ye et al., 2004; Tucker et al., 2007). The identifying feature is an AAA signature module, which includes a RecA-like mononucleotide binding domain and a C-terminal α-helical small domain. Characteristic features of a typical AAA module include Walker A and Walker B consensus sequences along with sensor-1 and 2 regions and an arginine-finger (Neuwald et al., 1999). Proteins belonging to the AAA family are divided into two classes: Class 1 AAA proteins feature two AAA modules and class 2 proteins feature a single AAA module. ClpB/Hsp104 proteins belong to class 1 with two AAA modules per subunit (Schirmer et al., 1996). Members of the AAA family form oligomers (Ogura and Wilkinson, 2001; Ye et al., 2004) and despite their diverse functions, follow similar mechanisms in converting energy from ATP hydrolysis to mechanical work (Hanson and Whiteheart, 2005; Wang 2004; Ye et al., 2004).

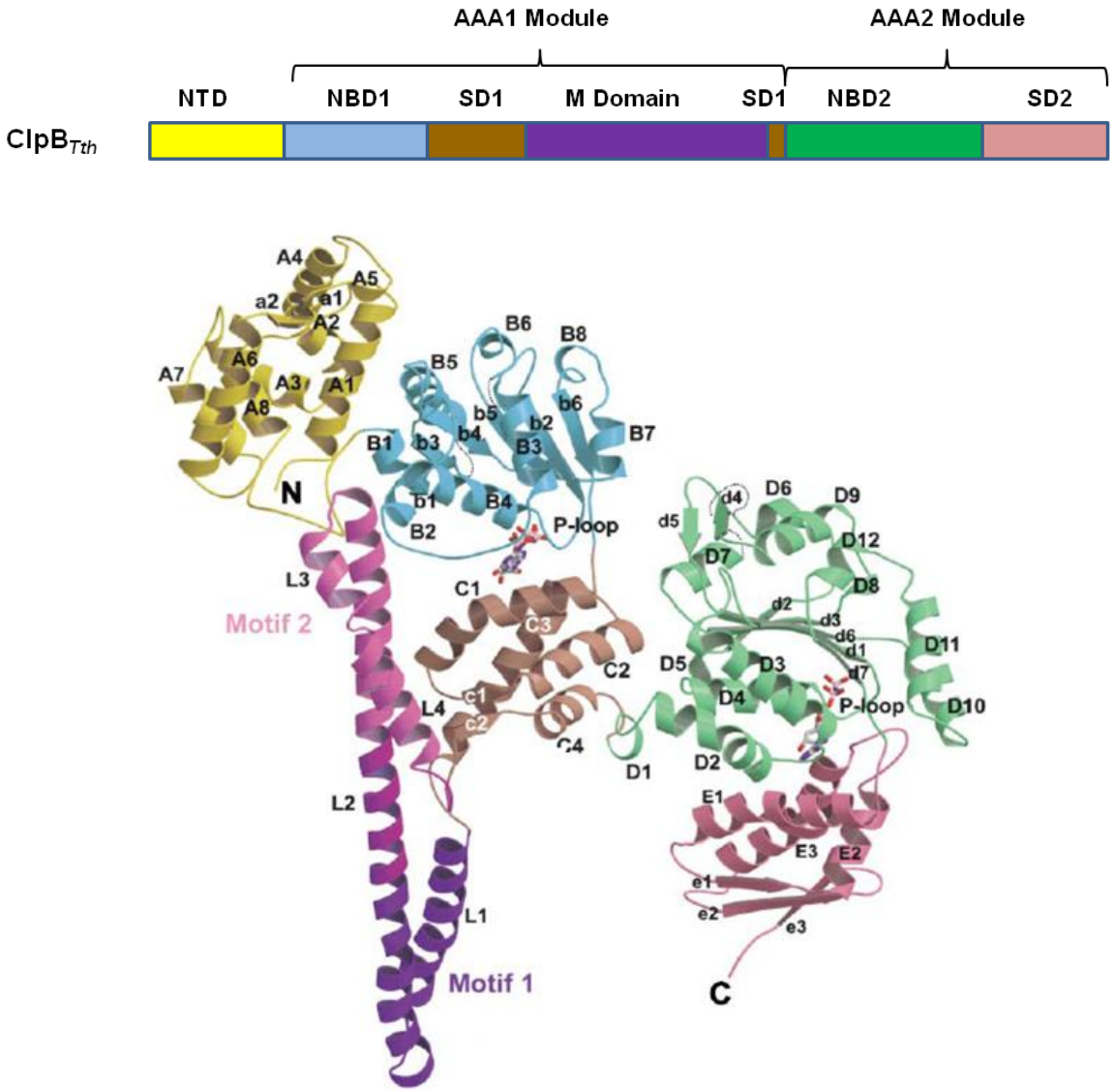

Fig 1.4: (A) Domain organization of *T. thermophilus* ClpB. ClpB$_{Tth}$ consist of three distinct parts. 1. N-terminal domain (NTD, Yellow). 2. The AAA1 module with the nucleotide binding domain 1 (NBD1, Blue), the small domain 1 (SD1, Brown) and the M domain (Violet). 3. The AAA2 module with the nucleotide binding domain 2 (NBD2, Green) and the small domain 2 (SD2, Pink).
(B) Structure of *T. thermophilus* ClpB. The two tandem AAA modules with N-terminal and M domains are shown in ribbon representation with AMP-PNP bound in *anti*-conformation (Obtained from Lee et al., 2003). **1.** NTD-*Yellow*: The N-terminal domain in ClpB$_{Tth}$ is mostly α-helical except for two parallel β strands at the beginning. **2.** AAA1 module: (NBD1-*Blue*, SD1-*Brown*, M domain-*Violet*): NBD1 of the AAA1 module features a RecA-like mononucleotide binding domain with an additional antiparallel β-strand inserted at the beginning. The small domain 1 is mostly α-helical except for two parallel β-strands, which connects the AAA1 module to the AAA2 module. The M domain, which appears as an insertion in SD1, consists of a long coiled-coil with two shorter coiled-coils. The two antiparallel α-helices of the M domain consist of leucine zipper motifs with three leucine-rich heptad repeats. **3.** AAA2 module: (NBD2-*Green*, SD2-*Pink*): NBD2 of the AAA2 module also features a RecA-like mononucleotide binding domain with a β-hairpin motif towards the end. A three stranded β-pleated sheet forms the end of the small domain 2; however, the rest of the domain is mostly α-helical.

In ClpB/Hsp104, the two tandem AAA modules (AAA1 and AAA2) consist of nucleotide binding domains (NBD1 and NBD2) and α-helical small domains (SD1 and SD2). The AAA modules are preceded by an N-terminal domain (NTD); whereas, an M domain exists as an insertion in SD1 of the first AAA module (Fig 1.4A). In *S. cerevisia* Hsp104, an additional 38 amino acid C-terminal extension is present, which is essential for thermotolerance in yeast (MacKay et al., 2008). ClpB/Hsp104 proteins from *E. coli*, *T. thermophilus* and *S. cerevisia* share approximately 50% identity in their protein sequence; however, sequence similarity between the two AAA modules within each protein is quite low (Schirmer et al., 1998; Schlee et al., 2001). The single AAA module of class 2 proteins shares high similarity with the second AAA module of ClpB/Hsp104 proteins.

The structure of *T. thermophilus* ClpB at 3.0 Å resolution revealed 3 distinct parts in the arrangement of the two tandem AAA modules with its N-terminal and M domains (Lee et al., 2003) (Fig 1.4B). A globular, N-terminal, non-NTPase domain (NTD) forms the first part of the protein, which is connected to the nucleotide binding domain of the AAA1 module through a flexible linker (Lee et al., 2003). Role of the N-terminal domain, although unclear, has been assigned to substrate binding but dispensable for chaperone activity (Beinker et al., 2002; Barnett et al., 2005; Lee et al., 2007, Wendler et al., 2007). The N-terminal domain (Part 1) is followed by the first AAA module consisting of NBD1 and SD1 with the M domain insertion (Part 2) and the second AAA module with NBD2 and SD2 (Part 3). Both NBD1 and NBD2 feature a RecA-like mononucleotide binding fold with small modifications (Lee et al., 2003). Both the NBDs carry Walker A and B consensus motifs, Sensor-1 and arginine-finger residues, which are important, for nucleotide binding and hydrolysis. Both the nucleotide binding domains bind ATP, although with different affinities.

Hydrolysis of ATP by ClpB/Hsp104 proteins follows sigmoidal kinetics (homotypic and heterotypic allostery) and is essential for chaperone activity (Schirmer et al., 2001; Barnett et al., 2000; Schlee et al., 2001; Watanabe et al., 2001; Hattendorf and Lindquist 2002). In the case of $Hsp104_{Yeast}$, the AAA1 module has higher ATP hydrolysis (Schirmer et al., 1998; Hattendorf and Lindquist 2002b), whereas ATP binding to the AAA2 module determines the oligomeric state (Parsell et al., 1994; Schirmer et al., 2001; Tkach and Glover 2004). In $ClpB_{Tth}$, the AAA2

module seems to have higher rate of hydrolysis. Upon isolation, the AAA2 module hydrolyzes ATP in a sigmoidal manner, indicating homotypic allosteric communications. The absence of AAA1 module appeared to have resulted in an increased rate of ATP hydrolysis; whereas, isolated AAA1 module does not bind or hydrolyze ATP on its own (Beinker et al., 2005). The mode of nucleotide hydrolysis in ClpB/Hsp104 proteins still remains very speculative. Evidence for both concerted and sequential ATP hydrolysis is available. The presence of heterotypic allostery in nucleotide hydrolysis and inter-subunit coupling favors a concerted mechanism for ATP hydrolysis (Werbeck et al., 2008). Structural basis for allosteric communications in $ClpB_{Tth}$ is unclear, owing to the lack of high resolution hexameric structures.

Mutations in the conserved regions of ClpB/Hsp104 proteins influence nucleotide binding and hydrolysis subsequently affecting the oligomeric state and chaperone activity (Fig 1.5A, B and Table 1.1). Mutating the conserved Walker A consensus residues (conserved lysine/threonine interacts with the phosphates of ATP) results in altered nucleotide binding and hydrolysis with a loss of allosteric behavior and chaperone activity (Schirmer et al., 1996; Schlee et al., 2001; Schirmer et al., 2001; Barnett et al., 2002; Mogk et al., 2003). Mutations in the Walker B consensus (conserved glutamic acid coordinates ATP hydrolysis by contacting water molecule, Mg^{2+} and ATP) results in complete loss of ATP hydrolysis, but nucleotide binding is not affected (Schirmer et al., 1996; Mogk et al., 2003; Lee et al., 2007). The so called TRAP mutant in ClpB/Hsp104 with Walker B mutations at both the AAA modules binds ATP but does not hydrolyze, hence extensively used to study the ATP-bound form of ClpB/Hsp104 proteins (Weibezahn et al., 2003; Lee et al., 2007). Mutation of the Sensor-1 residue (conserved asparagine/threonine interacts with the γ-phosphate of ATP) results in complete loss of hydrolysis in $Hsp104_{Yeast}$ (Schirmer et al., 1996; Hattendorf and Lindquist., 2002). Nucleotide binding domains of the ClpB/Hsp104 AAA modules are home to the so called 'arginine-finger', which is thought to be the basis for homotypic allosteric communications (conserved arginine interacts with the γ-phosphate of ATP bound at the neighboring AAA module). Loss of arginine side chain upon mutation, effects ATP hydrolysis and results in loss of function (Ogura et al., 2004; Mogk et al., 2003).

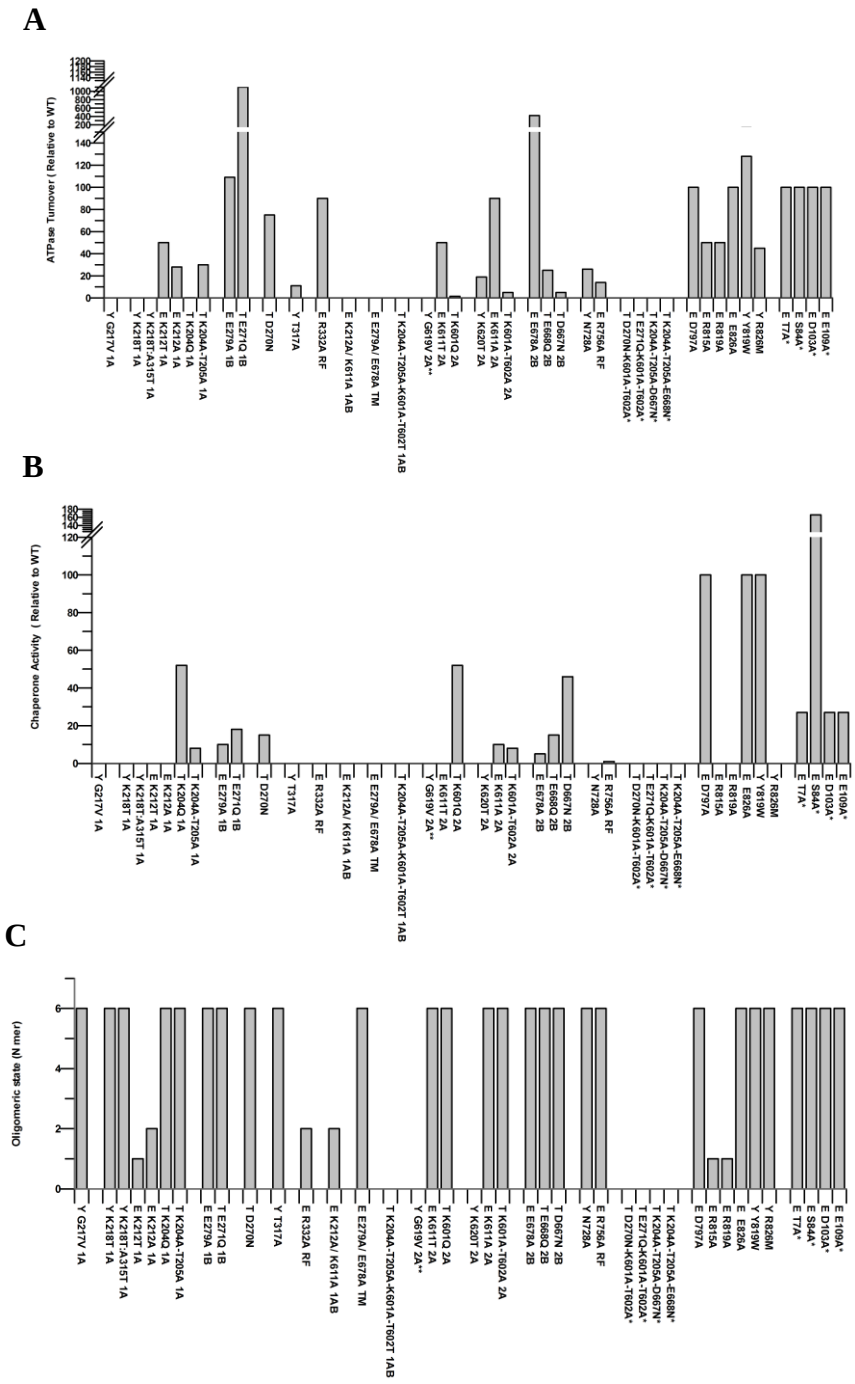

Fig 1.5: The effect of various mutations on the ATPase, chaperone activity and the oligomerization properties of ClpB/Hsp104 proteins. WT activity is taken as 100% in all cases. **Y:** *S. cerevisia* Hsp104, **E:** *E. coli* ClpB and **T:** *T. thermophilus* ClpB; **1A:** Walker A mutation in AAA1 module, **2A:** Walker A mutation in AAA2 module, **1B:** Walker B mutation in AAA1 module, **2B:** Walker B mutation in AAA2 module, **RF:** arginine-finger and **TM:** Trap Mutant.
(A) The effect on ATP hydrolysis: (*S. cerevisia* Hsp104: 76 ATP/ Min, *E. coli* ClpB: 1.26 ATP/ Min, *T. thermophilus* ClpB: 2.65 ATP/ Min).
(B) The effect on Chaperone activity.
(C) The effect on oligomerization.

Mutants K_D (µM)	ATP	ADP
T WT	21.4	1.5
Y WT	69	9.1
T K204Q 1A	43	3
T K204A-T205A 1A	45	6
T E271Q 1B	37	11
T D270N	55	10
T K601Q 2A	28	2
T K601A-T602A 2A	110	13
T E668Q 2B	17	3
T D667N 2B	17	1
T D270N-K601A-T602A*	370	15
T E271Q-K601A-T602A*	67	6
T K204A-T205A-D667N*	25	1
T K204A-T205A-E668N*	14	1
Y N728A	61	7

Table 1.1: The effect of various mutations on the nucleotide binding properties of ClpB/Hsp104 proteins.
Y: *S. cerevisia* Hsp104, **E:** *E. coli* ClpB and **T:** *T. thermophilus* ClpB; **1A:** Walker A mutation in AAA1 module, **2A:** Walker A mutation in AAA2 module, **1B:** Walker B mutation in AAA1 module, **2B:** Walker B mutation in AAA2 module and **RF:** arginine-finger.

The α-helical small domains (SD1 and SD2) also play a key role in the function of the ClpB/Hsp104 proteins. They feature the Sensor-2 or sensor-substrate discrimination motif (conserved arginine contacts the γ-phosphate of ATP). Mutations result in impaired nucleotide binding and loss of ATP hydrolysis (Hattendorf and Lindquist 2002; Barnett et al., 2002; Mogk et al., 2003). SD1 of the AAA1 module in ClpB/Hsp104 harbors the M domain; which differentiates ClpB/Hsp104 from the other Hsp100/Clp family proteins. Other than ClpB/Hsp104 a shortened M domain is seen in ClpC, a class 1 AAA ATPase, also involved in protein degradation. Deletion of the M domain results in loss of thermotolerance and chaperone activity (Cashikar et al., 2002, Mogk et al., 2003; Kedzierska et al., 2003; Schirmer et al., 2004). The M domain of $ClpB_{Tth}$ is an 85Å long coiled-coil divided into two motifs (Motif 1 has helices 1 and 2, whereas Motif 2 has helices 3 and 4) (Lee et al., 2003). In $Hsp104_{Yeast}$, mutations in helix 3 of the M domain resulted in different functional defects (Haslberger et al., 2007). Nucleotide binding driven, M domain mediated communication between the AAA modules, has been proposed to be crucial for function in both ClpB and Hsp104 (Cashikar et al., 2002; Watanabe et al., 2005).

Hsp104/ClpB and other ATPases belonging to the AAA family typically form dynamic, nucleotide- and ionic strength-dependent, hexameric structures (Beuron et al., 1998; Bochtler et al., 2000; Ishikawa et al., 2001; Lee et al., 2003; Ortega et al., 2000; Parsell et al., 1994; Sousa et al., 2000; Wang et al., 2001; Zolkiewski et al., 1999a; Haslberger et al., 2008; Werbeck et al., 2008). Hexamer formation in ClpB/Hsp104 is facilitated at high protein concentration, low ionic strength and in the presence of ATP; whereas, ADP drives the oligomeric equilibrium to lower order (Parsell et al., 1994; Schirmer et al., 1998; Zolkiewski et al., 1999; Schlee et al 2001; Schirmer et al., 2001; Hattendorf and Lindquist 2002b). Presence of both the AAA modules is essential for hexamer formation but not covalent linkage (Beinker et al., 2005). Upon reconstitution, isolated AAA modules of $ClpB_{Tth}$ were reported to display oligomer formation, nucleotide hydrolysis and subsequently chaperone activity.

In ClpB/Hsp104 proteins, deletion of the α-helical small domain (SD2) in the AAA2 module results in complete loss of oligomerization, (Mogk et al., 2003, MacKay et al., 2008). However, the exact mechanism remains unclear. In Hsp104, oligomerization is clearly assigned to nucleotide binding at the AAA2 module (Parsell et al., 1994; Schirmer et al., 2001). However, arginine-finger mutations in the AAA1 module have also been shown to affect nucleotide-dependent oligomer formation (Wendler et al., 2007). Although, dimer formation is reported in the case of isolated AAA2 module from $ClpB_{Tth}$ (Beinker et al., 2005), oligomerization has not been reported in the case of any other variants in $ClpB_{Tth}$, $ClpB_{E.coli}$ and $Hsp104_{Yeast}$. A mutation in the conserved regions which impair or alter nucleotide binding also affects nucleotide-mediated oligomer formation in ClpB/Hsp104 (Fig 1.7C and Table 1.1). Mutations of Walker A consensus lysine, Sensor-2 arginine and arginine-finger result in altered oligomerization properties (Schirmer et al., 1996; Schlee et al., 2001; Schirmer et al., 2001; Hattendorf and Lindquist 2002; Barnett et al., 2002; Mogk et al., 2003). The role of ADP-mediated dissociation of ClpB/Hsp104 oligomers in its function is still very ambiguous.

Two significantly different single particle reconstructions have been developed to date for the ClpB/Hsp104 hexamer ($ClpB_{Tth}$-AMP-PNP: Lee et al., 2003; $ClpB_{Tth}$-AMP-PNP, -ADP, *-apo* and $ClpB_{Tth}$ (TRAP)-ATP: Lee et al., 2007; $Hsp104_{Yeast}$ (AAA2 Sensor-1 mutant): Wendler et al., 2007) (Fig 1.6). Both the structures show a double barrel-like structure of varying sizes,

where the AAA modules from each subunit are placed in two separate rings, although in a staggered manner (Lee et al., 2007; Wendler et al., 2007). Arrangement of the NBDs of each AAA module is at the interface between the subunits, thereby forming contacts with the α-helical small domains and the neighboring AAA modules in both upper and lower rings. This forms a platform for propagation of the inter-subunit conformational changes. In both reconstructions, a central channel or cavity is present; however, of varying diameter (78 Å for $Hsp104_{Yeast}$ hexamer and 28 Å for $ClpB_{Tth}$ hexamer) (Fig 1.6A, B). Axial loops, which contain conserved tyrosines from both the AAA modules, line the central channel and are crucial for function of ClpB/Hsp104 proteins (Lum et al., 2004; Schlieker et al., 2004; Weibezahn et al., 2004). The central channel, a widely studied feature, has evolved as a ground for a universal mechanism of protein remodeling by Clp/Hsp100 proteins. It is extensively studied in Clp proteases that form the protein unfolding units of protease complexes (ClpA and ClpX of ClpAP and ClpXP proteases and HslU of HslUV complex).

Complete N-terminal domain and parts of the M domain are not visible in the $ClpB_{Tth}$ reconstruction owing to their high mobility (Lee et al., 2007), whereas, in the case of $Hsp104_{Yeast}$ structure, the N-terminal domains were shown to form a ring on top of the AAA1 (upper) ring (Wendler et al., 2007). Interestingly, the diameter of the central cavity decreased by 16 Å in the $Hsp104_{Yeast}$ NTD deletion mutants compared to the WT protein (Wendler et al., 2007). A notable difference was seen in the arrangement of the M domain (Fig 1.6 C, D and E). In the case of $ClpB_{Tth}$ structure, the M domains are placed at the periphery of the AAA1 (upper) ring with radial outward projections. Partial protrusions of the M domain at the periphery of the AAA1 (Upper) ring are nucleotide-dependent, which may be involved in mediating homotypic allosteric communications (Lee et al., 2003; Lee et al., 2007). In the case of $Hsp104_{Yeast}$ hexamer, the M domain is placed towards the cavity surface; where, it forms contacts with NTD and the AAA1 module of the same subunit and diagonally with the AAA2 module of the neighboring subunit. Conserved arginines, present on the M domain, have been proposed as the arginine-fingers which affect nucleotide hydrolysis (Wendler et al., 2007) instead of the established arginine-fingers of the AAA domains (Hanson and Whiteheart, 2005; Ogura et al., 2004). This arrangement of the M domain touted its role as a probable mediator in heterotypic allosteric communications.

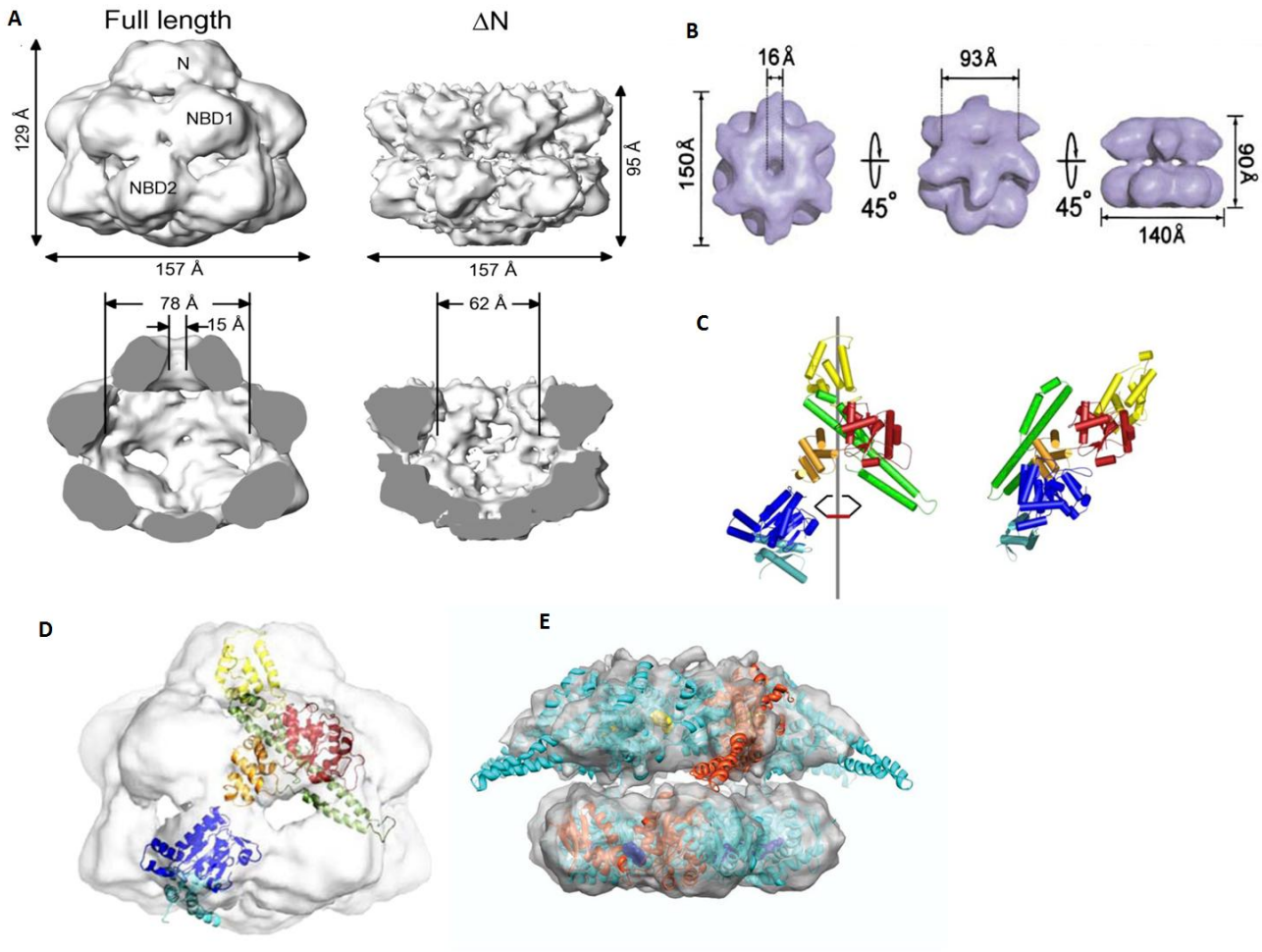

Fig 1.6: ClpB/Hsp104 Hexamer: (A) Dimensions of the Hsp104$_{Yeast}$ Hexamer (**Electron microscopic Reconstruction.** Overall dimensions of the Hsp104$_{Yeast}$ hexamer are bigger than typical AAA hexamers, of whose structures are known so far. The lack of N-terminal domain in ΔN structure results, in a change, in the orientation of the AAA1 modules; thereby, decreasing the central cavity size (Obtained from Wendler et al., 2007). **(B) Dimensions of the ClpB$_{Tth}$ Hexamer (Electron microscopic Reconstruction).** Size of the central cavity is smaller when compared to the Hsp104$_{Yeast}$ hexamer, owing to the domain arrangement (Obtained from Lee et al., 2003). **(C) Arrangement of the two AAA modules and the N-terminal domain in Hsp104$_{Yeast}$ and ClpB$_{Tth}$.** In the first figure (Hsp104$_{Yeast}$), the M domain is rotated 90º clockwise, placing it towards the inside of the protein. Second part of the figure shows domain arrangement in the ClpB$_{Tth}$ hexamer, where the M domain is placed towards the periphery (Obtained from Wendler et al., 2007). **(D) Homology model of the Hsp104$_{Yeast}$ structure docked to electron microscopic density map.** The staggered arrangement of the AAA modules is noticeable; where, the AAA1 module is arranged at the upper right hand corner of the AAA2 module. The M domain faces the cavity of the hexamer; thereby, interacting with the AAA1 module and the neighboring AAA2 module (Obtained from Wendler et al., 2007). **(E) The crystal structure of ClpB$_{Tth}$ docked to electron microscopic density map.** The staggered arrangement of the AAA modules can be noticed in the highlighted subunit (Red). The M domains are placed at the periphery; where, they undergo nucleotide-driven conformational changes (Obtained from Lee et al., 2007).

The M domain motion has been proposed to promote hexamer stabilization upon ATP binding at the AAA1 module and subsequent ATPase stimulation at the AAA2 module in $ClpB_{Tth}$ (Watanabe et al., 2005). Mutations in helix 3 of the M domain which disrupt the conformational rigidity have been shown to affect hexamerization and chaperone activity, but not the threading of substrate protein through the central channel (Watanabe et al., 2009). Similarly, in $ClpB_{E.coli}$ direct interactions between helix 3 of the M domain and the AAA1 module have been shown to be important for chaperone activity. However, in this case conformational flexibility has been shown to control these interactions (Haslberger et al., 2007). Mutations in helix 3 of the M domain disrupt interactions with the AAA1 module. These mutations have been shown to be affecting the conformation of the M domain helix 1. Motif 2 of the M domain which consists of helices 3 and 4 in $ClpB_{Tth}$ has additionally been shown to position between the neighboring AAA modules of the upper ring where it was speculated to be involved in ATP-dependent conformational changes (Lee et al 2007).

Although ClpB/Hsp104 shares the same loops in its central channel like ClpA, ClpX and HslU, preferential binding to aggregated substrates over folded proteins involves no recognition tags. Acidic amino acids, in the N-terminal domain, are involved in direct binding to protein aggregates, even in the absence of DnaK/Hsp70 system (Barnett et al., 2005). ClpB/Hsp104 along with the DnaK/Hsp70 system disaggregates both partially and completely aggregated proteins with similar refolding efficiency (Haslberger et al., 2008). Strict ATP dependence for substrate binding is observed (Schlieker et al., 2004; Weibezahn et al., 2003; Bosl et al., 2005). This occurs probably through stabilization of the central channel conserved loop residues, of the AAA1 ring, by interaction with the M domains (Lee et al., 2007). Flexibility in the M domain and orientation of its motif 2 which positions itself between the neighboring AAA1 modules in the AAA1 (upper) ring is also important for high affinity substrate binding (Lee et al., 2007).

ClpA, an AAA family member and part of the ClpAP protease complex, translocates proteins into the ClpP chamber for further degradation (Weber-Ban et al., 1999). Engineered variants of $ClpB_{E.coli}$ and $Hsp104_{Yeast}$ (helix-loop-helix in the AAA2 module is substituted with that of ClpA) bind the ClpP proteolytic chamber. Upon binding to ClpP, the engineered variant translocates proteins through its central pore like ClpA (Weibezahn et al., 2004b; Tessarz et al., 2008). This

provided hints at a possible mechanism, where aggregated proteins are pulled through the central pore of ClpB/Hsp104 proteins as a part of the disaggregation process. Threading of polypeptide chains through the central channel of the ClpB/Hsp104 oligomer has gained regard as a possible mechanism for protein disaggregation as well as prion propagation (Weibezahn et al., 2004; Tessarz et al., 2008; Haslberger et al., 2008; Tipton et al., 2008). Polypeptide translocation through the central channel, although essential, is not sufficient for disaggregation (Haslberger et al., 2007). Disaggregation of looped polypeptide chains as well as more than one polypeptide chain by threading through the central channel is shown as a possibility, owing to the size of the central channel in $ClpB_{E.coli}$ and $Hsp104_{Yeast}$ (Haslberger et al., 2008). Although these engineered variants acted as a 'degrading disaggregases', their function was shown to be dependent on the DnaK/Hsp70 system, and could not confer thermotolerance *in vivo* (Weibezahn et al., 2004b).

Further studies also showed that positively charged aggregated proteins bind to the negatively charged ClpB/Hsp104 channel entrance (Schlieker et al., 2004). It was proposed that substrate binding at the AAA1 (upper) ring occurs in the ATP-bound state (high affinity); hydrolysis and concomitant conformational changes thread the substrate through the central pore (Lee et al., 2007). Flexibility of the M domain and its nucleotide-dependent interaction with the AAA1 module plays a central role in substrate threading through the central channel (Haslberger et al., 2007; Lee et al., 2007; Wendler et al., 2007). The M domain motion, which seems to be central for the function of ClpB/Hsp104 proteins, was also postulated to generate a molecular crowbar-like force (Lee et al., 2003).

Protein disaggregation activity shown by ClpB/Hsp104 proteins is strictly dependent on concerted or sequential action along with the DnaK/Hsp70 system (Glover et al., 1998; Goloubinoff et al., 1999; Mogk et al., 1999; Motohashi et al., 1999 and Zolkiewski et al., 1999b). Chaperone activity of ClpB/Hsp104 and DnaK/Hsp70 proteins has been extensively studied using a wide variety of substrate proteins, both *in vivo* (thermotolerance) and *in vitro* (heat and chemical denaturation) (Parsell et al., 1994; Mogk et al., 1999; Glover et al., 1998; Motohashi et al., 1999; Zolkiewski et al., 1999; Goloubinoff et al., 1999; Beinker et al., 2001). Clear evidence is available for the action of DnaK/Hsp70 proteins both upstream and downstream of the disaggregation process (Weibezahn et al., 2004). This interaction was shown to be highly

specific to the organism as well as organelle and cannot be replaced by a counterpart from homologues or orthologues (Glover et al., 1998; Krzewska et al., 2001; Schlee et al., 2004). Presence of the N-terminal domain is dispensable, but mutations in the M domain affect this interaction (Schlee et al., 2004 and Haslberger et al., 2007). Nucleotide- and oligomeric state-dependent complex formation (K_D: 17 μM) was reported for *T. thermophilus* ClpB and DnaK proteins (Schlee et al., 2004). Recent studies showed that, DnaJ meditates binding of DnaK to the aggregated substrates, which in turn facilitates ClpB binding at the aggregate surface (Acebron et al., 2009).

ClpB/Hsp104 along with the DnaK/Hsp70 system reactivates aggregated substrate proteins both *in vivo* and *in vitro*, although the precise nature of the interaction between these proteins is not clearly known. A sequential mechanism of action has been proposed for the action of ClpB/Hsp104 and the DnaK/Hsp70 system from *E. coli*, where ClpB acts on aggregates and exposes hydrophobic binding sites for the DnaK system to act further (Goloubinoff et al., 1999). It has been proposed in several instances that ClpB/Hsp104 proteins break non-covalent contacts in aggregates thereby exposing hydrophobic surfaces for the DnaK/Hsp70 system to act (Glover et al., 1998; Schlee et al., 2004). A similar mechanism was proposed for ClpB and DnaK from *T. thermophilus* where, the transient complex formed between ClpB and DnaK proteins was hypothesized to be acting upon large aggregates using ATP hydrolysis-driven conformational changes. In further steps upon exposure of hydrophobic surfaces, these aggregates are acted upon by the DnaK system (Schlee et al., 2004). Recent studies showed that a mixture of ATP and ATPγS can elicit remodeling activity in ClpB/Hsp104 without DnaK/Hsp70 proteins (Doyle et al., 2007). A heterogeneous mixture of ClpB wild type and ClpB-TRAP mutant also results in remodeling activity in the absence of DnaK system (Hoskins et al., 2009).

1.4 Objective

Many fundamental processes of a living cell progress through consumption of energy. Fuelling biological processes occurs via various methods and sources. First and most important of them is the ATP hydrolysis. Energy released from the ATP hydrolysis is used to drive conformational changes in proteins, which in turn result in their function. ClpB/Hsp104, a member of AAA family, is an ATPase that disaggregates aggregated proteins with the help of Hsp70/DnaK system. Energy released from the ATP hydrolysis is used to fuel conformational changes that result in disaggregation of aggregates. The main aim of this work is to study the relationship between the nucleotide hydrolysis-mediated conformational changes and the resulting disaggregation activity by ClpB/Hsp104 proteins. Nucleotide binding and hydrolysis is an essential prerequisite which determines the rate and mechanism of ClpB/Hsp104 action, oligomeric state, complex formation with interacting partners and substrates. The detailed mechanism with which nucleotide binding and hydrolysis-mediated disaggregation reactions occurs still remains unclear. Several questions regarding the sequence of action of components of the bi-chaperone network and the mode of interaction with nucleotides and substrates is not well understood.

Studying nucleotide binding and hydrolysis mediated conformational changes in a hexameric protein like $ClpB_{Tth,}$ is intricate due to the occurrence of two AAA modules per subunit. It is often, if not always, difficult to study the contribution of each domain in a milieu and decode the complex interaction pattern. Although both AAA modules of $ClpB_{Tth}$ share the same consensus motifs and similar nucleotide binding fold, they exhibit different nucleotide binding properties (Schlee et al., 2001). Both the AAA modules of WT full-length $ClpB_{Tth}$ bind and hydrolyze ATP, which is necessary for oligomerization. Upon isolation, only AAA2 module shows oligomer formation and ATPase activity, which makes it an excellent candidate to investigate oligomeric properties of $ClpB_{Tth}$ in detail. It is also known that the C-terminal α-helical small domain (SD2) plays an important role in oligomerization in ClpB/Hsp104 proteins, but the exact mechanism through which this happens, remains unclear (Mogk et al., 2003, MacKay et al., 2008). Nucleotide binding measurements were performed to understand the mechanism with which nucleotide binding, hydrolysis and release cycles are influenced by SD2. Questions regarding the influence of nucleotides on the oligomeric state of $ClpB_{Tth}$, which is mediated by SD2, were

dealt with in this study. Conformational changes occurring in SD2 upon nucleotide binding at the nucleotide binding domains of $ClpB_{Tth}$ have been studied. The importance of the presence and flexibility of the SD2 motion was analyzed. To achieve this, experiments were performed using fluorescently labeled single-cysteine mutants of isolated AAA modules. Experiments were also performed to study complex formation between isolated AAA modules.

Allostery in ATP hydrolysis (Both homotypic and heterotypic) is essential for chaperone activity in $ClpB_{Tth}$, $ClpB_{E.coli}$ and $Hsp104_{Yeast}$ (Schirmer et al., 2000; Barnett et al., 2000; Schlee et al., 2001; Watanabe et al., 2001; Hattendorf and Lindquist 2002). However, most of the studies to understand the significance ATP hydrolysis of each AAA module, involve some perturbation to the active site of the protein or to its overall architecture. The second part of this work deals with understanding the nature of allosteric communication in $ClpB_{Tth}$. $ClpB_{Tth}$ mutants featuring single amino acid substitution at the interface between the AAA modules were studied. Effect of each interface mutation on the oligomeric nature, nucleotide binding and hydrolysis and chaperone activity was studied.

2. MATERIALS AND METHODS

2.1. Materials

2.1.1 Chemicals

Nucleotides: ATP, ADP, Mant-ADP (Sigma)

Fluorescence dyes: Alexa 488, Alexa 532 (Molecular Probes, Amersham GE Healthcare)

Chromatography materials and columns: Immobilized metal ion affinity chromatography: Ni NTA Super Flow (Qiagen); Gel permeation chromatography: S 200, S-75 Gel Permeation pre-packed Columns (Amersham)

ODS-Hypersil Reverse Phase C-18 (4.6 mm ∅ x 250 mm H, Bischoff, Leonberg)

2.1.2 Enzymes and Standard proteins

Restriction enzymes (New England Biolabs and Promega);

DNase I (Sigma)

T4 DNA Ligase (Promega)

Thrombin (Sigma)

Hog muscle Lactate dehydrogenase (Roche)

Rabbit muscle Pyruvate kinase (Roche)

Standard protein markers for SDS PAGE (Sigma)

BSA (Sigma)

2.1.3 Reagent and standard mixture kits

Plasmid mini purification kit (Promega)

PCR/ Gel Extraction kit for DNA (Promega)

Expand high fidelity PCR kit (Roche)

1 kb ladder marker for Agarose gel electrophoresis (Roche)

Low molecular weight protein marker for SDS PAGE (Roche)

EDTA free Protease inhibitor cocktail (Roche);

2.1.4 Bacterial strains

BL 21(DE3): E. coli B F–dcm ompT hsdS (rB –mB–) gal (Studier et. al., 1986)

Rosetta 2: Δ (ara–leu) 7697 ΔlacX74 ΔphoA PvuII phoR araD139 ahpC galE galK rpsL (DE3) F'[lac+ lacI q pro] gor522::Tn10 trxB pRARE2 (CamR, KanR, StrR, TetR);
XL 1 Blue: recA1, endA1, gyrA96, thi-1, hsdR17, supE44, relA1, lac, [F', proAB $lacI^qZ\Delta M15$, $Tn10\ (Tet^r)$] (Bullock et. al., 1986)

2.1.5 Media

Luria Bertini medium:10g/ L Bacto tryptone, 5g/ L yeast extract, 10g/ L NaCl;
Luria Bertini agar:10g/ L Bacto tryptone, 5g/ L yeast extract, 10g/ L NaCl, 15 g/L Bacto agar

2.1.6 Vectors

pET 27b (mod) (Novagen)

pET 27b (mod) is a modified version of pET 27b vector where the sequence following the EcoRI site till the end of HSV-tag is deleted. It comprises of a C-terminal hepta-histidine tag which is encoded right after the gene of interest. Stop codons are introduced right after the sequence for hepta-histidine tag. Expression is inducible with IPTG through *lac*-operator. Full-length WT and Mutant (All Interface mutants and ClpB-L757P) $ClpB_{Tth}$ proteins were cloned into this vector using NdeI and EcoRI restriction enzyme sites.

$ClpB_{Tth}$ WT, ClpB-I529A, ClpB-V521A, ClpB-E545Q, ClpB-E528Q, ClpB-E523Q, ClpB-R355A, ClpB-S357A, ClpB-Y371F, ClpB-L757P.

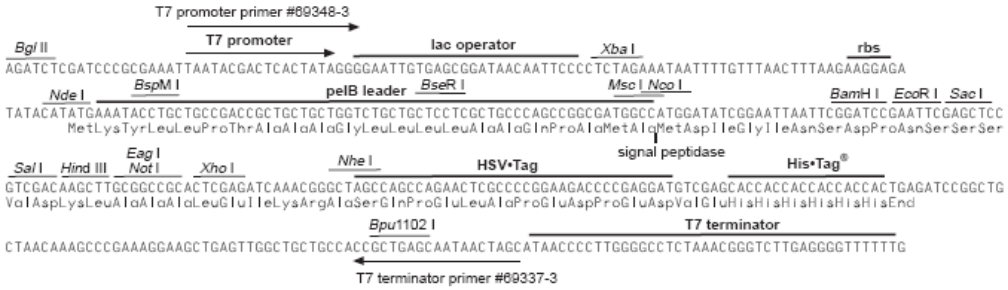

pET-27b(+) cloning/expression region

pET 28a (Novagen)

pET 28a vectors were used for recombinant cloning of various isolated modules of $ClpB_{Tth}$ were cloned using NdeI and EcoRI restriction sites. Stop codons are present right after the restriction site. Protein expression is inducible with IPTG through *lac*-operator. Proteins were expressed with a thrombin cleavable N-terminal hexa-histidine tag.

ClpB141-519-A434C: AAA1-A434C; ClpB519-854-R781C:AAA2-R781C; ClpB520-758: AAA2ΔSD2; ClpB520-854-I529A:AAA2-I529A.

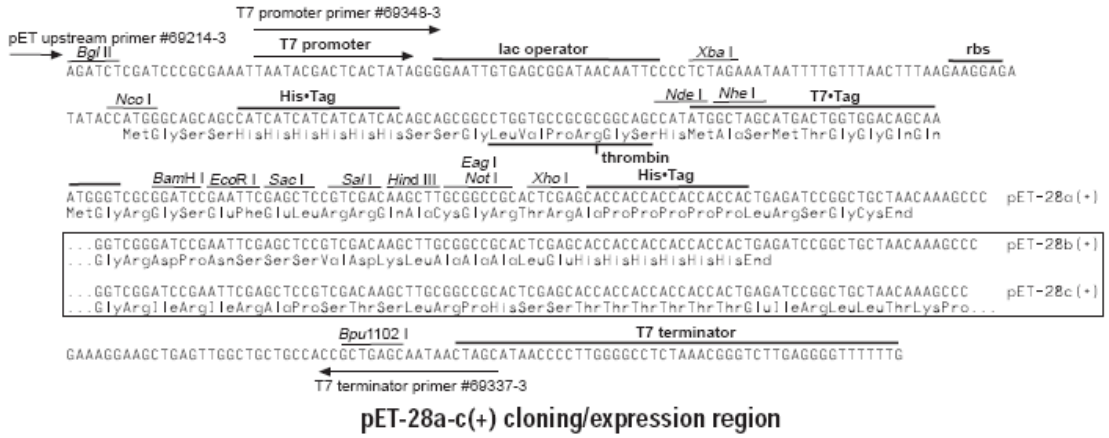

pET-28a-c(+) cloning/expression region

2.1.7 Oligonucleotides

All the oligonucleotides used for introducing mutation and variation in $ClpB_{Tth}$ are listed in table 2.1.

Mutation	Primer Sense/ Primer Anti-sense
A434C	CAA GTG CAT TGA GGC CGA GAT CGC C
	CAA TGC ACT TGA GGC GCT CCT GGG AG
R781C	GCC CGC CTC GCC GAG AAG TGC ATC TCC CTG GAG CTC ACC
	GGT GAG CTC CAG GGC GAT GCA CTT CTC GGC GAG GCG GGC CCG
I529A	GAG GTC ACC GAG GAG GAC GCC GCC GAG ATC GTC TCC CGC
	GCG GGA GAC GAT CTC GGC GGC GTC CTC CTC GGT GAC
V521A	GCC CGC TTC GTC CGC CTC GAG GCC ACC GAG GAG GAC ATC GCC GAG
	CTC GGC GAT GTC CTC CTC GGT GGC CTC GAG GCG GAC GAA GCG GGC
E528Q	GTC CGC CTC GAG GTC ACC CAG GAG GAC ATC GCC GAG ATC
	GAT CTC GGC GAT GTC CTC CTG GGT GAC CTC GAG GCG GAC
E523Q	GTC CGC CTC GAG GTC ACC GCG GAG GAC ATC GCC GAG ATC
	GAT CTC GGC GAT GTC CTC CGC GGT GAC CTC GAG GCG GAC
R355A	GAG GTC CAC CAC GGG GTG GCC ATC TCC GAC AGC GCC ATC
	GAT GGC GCT GTC GGA GAT GGC CAC CCC GTG GTG CAG CTC
S357A	CAC CAC GGG GTG CGC ATC GCC GAC AGC GCC ATC ATC GCC
	GGC GAT GAT GGC GCT GTC GGC GAT GCG CAC CCC GTG GTG
Y371F	GCC GCC ACC CTC TCC CAC CGG GCC ATC ACG GAA AGG CGC CTT CCC
	GGG AAG GCG CCT TTC CGT GAT GGC CCG GTG GGA GAG GGT GGC GGC
L757P	ATC GTG GTC TTC CGG CCC CCC ACC AAG GAG CAG ATC CGC
	GCG GAT CTG CTC CTT GGT GGG GGG CCG GAA GAC CAC GAT
ClpB 519-758	GCG GAT GAA TTC ATT GGT GAG GGG CCG

Table 2.1: Oligonucleotides

2.2 Cloning and DNA based methods

2.2.1 DNA concentration estimation

Quantification of DNA was performed by making use of the absorption of DNA at 260 nm following Beer-Lambert's law. Spectrophotometric measurements were performed using 1 µL of undiluted sample solution (NanoDrop ND-1000, NanoDrop Technologies). Quality of isolated DNA was estimated using the ratio between absorbance at 280 nm to 260 nm; which, for a pure preparation lies in the range of 1.8-2.0 (Glasel et al., 1995).

2.2.2 Agarose gel electrophoresis

Agarose gel electrophoresis was used to examine the quality and size of plasmids and DNA fragments. DNA sample preparation is done in loading buffer containing Glycerol, Bromophenol blue and Xylene cyanol for application on Agarose gels. When applied on a 1% Agarose gel under low electric current, in standard running buffer, negatively charged DNA molecules based on their length and secondary structure move towards the anode. Migration of DNA during the run was observed by tracking Bromophenol dye (Studier et al., 1986). Visualization of DNA on 1% Agarose gel is facilitated by soaking the gel in ethidium bromide solution (Dilute solution of Ethidium bromide in water). Excess dye is washed by soaking the Agarose gel in water. Ethidium bromide, a fluorescent dye, intercalates between the base pairs of DNA, which helps in visualizing DNA under ultra violet light.

Running Buffer: 40 mM Tris-Acetate pH 7.5, 1x TAE and 0.5 mM EDTA

2.2.3 Site directed mutagenesis by Overlap extension method

Site directed mutagenesis in $ClpB_{Tth}$ gene was performed by PCR-based overlap extension method, using a thermo stabile High fidelity Expand Polymerase (Ho et. al., 1989). pET 27b (mod) plasmid carrying $ClpB_{Tth}$ gene was used as a template for interface mutants and ClpB-L757P whereas, pET28a plasmids carrying genes for isolated AAA modules were used to generate point mutations A434C (AAA1 module), R781C and I529A (AAA2 module) (See 2.1.6 for list of clones). Fragments with overlapping ends were prepared using complimentary oligonucleotides carrying the required mutation. Primers used for each specific mutation are listed (Table 3.1.2). Thus generated DNA fragments were fused in a further amplification step to

generate the whole gene carrying the required mutation. Temperature, time for each cycle and other parameters for amplification are listed below. One nanogram of template was used in buffer containing 50 mM Tris HCl pH 7.5, 100 mM KCl, 5 mM MgCl2 and 2 mM EDTA along with 10 pmols of each primer. 5 Units of polymerase is used with the following temperature cycling: 1'- 95˚C, 25 times (1'- 95˚C, 2'- 55˚C, 1'-72˚C), 10'-72˚C. Annealing temperature was calculated based on the nucleotide base content as 2*(AT) +4*(GC)

2.2.4 Restriction digestion

The newly amplified DNA (insert DNA) and the vector were separately digested using specific restriction enzymes to generate compatible terminal sequence with 5' phosphate residues and 3' hydroxyl moieties. $ClpB_{Tth}$ mutants and variants in pET27b (mod) and pET28a vectors are prepared using NdeI and EcoRI sites at 5' and 3' ends respectively. Both vector and insert DNA were digested with NdeI and EcoRI in compatible buffer for 4 hrs at 37˚C. 5-10 U of either enzyme was used per one microgram of DNA.

2.2.5 Purification of DNA fragments

DNA extraction from 1% Agarose gel was performed using PROMEGA PCR/ DNA purification kit following manufacturer's protocol (PCR/ Gel Extraction kit for DNA (Promega)). Both vector and insert DNA following restriction digestion was extracted, after separation on a quantitative 1% Agarose gel. Agarose gel pieces containing insert and vector DNA both were then dissolved in binding buffer at 65˚C for 15-20' and then adsorbed on to glass beads and washed with washing buffer to remove salts, free nucleotides and protein content. DNA was eluted in nuclease free water (Browlee et al., 1969; Carter et al., 1993).

Binding Buffer: 10 mM Tris-HCl pH 6.6, 3M Guanidine thiocyanate, 5% ethanol (v/v)

Washing Buffer: 2 mM Tris-HCl pH 7.5, 20 mM NaCl, 5% ethanol (v/v)

2.2.6 Ligation

Vector and Insert DNA after purification from Agarose gel were diluted into a mixture containing T4 Ligase, 1x T4 Ligase buffer in a final volume of 20 µL was prepared. 1:3 molar ratio of vector to insert DNA was used and the reaction mixture was incubated at 16˚C overnight

(Bercovich et al., 1992; Michelsen et al., 1995). Ligated products are further purified as described in 3.2.4, exception being here DNA is directly mixed with binding buffer.

2.2.7 DNA Transformation

Ligated products following purification were used to transform XL1 Blue Ultra competent cells. 5ng of ligated product was added to a gently thawed competent cell preparation and incubated on ice for nearly 30'. Cells were then subjected to heat shock at 42˚C for nearly 11/2' and immediately transferred to ice. 1ml of SOB medium without any antibiotics was added and cells were grown for 1 hr at 37˚C followed by plating 100 µL of this cell suspension on a petri dish containing LB Agar medium with kanamycin (1g/L) (Cohen et al., 1972).

2.3 Protein preparation methods

2.3.1 Protein Expression

$ClpB_{Tth}$ wild type, mutants and are expressed and purified from BL21 (DE3) strain of E Coli cells whereas isolated AAA modules of $ClpB_{Tth}$ were expressed in Rosetta 2 strain.

BL21 (DE3): $ClpB_{Tth}$ WT, I529A, V521A, E545Q, E528Q, E23Q, H369A, R355A, S357A, Y371F, L757P.

Rosetta 2: AAA1 module, AAA2 module, AAA1-A434C, AAA2-R781C, AAA2ΔSD2, AAA2-I529A.

Antibiotic doses: BL 21(DE3): Kanamycin 25 µg/ mL; Rosetta 2: Kanamycin 25 µg/ mL and Chrolamphenicol 30 µg/ mL

A primary culture of cells was initially prepared by inoculation from a freshly streaked plate and overnight incubation at 37˚C. Overnight primary culture was then diluted 20 times to LB Agar medium containing required antibiotic. Cells were incubated at 37˚C to reach an optical density of 0.6 at 600 nm. Expression of recombinant protein was induced using 1 mM IPTG, and cells were incubated at 37˚C for 4 hrs. Centrifugation of cell cultures was done at 4000 rpm for 20 min at 4˚C. Cell pellets obtained from centrifugation were resuspended in 50 mM Tris-HCl pH 7.5 and subjected to another centrifugation step at 4˚C for 20 min at 4000 rpm. Protein expression at various time intervals was monitored by drawing samples and analysis using 15% SDS PAGE.

2.3.2 Protein Purification

Purification for $ClpB_{Tth}$ proteins was done by making use of histidine tag either at the N or C termini of the protein. Proteins with C-terminal non-cleavable histidine tag and N-terminal thrombin cleavable histidine tag were purified essentially with the same steps; only exception being, the thrombin cleavage of the histidine tags in case of the proteins with the N-terminal cleavable histidine tag.

2.3.2.1 Cell lysate preparation

Cell pellets with over expressed protein were thawed and/or dissolved in buffer A and homogenized manually. EDTA-free protease inhibitor cocktail was included in this mixture to

prevent unwanted proteolysis during cell lysis. Thoroughly homogenized cell suspension was subjected to lysis in a micro fluidizer (Microfluidics Corp, USA) by applying a pressure of 600 kPa. Fluidized cell suspension was then centrifuged at 35000 rpm, for 45 min at 4˚C (Beckmann L8-70M ultra centrifuge Ti45 Rotor) to extract the protein in the soluble fraction. Presence of the protein of interest in the supernatant after centrifugation was confirmed by 15% SDS-PAG electrophoresis.

2.3.2.2 Immobilized metal ion affinity Chromatography

Thoroughly filtered (5 μM filters) cell lysate containing histidine tagged protein was then applied on to a immobilized metal ion affinity chromatographic (Ni-NTA) column pre-equilibrated with buffer A (Qiagen 22 mL in 12 x 2 cm sized Glass Column with fitted temperature regulated jacket) (Merck Biosciences). Cell lysate application was followed by extensive washing with buffer B to remove non-specific binding of unwanted proteins to column material. Bound histidine tagged $ClpB_{Tth}$ proteins were then eluted with a gradient of imidazole in buffer B to buffer C over 80 Min. Samples which were drawn at various steps of the purification were analyzed using 15% SDS PAG electrophoresis. Peak fractions which represented highest purity were pooled for further purification.

Buffer A: 50 mM Tris-HCl pH 7.5, 300 mM KCl and 10 mM Imidazole

Buffer B: 50 mM Tris-HCl pH 7.5, 300 mM KCl and 20 mM Imidazole

Buffer C: 50 mM Tris-HCl pH 7.5, 300 mM KCl and 500 mM Imidazole

2.3.2.3 Thrombin cleavage of histidine Tag

Protein pool obtained from immobilized metal ion affinity chromatography column was then subjected to cleavage of histidine tag using thrombin protease for proteins carrying N-terminal cleavable histidine tag. Protein pool was incubated with thrombin at 37 ˚C for 2 hrs. Histidine tag cleavage is monitored by drawing 10 μL aliquots at regular intervals and comparing them to non-cleaved protein on 15% SDS-PAG electrophoresis. To remove the cleaved histidine tag, protein pool was dialyzed in buffer A and was again applied to a Ni NTA Affinity column. Pure protein was then collected in the flow through and the bound his tag was washed from the column by eluting with buffer C containing high concentration of Imidazole.

Buffer A: 50 mM Tris-HCl pH 7.5, 300 mM KCl and 10 mM Imidazole

Buffer C: 50 mM Tris-HCl pH 7.5, 300 mM KCl and 500 mM Imidazole

2.3.2.4 AmSO4 precipitation

N-terminal histidine tagged proteins after thrombin cleavage and C-terminal histidine tagged proteins directly after immobilized metal ion chromatography step were subjected to ammonium sulfate precipitation. Ammonium sulfate was added to protein solution in steps to a final concentration of 40% (W/V) and then centrifuged at 35000 rpm for 45 min at 4˚C. The protein pellet obtained after centrifugation was resuspended in buffer D. Integrity of protein in preparation was assessed using 15% SDS-PAG electrophoresis by obtaining samples before and after precipitation.

Buffer D: 50 mM Tris-HCl pH 7.5 and 25 mM KCl.

2.3.2.5 Gel Filtration Chromatography

Resuspended pellet containing $ClpB_{Tth}$ protein was then applied to a Gel Filtration chromatography column pre-equilibrated with buffer D (Amersham Biosciences; Superose 200 for full-length $ClpB_{Tth}$ proteins and Superose 75 for Isolated AAA modules). Samples were applied in a volume of 4-6 mL at a flow rate of 2 mL/min. Entire elution was collected in fractions of 6 ml each. Fractions representing the peak area of the chromatogram were analyzed for purity and integrity on a 15% SDS PAG electrophoresis and the peak fractions with highest amount of purity were pooled.

Buffer D: 50 mM Tris HCl pH 7.5 and 25 mM KCl

2.3.2.6 Ion Exchange Chromatography

For the isolated WT AAA1 module and single-cysteine mutant of AAA1 module, instead of gel filtration, ion exchange chromatography was used for second purification step. Resuspended pellet after ammonium sulfate precipitation was applied on to buffer E pre equilibrated Resource Q Ion exchange column. Samples were applied in a volume of 4-6 mL at a flow rate of 2 mL/Min. Non-specific binding was eliminated by washing the column with buffer E mixed with 10, 20 and 50 mM NaCl in steps. To elute bound protein a step elution was performed using a gradient between Buffer E and 500 mM NaCl. Samples were drawn at various time intervals and

analyzed using 15% SDS-PAG electrophoresis. Fractions containing highest amount of pure protein were then pooled.

Buffer E: Tris-HCl pH 8.0

2.3.2.7 Protein concentration by ultra filtration

Proteins pools after gel filtration or ion exchange chromatography steps were concentrated using centrifugal concentrators (Amicon). Protein pools were concentrated by centrifuging the protein solution at 3000 rpm/ 4˚C (Cut off filters of 30 kDa for full-length $ClpB_{Tth}$ and 10 kDa for isolated AAA modules). After concentrating the protein to required molarity (protein concentration estimation in section 3.4.1), protein solutions were alliquoted and freezed in Liq.N2 and stored at -80˚C.

2.3.3. SDS-PAG electrophoresis

For analysis of purity and integrity of proteins a discontinuous single dimensional poly-acrylamide gel electrophoresis under denaturing conditions was performed. This type of electrophoresis comprises of a stacking (5%) and following a separating gel (15%). Protein samples were prepared by dissolving in SDS-loading buffer and boiling the mixture at 95˚C for 5 min prior to loading. Gels were run at 40 mA for 45 min. Staining of the gels was done by boiling the gel in staining solution containing Coomassie blue for 2 min at 100˚C followed by removal of excess stain was done in destaining solution for 1 hr by repeated exchange for fresh buffer.

Stacking gel: 1.1 ml 40% poly-acrylamide, 7.1 ml water, 1.25 ml 1M Tris-HCl pH 6.8, 0.1 ml 10% SDS, 0.5 ml Ammonium per sulfate, 0.02 ml TEMED.

Separating gel: 3.8 ml water, 2.5 ml 1M Tris-HCl pH 6.8, 0.1 ml 10% SDS, 0.5 ml Ammonium per sulfate, 0.02 ml TEMED, 3.1 ml 40% poly-acrylamide .

SDS-Loading buffer: 130 mM Tris-HCl pH 6.8, 200 mM DTE, 4% SDS, 0.2% (W/V) Bromophenol blue, 40% (V/V) Glycerol;

Running buffer: 25 mM Tris, 192 mM Glycine, and 0.01% (W/V) SDS;

Staining solution: 25% (V/V) Isopropanol, 10% (V/V) Acetic acid, 0.1% (W/V) Coomassie blue R-250, and 0.01% (W/V) Coomassie blue G-250;

Destaining solution: 20% (V/V) Acetic acid, 10% (V/V) Ethanol

2.3.4. Nucleotide content analysis by reverse phase chromatography

All the purified wild type $ClpB_{Tth}$ and mutant proteins were analyzed for bound nucleotide content by reverse phase chromatography. 16 µL of approximately 10 mg/mL protein was incubated with 4 µL of 50% TCA on ice for 15 min. Upon incubation the mixture was centrifuged at 13K rpm for 10 min at 4°C and the supernatant was collected. 20 µL of 2 M KAc was added to 10 µL of supernatant and applied onto an ODS-Hypersil Reverse Phase C-18 (4.6 mm ∅ x 250 mm H) (Bischoff, Leonberg) column equilibrated with 50 mM Kpi, pH 6.5. The amount of intrinsic nucleotide was calculated by referring to standard chromatograms of ATP, ADP and AMP of 10 µM of each.

2.3.5. Covalent modification of proteins with fluorescent probes

Single-cysteine mutants of full-length $ClpB_{Tth}$ and isolated AAA modules proteins were labeled with fluorescent dyes. Alexa 488 and Alexa 532 dyes (Molecular probes, Amersham GE Health Care) were used by following manufacturers protocol with slight modification. A solution containing 10 times molar excess dye to protein (Approximately 2 mg protein was used) was prepared in labeling buffer and incubated at room temperature for 4-5 hrs with gentle mixing. Excess label is removed by extensive washing in a centrifugal concentrator (Amicon) to simultaneously concentrate the labeled protein using 10 kDa cut off filter. Concentrated labeled protein was then analyzed for labeling efficiency by measuring the protein and dye absorption spectra.

% of labeling is estimated by the following equation:

$$\mathbf{A}_{Dye} / \mathbf{E}_{Dye} \times \mathbf{MW}_{Protein} / \mathbf{Protein\ concentration}_{(mg/ml)} = \mathbf{Moles}_{Dye} / \mathbf{Moles}_{Protein} \quad \text{Eq. 1}$$

A_{Dye}: Absorbance of dye at its absorption maximum; $E_{Dye:}$ Molar Extinction coefficient for the dye molecule; $MW_{Protein}$: Molecular weight of the protein

Labeling Buffer: 25 mM Tris HCl pH 7.5 and 25 mM KCl

2.4. Spectroscopic methods

2.4.1. Protein concentration measurement: Absorption spectroscopy

Protein concentration estimations were performed making use of the Ehresman method (Laemmle 1970). Absorption of $ClpB_{Tth}$ proteins at 232 and 228 nm was measured and the concentration was estimated using the following equation:

$$\mathbf{C_{Protein} = (A_{222} - A_{234} / 3.154)} \qquad \text{Eq. 2}$$

C: Concentration of the protein; A_{222} : Absorbance at 222 nm; A_{234} : Absorbance at 234 nm

Protein concentration was also estimated using Bradford assay (Bradford 1976). Upon binding to the arginine or any aromatic amino acid residues in a protein, coomassie brilliant blue dye undergoes a shift in its absorption properties. The protein bound anionic form absorbs at 595 nm which was used to estimate protein concentration.

2.4.2. Coupled colorimetric assay for measuring steady state ATP Hydrolysis

ATP hydrolysis by WT $ClpB_{Tth}$ and its variants and mutants was measured under steady state conditions in a coupled colorimetric assay using an ATP regeneration system (Schlee et al., 2001 and Beinker et al., 2005). ATP hydrolysis of 10 µM WT or mutant $ClpB_{Tth}$ was measured at 25°C in a standard ATPase buffer with varying ATP concentration from 0.02 – 2 mM. In case of reconstituted complex of isolated AAA modules an equimolar mixture of participating proteins was prepared. Reaction mixtures with all the buffer components, enzymes and $ClpB_{Tth}$ protein with varying amounts of ATP were prepared in a micro titer plate (Corning flat bottomed 4695 transparent plates) and adjusted to a final volume of 75 µL with water. The reactions were initiated by dispensing 75 µL of 10 mM $MgCl_2$ and followed for 10 min by taking a measurement every 6 seconds in a micro titer plate reader (Varioskan; Thermo Electron Corporation).

Standard ATPase buffer: 50 mM Tris-HCl pH 7.5, 200 mM KCl, 2 mM DTE, 2 mM EDTA, 0.4 mM NADH, 0.4 mM PEP, 0.1 mg/ml BSA, 0.02 mg/ml LDH (Hog Muscle, Roche), and 0.05 mg/ml PK (Rabbit Muscle, Roche),

Reaction rates were calculated from the slope of the observed reaction using the following equation.

$K = \Delta A / (E_{NADH} . C . d)$ Eq. 3

K: Observed rate per minute; ΔA: Change of absorption per minute; E_{NADH}: Molar extinction coefficient of NADH; C: Molar concentration of protein; d: Path in cm (0.36)

Observed rate at each ATP concentration measured were plotted against Mg*ATP concentration. Data was analyzed using GRAFIT (Version 5.0.1.0 Erithacus Software Limited.) with the Hill equation which phenomenologically describes cooperativity in ATP hydrolysis.

$$k = \frac{k_{cat} \cdot [S]^n}{Km^n + [S]^n}$$ Eq. 4

k: Rate of hydrolysis at given ATP concentration; k_{cat}: Turnover number; K_m: Concentration of substrate required to attain half maximal rate; S: Substrate concentration; n: Hill coefficient

2.4.3. Refolding Assays using heat denatured substrate proteins

Efficiency of mutant $ClpB_{Tth}$ proteins compared to the wild type in refolding heat denatured proteins in cooperation with the $DnaK_{Tth}$ system ($DnaK_{Tth}$, $DnaJ_{Tth}$, and $GrpE_{Tth}$) was estimated using *Bacillus stearothermophilus* α-Glucosidase (Sigma) and Lactate dehydrogenase (Purified by Philipp Beinker) were used as model substrates (Ken et al., 1999, Beinker et al., 2002 and Beinker et al., 2005)

2.4.3.1 α-Glucosidase Assay

Thermal denaturation of α-Glucosidase (0.2 µM) was performed at 75°C for 8 min in denaturation buffer. Activity native α-Glucosidase directly after dilution into denaturation buffer was measured and referred to as native activity. Denatured α-Glucosidase was incubated with WT $ClpB_{Tth}$ or mutant (1.0 µM) along with the $DnaK_{Tth}$ system (1.6 µM $DnaK_{Tth}$, 0.4 µM $DnaJ_{Tth}$ and 0.4 µM $GrpE_{Tth}$) at 55°C for 2 hours. In case of reconstituted complex of isolated AAA modules an equimolar mixture of participating proteins was prepared. Control mixtures containing denatured α-Glucosidase incubated with none or only one of the chaperone proteins were also included. Samples were drawn at regular time intervals (10, 30, 60, 90, 120, and 180 min) and diluted 10 fold into assay buffer. 200 µL of this mixture was monitored for increase in

the absorbance at 405 nm for 10 min in a 96-well micro titer plate (Corning flat bottom plate 4695) with a Micro titer plate reader (Varioskan with data acquisition Software Sknalt (version 2.0.); Thermo Electron Corporation). Catalysis the cleavage of the glycosidic bond in *para*-nitro phenyl α-*d* gluco pyranoside by α-Glucosidase was monitored by an increase in absorbance at 405 nm of released *para*-nitro phenol. Heat denatured α-Glucosidase upon refolding by $ClpB_{Tth}$ and $DnaK_{Tth}$ system resumes its enzymatic activity which is a direct measure of the refolding ability of chaperone proteins. Calculated slope for each control as well as experimental mixtures were then plotted at all the time points measured to asses the % of refolding.

Denaturation buffer: 50 mM MOPS-NaOH pH 7.5, 150 mM KCL, 10 mM MgCl2, 5 mM ATP, and 2 mM DTE;

Assay Buffer: 50 mM Kpi pH 6.8, 2 mM *para*-nitro phenyl α-*d* Glucopyranoside and 0.1 mg/ml BSA

2.4.3.2 Lactate dehydrogenase Assay

Thermal denaturation of 0.1 µM LDH was performed at 80°C for 30 min in denaturation buffer Activity of LDH directly after dilution into denaturation buffer was measured and referred to as native activity. Denatured LDH was incubated with wild type or mutant $ClpB_{Tth}$ (1.0 µM) along with the $DnaK_{Tth}$ system (1.6 µM $DnaK_{Tth}$, 0.4 µM $DnaJ_{Tth}$ and 0.4 µM $GrpE_{Tth}$) at 55°C for 2 hours. In case of reconstituted complex of isolated AAA modules an equimolar mixture of participating proteins was prepared. Control mixtures containing denatured LDH incubated with none or only one of the chaperone proteins were also included. Samples were drawn at regular time intervals (10, 30, 60, 90, 120, and 180 min) and diluted 10 fold into 2X assay buffer for a final volume of 110 µL. Reaction for refolded LDH was initiated by dispensing 90 µL of 2X solution of Pyruvate (20 mM). 200 µL of this mixture was monitored for decrease in the absorbance at 340 nm for 10 min in a 96-well micro titer plate (Corning flat bottom plate 4695) with a Micro titer plate reader (Varioskan with data acquisition Software Sknalt (version 2.0.); Thermo Electron Corporation). Lactate dehydrogenase (LDH) from *Bacillus stearothermophilus* converts pyruvate to lactate by oxidation of NADH to NAD+ which can be monitored by a decrease in the absorbance at 340 nm. Heat denatured LDH upon refolding by $ClpB_{Tth}$ and $DnaK_{Tth}$ system resumes its enzymatic activity which is a direct measure of the refolding ability of chaperone proteins. Slope for each control as well as experimental mixtures were then plotted

at all the time points measured. Fractional refolding is reported upon comparison with native of activity of the substrate protein.

Denaturation buffer: 50 mM MOPS-NaOH pH 7.5, 150 mM KCL, 10 mM MgCl2, 5 mM ATP, and 2 mM DTE;

Assay Buffer: 50 mM Bis-Tris 6.5, 100 mM KCl and 0.5 mg/ml BSA

2.4.4. Fluorescence Spectroscopy

Fluorescence spectroscopy measurements were performed using Fluormax-III spectrofluorimeter (Jobin yvon, Edison, NJ USA) in 1 ml quartz cuvettes at 25ºC in buffer containing 50 mM Tris-HCl pH 7.5, 50 mM KCl and 5 mM MgCl2. Emission scans for labeled proteins (AAA1-A434C*$^{\text{Alexa 488}}$ and AAA2-R781C*$^{\text{Alexa 532}}$) was performed by measuring at the fluorophore's maximum absorption wavelength. For experiments using A434C*$^{\text{Alexa 488}}$ excitation and emission wavelengths of 488 and 532 nm were used. For experiments with AAA2-R781C*$^{\text{Alexa 532}}$ excitation and emission wavelengths of 528 and 555 nm were used. A slit width of 1nm/ 1nm, integration time of 0.2 sec and a scan rate of 0.5 sec were used for all the experiments performed.

Experiments where binding of AAA2-K601Q protein to AAA2-R781C*$^{\text{Alexa 532}}$ was studied, fluorescence emission amplitude of AAA2-R781C*$^{\text{Alexa 532}}$ after correction for volume changes was plotted against concentration of AAA2-K601Q for each titration. K_D value was calculated by fitting the titration data to the quadratic equation using GRAFIT software (version 5.0.6, Erithacus Software Ltd., Staines, UK).

$$\mathbf{F = Fo + (Fmax - Fo) * (((((Vo + Co + K_D) / 2)) - sqrt(sqr((Vo + Co + K_D / 2) - Vo * Co)) / Co)} \quad \text{Eq.5}$$

F: Fluorescence emission after volume correction at a given protein concentration; *Fo:* Fluorescence of the free Fluorophore; *Fmax:* Fluorescence emission at saturated substrate concentration; *Vo:* Total protein concentration in µM; *Co:* Total ligand concentration in µM; K_D*:* Dissociation constant of complex in µM

Experiments where binding of ADP to AAA2-R781C*$^{\text{Alexa 532}}$ or AAA2-R781C*$^{\text{Alexa 532}}$+ AAA2-K601Q complex was studied, fluorescence emission amplitude of AAA2-R781C*$^{\text{Alexa 532}}$ after correction for volume changes was plotted against concentration of ADP for each titration. Data

were then fit into a biphasic binding model by assuming two binding sites with different affinities using scientist software (Micromath Version etc) to obtain K_D1 and K_D2. For more information regarding the model refer to appendix A.

Fluorescence resonance energy transfer measurements were performed for AAA1-A434C*$^{Alexa\ 488}$ (Donor) and AAA2-R781C*$^{Alexa\ 532}$ (Receptor) at both 25ºC and 45ºC. A wavelength of 450 nm was used for excitation of AAA1-A434C*$^{Alexa\ 488}$ (Donor). Donor emission, acceptor emission at donor excitation wavelengths was independently measured using 0.5 µM protein each. Emission spectrum for donor and acceptor complex was obtained by incubating 0.5 µM of each protein. Energy transfer was estimated by subtracting acceptor alone emission spectrum from donor and acceptor complex emission spectrum.

2.5. Thermodynamic Methods

2.5.1 Isothermal Titration Calorimetry

Binding of protein-protein and protein-ligand complexes were analyzed using isothermal titration calorimetry. Measurements were performed using MicroCal MCS isothermal titration calorimeter (MicroCal LLC, Northampton, MA) and data was analyzed using manufacturers software to obtain binding affinity, stoichiometry, enthalpy and entropy of binding. Proteins and ligand molecules were always incubated at 1°C less than the appropriate measurement temperature prior to beginning of the measurement in a temperature controlled jacket. After the completion of the binding reactions the contents of the reaction cell were always analyzed in a 15% SDS PAGE for the presence of the both the protein components in case of protein-protein complex analysis. Analysis of protein-protein complexes involved binding studies between AAA1 module and AAA2 module of $ClpB_{Tth}$ where measurements were performed at 25°C and 45°C in standard ITC buffer. AAA1 module (10 µM) was titrated to AAA2 module (90µM) in 10 µL each injection. 29 injections were performed with a spacing of 240 seconds at a rate of 0.5µL/ Second. Binding studies involving nucleotide binding to isolated AAA2 module and AAA2ΔSD2 of $ClpB_{Tth}$ were performed in a similar manner. Nucleotide (100 µM) titrated to AAA2 module or AAA2ΔSD2 (10 µM) 29 injections at 25°C in standard ITC buffer. 10 µL injections were performed with a spacing of 240 seconds each and with an injection speed of 0.5 µL/ Second.

Standard ITC buffer: 50 mM HEPES-NaOH pH 7.5, 100 mM KCl, 5 mM MgCl2.

2.6 Molar Mass estimation methods

Molar mass of various chaperone proteins including WT $ClpB_{Tth}$, Interface Mutants and Isolated AAA modules (Both WT and Mutants) was estimated using gel permeation chromatography (GPC) coupled with multi-angle light scattering measurements. Proteins samples were applied using an injection device (WATERS 717 plus Auto sampler) and further separated on a GPC column. The eluate from the GPC column was then monitored by the light scattering detector (DAWN HELEOS Wyatt Tech Corp.), refractive index increment (WATERS 2414 RI Detector) and absorption (WATERS 2996 Photodiode Array Detector) detectors. For detailed information regarding hardware, software, data acquisition and instrument calibration refer to appendix B.

Protein samples prior to injection were subjected to centrifugation for 5 minutes at 13k rpm/ 4˚C to remove aggregates whereas, buffers were pre-filtered using 0.2 µM filters. Sample quality was preserved by a set of inline filters (0.02 µM, Millipore) both before injection and after the GPC column. Typically 100-200 µg of protein was injected per each experiment however, for lower molecular weight proteins (≤ 30 kDa) masses up to 500 µg were injected. Experiments were performed at a flow rate of 0.4-0.5 ml/min. For proteins or protein-protein complexes ≤100 kDa a Superdex 75 HR 10/30 (25mL) GPC column (Amersham) was used. For proteins or protein-protein complexes ≥100 kDa a Superdex 200 HR 10/30 (25mL) GPC column (Amersham) was used. For analysis of proteins in buffers containing no nucleotides, protein absorbance at 280 nm was monitored. For analysis in buffers containing nucleotides, nucleotide absorbance at wavelengths where protein absorption spectrum does not overlap was used.

Absolute molecular weight distributions of proteins and protein-protein complexes were estimated using manufacturer's software and protocol (ASTRA Version 5.1.7.3; Wyatt Tech. Corp.). Distribution of various molar masses in the protein sample was calculated by analyzing the entire chromatogram and % of particular molar mass species in total protein is reported. Molar mass analysis of a given protein was estimated by initially estimating its concentration using refractive index increment signal. One or more peak regions of the chromatogram were selected and molar mass of the protein species present in those particular areas was calculated using Zimm fitting method. The light scattered by a macromolecule is proportional to its weight averaged molar mass and concentration, explained by Debye-Zimm equation which applies well

for macromolecules of dimensions ranging from λ/20 to λ (λ= 658 nm). The ratio of K*c/ R(θ) from the following equation when extrapolated to zero $Sin^2(\theta/2)$ yields 1/Molecular Weight from intercept and root mean square radius from slope of the fit (Zimm plot).

$$\frac{K.c}{R(\theta)} = \frac{1}{M.P(\theta)} + 2A_2c$$

Where $K = \frac{4\pi^2 n^2 (dn/dc)^2}{\lambda_0^4 N_A}$

c: Sample concentration; *n:* refractive index of the solvent; *dn/dc:* refractive index increment (A standard dn/dc value of 0.185 is used for all the proteins analyzed.); N_A*:* Avogadro's number; λ_0*:* Wavelength of the scattered light in vacuum; *R(θ):* Intensity of scattered light at angle θ; *M:* Weight averaged molar mass; $2A_2c$*:* Second viral coefficient (mL.mol/ g^2); *P(θ):* governs the angular dependence of scattered light.

Molar mass limits for oligomeric forms of ClpB WT, mutants and variants for distribution analysis was set as follows.

For ClpB WT and Interface mutants: 96.2 kDa

Molecular Mass (kDa)	Oligomer
80-150	Monomer
150-240	Dimer
240-330	Trimer
330-420	Tetramer
420-510	Pentamer
510-600	Hexamer

For ClpBΔN and Reconstituted complex of isolated AAA modules: 80.1 kDa

Molecular Mass (kDa)	Oligomer
60-130	Monomer
130-200	Dimer
200-290	Trimer
290-380	Tetramer
380-470	Pentamer

For Isolated AAA1 module and AAA1-A434C: 43.2 kDa

Molecular Mass (kDa)	Oligomer
30-50	Monomer
60-100	Dimer

For Isolated AAA2 module and AAA2-R781C: 38.3 kDa

Molecular Mass (kDa)	Oligomer
25-45	Monomer
45-90	Dimer

For Isolated AAA2ΔSD2: 28 kDa

Molecular Mass (kDa)	Oligomer
20-40	Monomer
40-60	Dimer

3. RESULTS

3.1 Studies on nucleotide binding to the isolated AAA modules of $ClpB_{Tth}$.

To understand the role of various domains of $ClpB_{Tth}$ in nucleotide-mediated oligomer formation and dissociation, experiments were conducted on the isolated AAA modules carrying single-cysteine substitutions. The isolated AAA1 module comprises of the nucleotide binding domain 1 (NBD1) and the α-helical small domain 1 (SD1) with its M domain insertion; whereas, the isolated AAA2 module consists of a section of SD1, the nucleotide binding domain 2 (NBD2) and the α-helical small domain 2 (SD2) (Fig 3.2A). The isolated AAA modules with single-cysteine substitutions were fluorescently labeled and monitored for conformational changes upon nucleotide binding. An emphasis was given to the role of the α-helical small domain 2 of the AAA2 module, in nucleotide-dependent oligomer formation and dissociation of $ClpB_{Tth}$.

3.1.1 Cysteine mutant engineering in the isolated AAA modules of $ClpB_{Tth}$.

3.1.1.1 Structural analysis of $ClpB_{Tth}$ for site directed mutagenesis.

Amino acids for mutagenesis were selected from the domains, which cover the perimeter of the upper and lower rings of $ClpB_{Tth}$ hexamer, and which exhibit pronounced mobility during ATP hydrolysis. Hexameric $ClpB_{Tth}$ forms a double barrel-like structure with a central cavity (Fig 3.1). AAA1 and AAA2 modules form the distinctive upper and lower rings of the double barrel. The cavity side of the two rings is lined by NBD1 and NBD2, of the AAA modules. Perimeter of the upper ring is formed by SD1 along with its M domain insertion and that of the lower ring by SD2 (Fig 3.1).

The M domain of $ClpB_{Tth}$, a unique feature of ClpB/Hsp104 proteins, is essential for chaperone activity (Cashikar et al., 2002; Mogk et al., 2003). Sulfhydryl cross linking in double-cysteine mutants of $ClpB_{Tth}$, which render the M domain immobile, result in impaired chaperone activity indicating the importance of its motion during the functional cycle (Lee et al., 2003). SD2 forms a tight interface with the neighboring AAA2 module, and its deletion is known to impair nucleotide hydrolysis, oligomer formation and chaperone activity (Barnett et al., 2000; Mogk et

al., 2003; Lee et al., 2003). Hence, amino acids were selected from these two domains for mutagenesis.

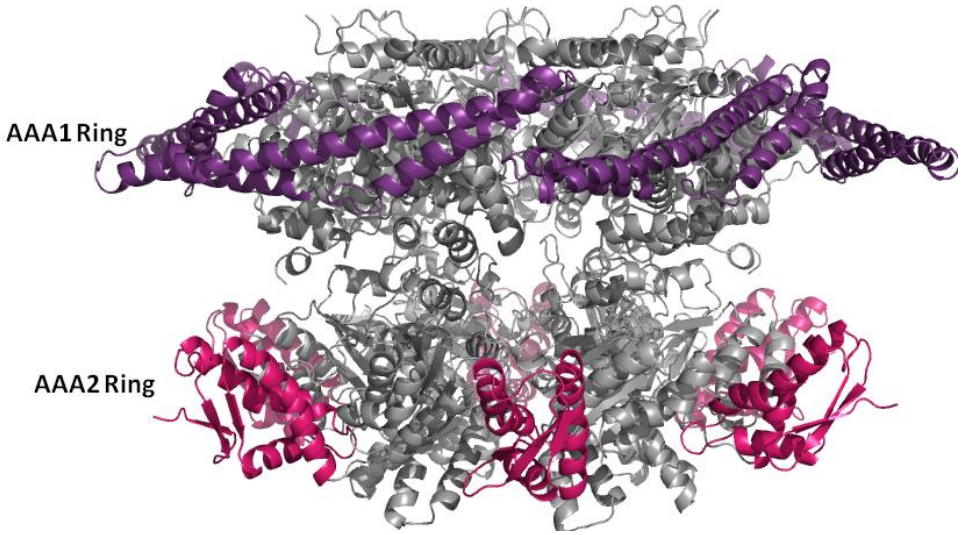

Fig 3.1: Structure of the ClpB$_{Tth}$ hexamer. Ribbon representation of the ClpB$_{Tth}$ hexamer, with M domain and SD2 from each subunit highlighted. The upper ring of the hexameric structure is formed by the AAA1 modules (NBD1, SD1 and the M domain) from each subunit; whereas, the lower ring is formed by AAA2 modules (NBD2 and SD2). The M domains in the AAA1 ring are shown in purple; whereas, the α-helical small domains from the AAA2 ring are shown in pink. Rest of the protein is shown in grey. The N-terminal domains are not shown in this representation. Structural information is obtained from Diemand and Lupas 2006 and rendered using Pymol software.

Aided by the published crystal structure of ClpB$_{Tth}$ (Lee et al., 2003), amino acids for site directed mutagenesis were selected in the isolated AAA modules. Of the AAA1 module, alanine 434 located at the tip of the long coiled-coil of the M domain (Helix 2 of Motif 1) was selected for mutagenesis (Fig 3.2B). Of the AAA2 module, arginine 781 was selected for mutagenesis. R781 is located on the loop connecting α-helix (E1) and β sheet (e1) of SD2, in the AAA2 module (Fig 3.2B). Both the amino acids showed no sequence conservation, when compared to ClpB$_{EColi}$ and Hsp104$_{Yeast}$.

A

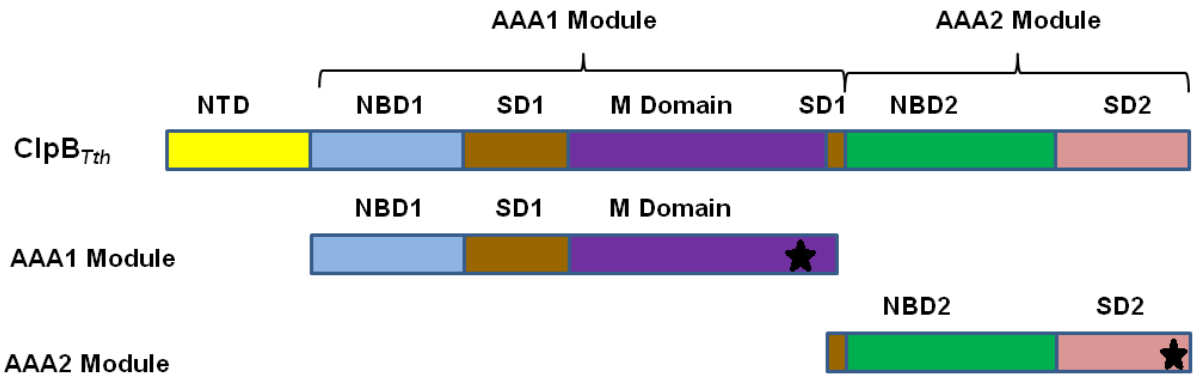

B

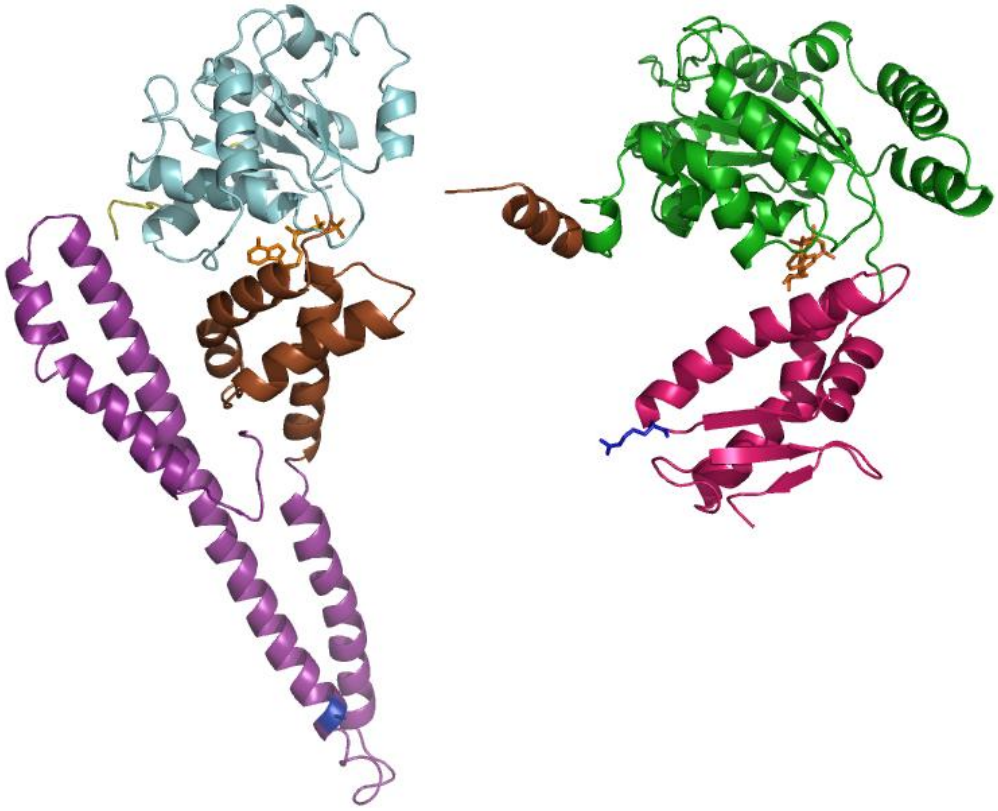

Fig 3.2: The isolated AAA modules of ClpB$_{Tth}$. (A) A schematic depicting domain organization of ClpB$_{Tth}$. The isolated AAA1 module (AA 141-519) features the nucleotide binding domain 1 (NBD1) and the α-helical small domain 1 (SD1). The isolated AAA2 module (AA 520-854) features the nucleotide binding domain 2, the α-helical small domain 2 (SD2) and a section of SD1 (AA 520-535).
NTD- Yellow (AA 1-152), NBD1- Blue (AA 153-331), SD1- Brown (AA 332-400 and 519-535), M domain- Violet (AA 401-518), NBD2- Green (AA 536-758) and SD2- Pink (759-854)
(B) A ribbon representation of the isolated AAA1 and AAA2 modules, with alanine 434 and arginine 781 highlighted in blue (stick representation) respectively. Bound AMP-PNP molecules are shown in orange (stick representation). Structural data were obtained from PDB entry 1QVR (Lee et al., 2003) and rendered using Pymol software.

3.1.1.2 Purification of AAA1-A434C and AAA2-R781C.

AAA1-A434C and AAA2-R781C mutants were purified using immobilized metal ion affinity chromatography. The AAA1-A434C mutant was further purified using ion exchange chromatography and the AAA2-R781C protein using gel permeation chromatography (Methods 2.3). Proteins were purified to 95% purity, as assessed by 10% poly-acrylamide gel electrophoresis. Intrinsic nucleotide content of the purified proteins was assessed using HPLC-based reverse phase chromatography (Methods 2.3.4). Upon comparison with chromatograms of standard nucleotides, both AAA1-A434C and AAA2-R781C proteins were found to be nucleotide-free (Data not shown).

Upon reconstitution, the isolated AAA modules of $ClpB_{Tth}$ exhibit chaperone activity (Beinker et al., 2005). This chaperone activity depends on the AAA modules' ability to bind and hydrolyze ATP, and form higher order oligomers. Deletion of the N-terminal domain has no effect on afore mentioned properties of $ClpB_{Tth}$ (Beinker et al., 2003); hence lack of it has no effect on the reconstituted complex of AAA modules (AAA1 module +AAA2 module= ClpBΔN). Therefore, the impact of introduced single-cysteine mutations on all the above mentioned properties in isolated AAA modules, of $ClpB_{Tth}$, was studied in the following experiments.

3.1.1.3 Oligomeric state analysis of AAA1-A434C and AAA2-R781C.

The isolated AAA modules of $ClpB_{Tth}$ were reported to show different oligomerization properties, when compared to each other and wild type $ClpB_{Tth}$ (Beinker et al., 2005). The isolated AAA1 module remains monomeric with varying ionic strength as well as in nucleotide presence or absence. However, oligomer formation was reported for the AAA2 module at a low-salt concentration, irrespective of the nucleotide present. Hence, the influence of cysteine mutations on the oligomeric state of isolated AAA modules, both individually and upon reconstitution, was studied. Experiments were performed using gel permeation chromatography coupled with multi-angle light scattering measurements (Methods 2.6). Data was analyzed using manufacturer's software (ASTRA Version 5.1.7.3, Wyatt Tech Corp).

For the isolated wild type AAA1 module, the peak portion of the chromatogram yielded a molar mass of 44 kDa, which corresponds to a monomeric molecular mass (Fig 3.3A and Table 3.1).

AAA1-A434C mutant yielded a molar mass of 42.3 kDa and showed an elution profile similar to its wild type counterpart (Fig 3.3A and Table 3.1). The peak portion of the chromatogram for the wild type AAA2 module yielded a molecular mass of 51 kDa; whereas, AAA2-R781C yielded 56 kDa (Fig 3.3B and Table 3.1). Both, the wild type AAA2 module and AAA2-R781C showed molecular weights indicative of a mixture of monomers and dimers.

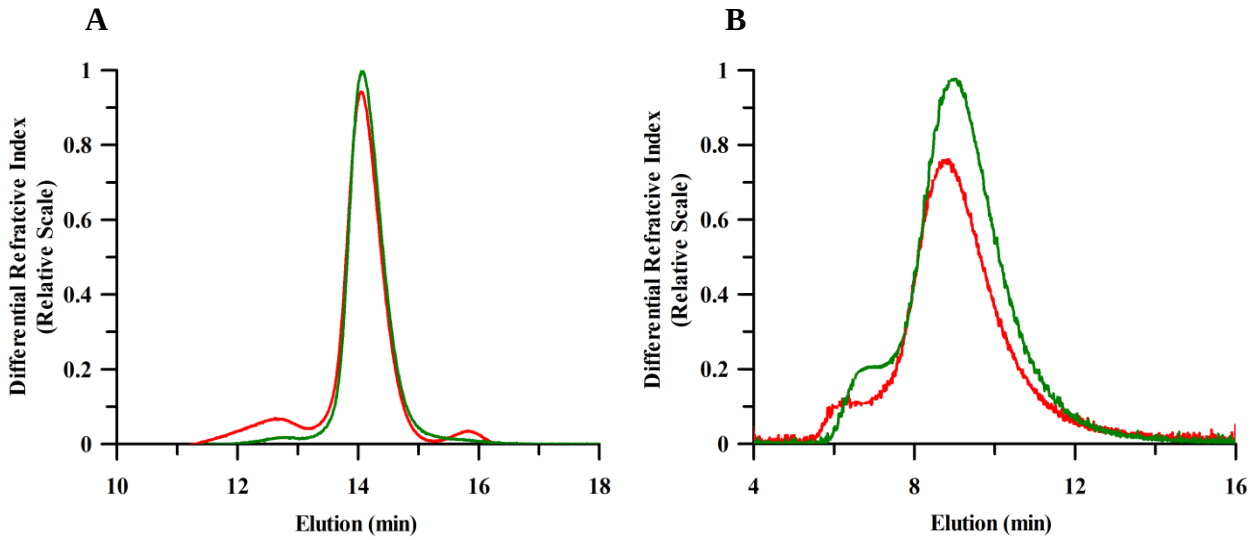

Fig 3.3: Oligomeric state of the isolated AAA modules of ClpB$_{Tth}$. Elution profile of **(A)** the isolated wild type AAA1 module (Red) and AAA1-A434C (Green) (**B)** the isolated wild type AAA2 module (Red) and AAA2-R781C (Green) in a buffer containing 50 mM Tris-HCl pH 7.5, 100 mM KCl and 5 mM MgCl2.

Reconstituted complex of equimolar amounts of the isolated wild type AAA modules (AAA1+AAA2), as well as the AAA modules carrying cysteine mutations (AAA1-A434C+AAA2-R781C), were studied under the same buffer conditions. Elution profile and molar masses obtained were compared to that of ClpBΔN. The peak portion of the ClpBΔN chromatogram corresponded to a molar mass of 279 kDa, which is closer to a theoretical trimer of the protein (Fig 3.4 and Table 3.1). Similarly, peak portions of the chromatograms for both the reconstituted complexes (wild type AAA modules and cysteine mutant AAA modules) yielded a molar mass of 254 and 284 kDa respectively (Fig 3.4 and Table 3.1). All the results obtained, were in agreement with previously published data (Beinker et al., 2005). These observations suggest that the introduction of single-cysteine mutations in the isolated AAA modules does not seem to have any effect on their oligomeric properties.

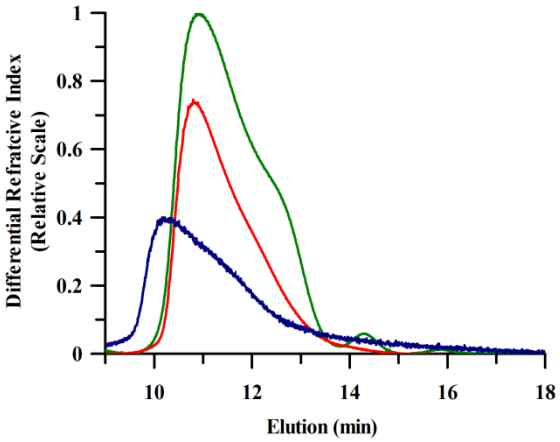

Fig 3.4: Oligomeric state of reconstituted complex of isolated AAA modules. Elution profile of reconstituted complex of the isolated wild type AAA modules (Red), the cysteine mutant AAA modules (AAA1-A434C+ AAA2-R781C) (Green) and ClpBΔN (Navy) in a buffer containing 50 mM Tris-HCl pH 7.5, 100 mM KCl and 5 mM MgCl2.

Protein	Theoretical Molar Mass (Monomer)	Predominant Molar Mass	Predominant Oligomeric species
AAA1 Module	43.2	44	Monomer
AAA1-A434C	43.2	42.3	Monomer
AAA2 Module	38.3	51	Monomer/ Dimer
AAA2-R781C	38.3	56	Monomer/ Dimer
ClpBΔN	81.5	279	Trimer
AAA1+ AAA2	81.5	254	Trimer
AAA1-A434C+ AAA2-R781C	81.5	284	Trimer

Table 3.1: Oligomeric state analysis for the isolated and reconstituted complexes of the AAA modules.

3.1.1.4 ATP hydrolysis properties of AAA1-A434C and AAA2-R781C.

The isolated AAA modules, upon reconstitution, form oligomers and hydrolyze ATP (Beinker et al., 2005). The isolated AAA1 module alone does not bind or hydrolyze ATP, whereas the isolated AAA2 module alone shows a higher rate of hydrolysis when compared to wild type $ClpB_{Tth}$ (Beinker et al., 2005). Therefore, the effect of cysteine mutations on ATPase activity of the isolated AAA modules was studied (Methods 2.4.2).

Isolated AAA1-A434C, like its wild type counterpart, showed no ATPase activity (Data not shown). On the other hand, AAA2-R781C exhibited sigmoidal behavior similar to that of the isolated wild type AAA2 module (Fig 3.5). Data analysis yielded a k_{cat} value of 7.9 ±0.4 min^{-1}, which is close to that reported for wild type AAA2 module (6.9 ±0.2 min^{-1}) (Beinker et al., 2005). Both the K_m value of 1.02 ±0.09 mM and the Hill coefficient of 1.87 ±0.3 are comparable to the values reported for the wild type isolated AAA2 module (Table 3.2). The undisturbed Hill coefficient value indicated that the introduction of R781C mutation did not affect homotypic allosteric interactions, present in the isolated AAA2 module oligomer.

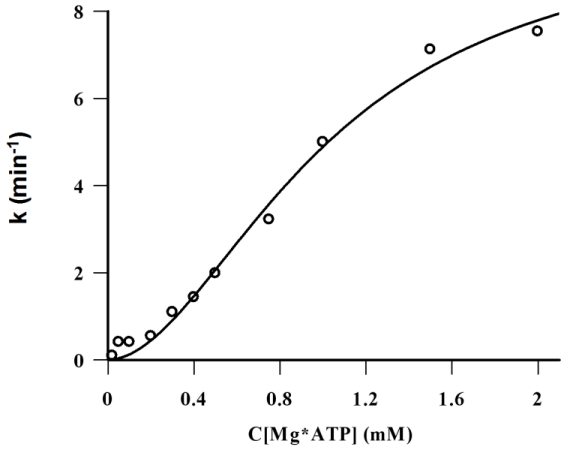

Fig 3.5: Steady-state ATPase activity. ATPase activity of 10 µM AAA2-R781C was measured at 25°C using an ATP regeneration system. The obtained rate constants were plotted against Mg*ATP concentration. The solid line represents data fitted with the Hill equation.

Protein	k_{cat} (min^{-1})	K_m (mM)	n
AAA2 module	6.9 ±0.2	0.76 ±0.04	2.08 ±0.21
AAA2-R781C	7.9 ±0.4	1.02 ±0.09	1.87 ±0.3

Table 3.2: ATPase activity of the isolated AAA2 module: The isolated wild type AAA2 module values shown here are as reported (Beinker et al., 2005).

3.1.1.5 Refolding denatured α-Glucosidase by AAA1-A434C and AAA2-R781C.

$ClpB_{Tth}$ refolds denatured substrate proteins with the help of $DnaK_{Tth}$ chaperone, and its co-chaperones $DnaJ_{Tth}$ and $GrpE_{Tth}$ (Parsell 1994; Glover et al., 1998; Motohashi et al., 1999). Upon reconstitution, the isolated AAA modules are active in refolding heat denatured α-Glucosidase from *Bacillus stearothermophilus* (Beinker et al., 2005). However, the isolated AAA modules 1 or 2 are not active in chaperone assays on their own. The effect of single-cysteine mutations on

the ability of the reconstituted complex of AAA modules to refold heat denatured α-Glucosidase was studied (Methods 2.4.3.1). An equimolar mixture of AAA1-A434C and AAA2-R781C was prepared and its ability to refold denatured α-Glucosidase was studied and compared to that of wild type AAA modules 1 and 2. Complex of AAA1-A434C and AAA2-R781C refolded heat denatured α-Glucosidase to 14% of its native activity, which is closer to 15% shown by its wild type counterpart (Fig 3.6) (Table 3.3).

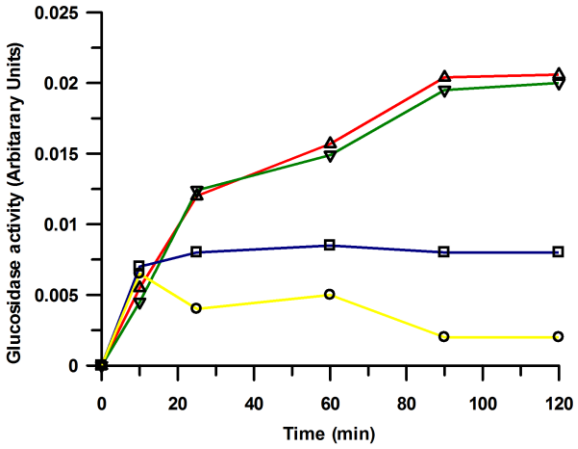

Fig 3.6: α-Glucosidase assay. Refolding of heat denatured α-Glucosidase by the reconstituted complex of AAA1-A434C and AAA2-R781C (Green) was compared with the reconstituted complex of wild type AAA1 and wild type AAA2 modules (Red). α-Glucosidase, upon denaturation at 75°C for 10 min, was subjected to refolding at 55°C for 120 min in the presence of 1.0 µM reconstituted complex, 1.6 µM $DnaK_{Tth}$, 0.4 µM $DnaJ_{Tth}$ and 0.4 µM $GrpE_{Tth}$. Activity of refolded α-Glucosidase at various time points during the refolding reaction was plotted against time (min). The blue and yellow lines represent activity of α-Glucosidase after refolding in the presence of $DnaK_{Tth}$ system alone and no chaperones respectively.

Protein	Fraction of refolded α-Glucosidase (%)
Wild type AAA1+ Wild type AAA2	15
AAA1-A434C + AAA2-R781C	14
$DnaK_{Tth}$ system alone	2-3

Table 3.3: Refolding yields of heat denatured α-Glucosidase by the AAA modules of $ClpB_{Tth}$. Catalysis of cleavage of the glycosidic bond in p-nitrophenyl-α-D-glucopyranoside by refolded α-Glucosidase was quantified and expressed as fraction of its native activity regained. Native activity refers to the activity of α-Glucosidase prior to heat denaturation.

Both, AAA1-A434C and AAA2-R781C alone showed little or almost no refolding activity as expected (Data not shown). Refolding by the $DnaK_{Tth}$ chaperone system alone resulted in very low yield (2-3%). Based on these observations, it was concluded that the introduction of single-

cysteine mutations did not affect the ability of the AAA modules to refold heat denatured substrate proteins, upon reconstitution.

3.1.1.6 Fluorescent labeling of AAA1-A434C and AAA2-R781C.

Fluorescently labeled isolated AAA modules were prepared by labeling AAA1-A434C with Alexa 488 (AAA1-A434C*$^{Alexa\ 488}$) and AAA2-R781C with Alexa 532 (AAA2-R781C*$^{Alexa\ 532}$) labels in separate batches (Methods 2.3.5). Labeled proteins after concentration were analyzed for their purity using 10% poly-acrylamide gel electrophoresis. Calculated labeling efficiencies for the labeled proteins ranged from 95% to 98% (Methods 2.3.5). Emission and excitations scans were performed for AAA1-A434C*$^{Alexa\ 488}$ and AAA2-R781C*$^{Alexa\ 532}$, to determine excitation and emission maxima. For AAA1-A434C*$^{Alexa\ 488}$, the excitation and emission maxima were at 488 and 532 nm respectively (See Fig 3.7A). For AAA2-R781C*$^{Alexa\ 532}$, the excitation and emission maxima were at 528 and 555 nm, respectively (Fig 3.7B).

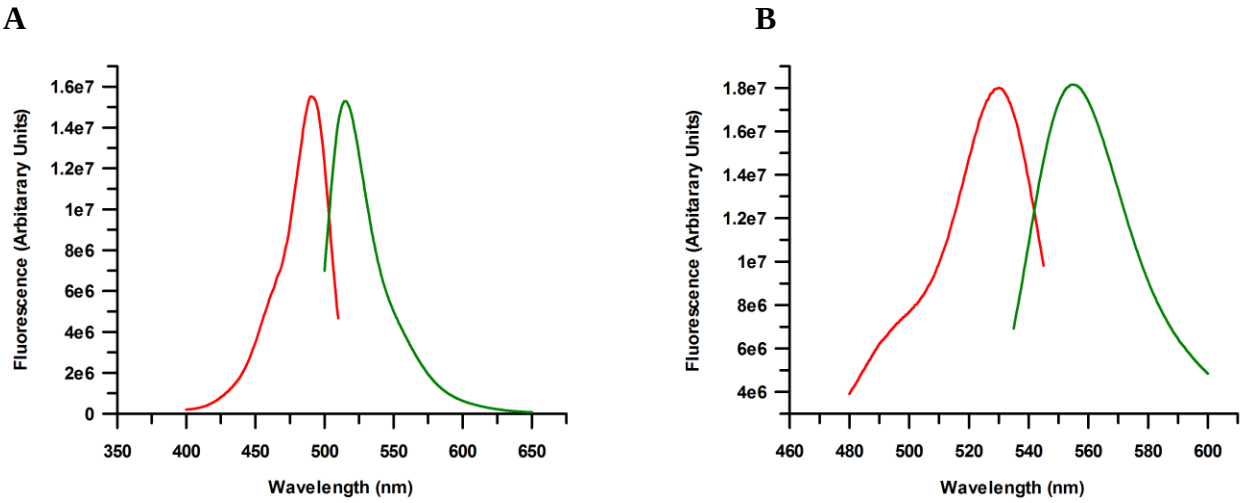

Fig 3.7: Excitation and emission scans of the fluorescently labeled isolated AAA modules of ClpB$_{Tth}$.(A) AAA1-A434C$^{*Alexa\ 488}$: Red line shows excitation spectrum of the Alexa 488 label attached to AAA1-A434C, at an emission maximum of 532 nm. Whereas, the green line represents the emission spectrum of the Alexa 488 label, at an excitation maximum of 488 nm.
(B) AAA2-R781C$^{*Alexa\ 532}$: Red line shows excitation spectrum of the Alexa 532 label attached to AAA2-R781C, at an emission maximum of 555 nm. Whereas, the green line represents the emission spectrum of the Alexa 532 label, at an excitation maximum of 528 nm.

3.1.2 Studies on nucleotide binding to the isolated AAA modules of $ClpB_{Tth}$.

Nucleotide binding to the fluorescently labeled isolated AAA modules was studied (AAA1-A434C and AAA2-R781C), to understand nucleotide-mediated conformational changes in $ClpB_{Tth}$.

3.1.2.1 ATP binding to the isolated AAA1 module.

ATP binding to the AAA1 module in the presence and absence of the AAA2 module was studied (Methods 2.4.4). Addition of 200 µM ATP to 0.5 µM AAA1-A434C*$^{Alexa\ 488}$ resulted in no fluorescence change (Fig 3.8). This suggests that addition of ATP may not have resulted in any conformational changes, in the M domain of the AAA1 module. Addition of 0.5 µM AAA2-R781C to this mixture also did not have any effect on the fluorescence signal (Fig 3.8). Although oligomer formation could be expected in this case, it did not appear to have any impact on the fluorescence signal of the Alexa 488 label present on the M domain of the AAA1 module.

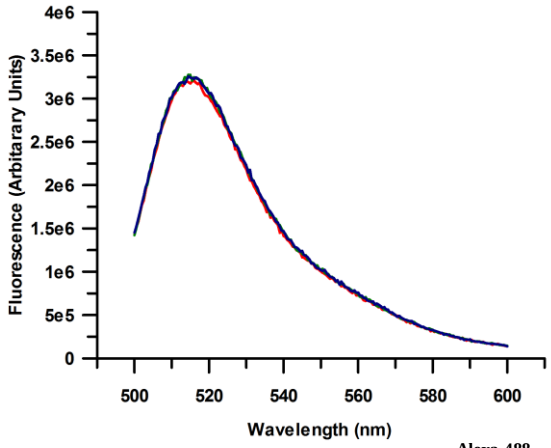

Fig 3.8: Effect of addition of AAA2-R781C to AAA1-R781C*$^{Alexa\ 488}$ in the presence of ATP. Fluorescence of the Alexa 488 label attached to the M domain in the AAA1 module, before (Red) and after (Green) addition of ATP and AAA2-R781C (Blue). Upon excitation at 488 nm, fluorescence of the Alexa 488 label was monitored at 532 nm, in a buffer containing 50 mM HEPES-NaOH pH 7.5, 50 mM KCl, 5 mM MgCl2 at 25°C.

3.1.2.2 Nucleotide binding to the isolated AAA2 module.

The effect of ATP binding to the isolated AAA2 module was studied (Methods 2.4.4). A change in the fluorescence signal might indicate a conformational change in the α-helical small domain 2 (SD2). Addition of 200 µM ATP to 0.5 µM AAA2-R781C*$^{Alexa\ 532}$ resulted in quenching of the Alexa 532 fluorescence (Fig 3.9A). This signal change hints at a possible conformational change in SD2. The time scale of the experiment and ATP hydrolysis properties of the isolated AAA2

module (turnover of 6.9 min^{-1}) make it difficult to conclude the underlying cause. Oligomer formation has been reported for the isolated AAA2 module, in the presence of either ATP or ADP, at low ionic strength (Beinker et al., 2005). Therefore, the signal change observed here might be due to either ATP binding, hydrolysis, ADP release or dissociation of the isolated AAA2 module dimer. For understanding the above mentioned signal changes, the effect of ADP binding to the isolated AAA2 module was studied. Addition of 200 µM ADP to 0.5 µM AAA2-R781C*$^{Alexa\ 532}$ resulted in a decrease, in the emission intensity of Alexa 532 label (Fig 3.9B).

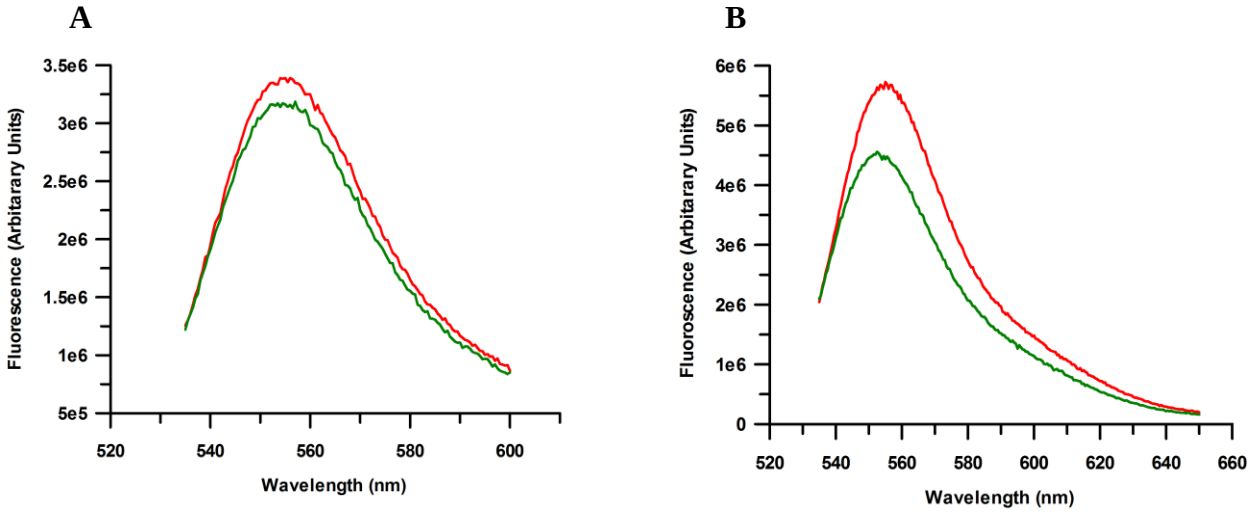

Fig 3.9: Effect of addition of nucleotides to AAA2-R781C*$^{Alexa\ 532}$. Upon excitation at 528 nm, fluorescence of the Alexa 532 label was monitored at 555 nm, in a buffer containing 50 mM HEPES-NaOH pH 7.5, 50 mM KCl, 5 mM MgCl2 at 25°C.
(A) Fluorescence of the Alexa 532 label attached to the α-helical small domain (SD2) in the AAA2 module before (Red) and after addition of ATP (Green). **(B)** Fluorescence of the Alexa 532 label attached to the α-helical small domain (SD2) in the AAA2 module before (Red) and after addition of ADP (Green).

Needless to say, this might signify a conformational change occurring in SD2 of the isolated AAA2 module upon ADP binding at its nucleotide binding domain. This conformational change occurring in SD2 of the isolated AAA2 module could either be due to ADP binding or dissociation of the dimeric AAA2 module upon ADP binding. A decrease in the fluorescence signal also indicates that the conformational change observed in SD2, is probably its movement away from the protein core. The conformational change occurring in SD2 upon addition of ATP to AAA2-R781C*$^{Alexa\ 532}$ is probably similar to the one observed with the addition of ADP (Fig 3.9A and 3.9B). In the first case, it could be due to ADP formation upon ATP hydrolysis and the later due to binding of ADP. The possibility of ADP binding-mediated dissociation of the dimeric AAA2 module cannot be excluded in both cases.

3.1.2.3 Titration of ADP to the isolated AAA2 module.

To understand the nature of ADP binding to the isolated AAA2 module and related conformational change(s), titration experiments were performed. Addition of increasing amounts of ADP (0.02 µM to 700 µM) to 0.5 µM AAA2-R781C*$^{Alexa\ 532}$ decreased the fluorescence intensity of the Alexa 532 label (Methods 2.4.4). The fluorescence emission amplitude (after correction for volume changes), when plotted against ADP concentration, yielded a rectangular hyperbola (Fig 3.10 A). Data analysis using the quadratic equation resulted in a poorly fitted curve and a dissociation constant of 1.13 (±0.3) µM. Although this is close to the K_D of 1.5 µM reported for the isolated AAA2 module with Mant-ADP displacement titrations (Philipp Beinker Dissertation, 2003), the error remains remarkably high (27%).

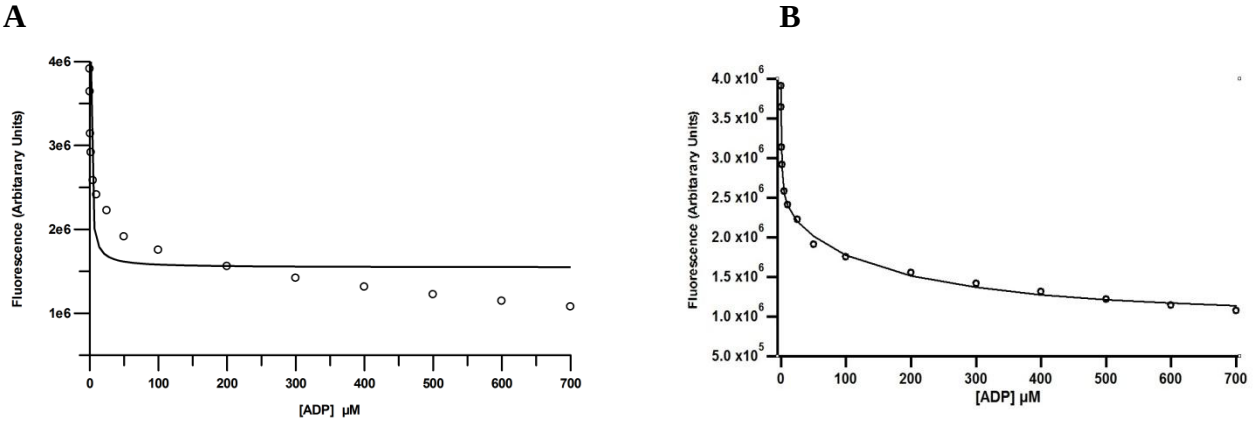

Fig 3.10: Titration of ADP to AAA2-R781C*$^{Alexa\ 532}$. Upon excitation at 528 nm, fluorescence of the Alexa 532 label was monitored at 555 nm, in a buffer containing 50 mM HEPES-NaOH pH 7.5, 50 mM KCl, 5 mM MgCl2. Fluorescence emission intensity decrease of the Alexa 532 label attached to the isolated AAA2 module upon addition of increasing amounts of ADP was plotted against ADP concentration.
(A) Solid line indicates the fit obtained upon analysis with the quadratic equation. **(B)** Solid line indicates the fit obtained upon analysis with the biphasic binding model.

The shape of the obtained curve and the observation that AAA2 module exists in a monomer-dimer mixture has indicated a possibility for two phases in the binding reaction. Therefore, a model was developed using Micromath SCIENTIST software to study possible biphasic binding of ADP to the isolated AAA2 module (Methods 2.4.4). Data obtained from the fluorescence titration experiment fitted well with the simulated curve suggesting biphasic binding (Fig 3.10 B). Data analysis yielded two dissociation constants (K_D1: 0.6 µM and K_D2: 145 µM), indicating a high affinity and a low affinity binding site in the isolated AAA2 module dimer. The K_D1 of

0.66 µM for ADP binding to the AAA2 module is also in agreement with 0.5 µM reported for the isolated wild type AAA2 module (Werbeck et al., 2009).

However, the biphasic nature in ADP binding to the isolated AAA2 module looks ambiguous due to the nature of the fluorescence signal changes observed during the ADP titration. Upon addition of 200 µM ADP, a signal loss of approximately 25% was observed (Fig 3.9B). In the titration experiment, at the same ADP concentration of 200 µM, a signal loss of nearly 65% could be observed (Fig 3.10A and 3.10B). This might indicate a possible photo bleaching effect. However, the oligomeric state of the isolated AAA2 module and $ClpB_{Tth}$ in general is so dynamic, that addition of 200 µM ADP at once might result in different changes in the protein compared to addition in steps. Alexa fluor labels are known for their photo stability; hence, biphasic binding most probably cannot be excluded. However, future experiments might be required to understand the reason for this ambiguity.

3.1.2.4 Isothermal calorimetric titration of ADP to the isolated AAA2 module.

Isothermal titration calorimetry measurement was performed to study binding of ADP to the isolated AAA2 module (Methods 2.5.1). The measurement was performed at 25°C by titrating 100 µM ADP to 10 µM AAA2-R781C in 29 injections of 10 µL each.

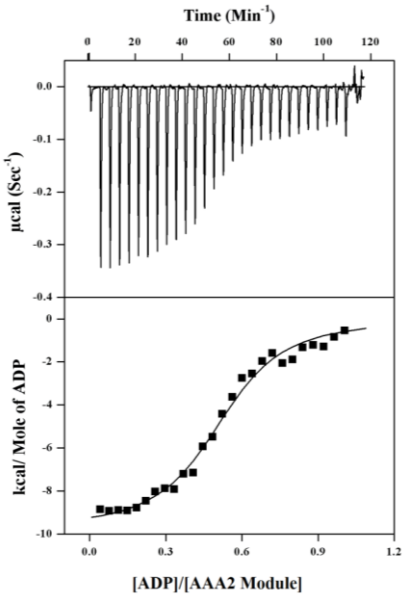

Fig 3.11: Binding of ADP to AAA2-R781C. The upper part of the figure features thermodynamics of the heat release due to the addition of ADP to AAA2-R781C at 25°C. The lower part of the figure shows a plot of heat release and molar ratio of ADP and the AAA2 module (AAA2-R781C).

Binding of ADP to the AAA2 module resulted in a pronounced heat release. Data upon analysis fitted into a single site binding model, which yielded an association constant of 1.51x 10^6 M^{-1} (Fig 3.11). The corresponding K_D of 0.66 µM obtained here is in agreement with K_D1 obtained from the fluorescence titration measurements (Fig 3.10B). Data analysis also yielded a stoichiometry of 0.5 for binding of ADP to the AAA2 module. This probably suggests that one molecule of ADP binds to two molecules of the isolated AAA2 module or in other words, probably one ADP per the isolated AAA2 module dimer.

The presence of two phases in ADP binding and the oligomeric state of the isolated AAA2 module raised questions regarding the nature of the conformational change occurring in SD2. The isolated AAA2 module forms a mixture of monomers and dimers (Results 3.1.1.3), which indicated the possibility for an inter-subunit conformational change. To investigate the nature of the conformational change occurring in SD2 upon ADP biding, further experiments were designed and conducted. Dimer formation would be an essential prerequisite to observe an inter-subunit conformational change. Hence, experiments were conducted to estimate the oligomeric state of AAA2 module at the ionic strength and protein concentrations where ADP binding experiments were performed.

3.1.2.5 Oligomeric state analysis of the isolated AAA2 module.

The following experiments were performed to estimate the oligomeric state of the isolated AAA2 module at the ionic strength where ADP binding experiments were conducted. Experiments were conducted using gel permeation chromatography coupled with multi-angle light scattering measurements (Methods 2.6). Measurements were performed in buffers containing 50 mM Tris-HCl pH 7.5, 5 mM MgCl2 and varying KCl concentrations of 25, 100 and 200 mM. Molar mass distribution analysis was performed using manufacturer's software (ASTRA Version 5.1.4.3 Wyatt Tech Corp) and tabulated (Table 3.5).

For all the salt concentrations measured, neither the isolated wild type AAA2 module nor AAA2-R781C yielded molar masses that correspond to one particular oligomeric species. At 25 mM KCl, the isolated wild type and AAA2 module and AAA2-R781C remained at molar masses close to that of a theoretical dimer (76.6 kDa) (See Table 3.5). 72% of the injected protein was

present in molar masses ranging from 55-65 kDa, for the isolated wild type AAA2 module. The peak portion of the chromatogram yielded an average molar mass of 68.8 kDa, which consists of 75 µg of 115 µg total protein analyzed. For AAA2-R781C, more than 90% of the protein was present in molar masses ranging from 55-65 kDa. The peak portion of the chromatogram yielded an average molar mass of 63 kDa, which consists of 131µg of 136 µg total protein analyzed. For both the proteins, the calculated molar mass is closer to the theoretical molar mass of a dimer (76.6 kDa), rather than a monomer (38.3 kDa).

M. Wt (kDa)	**25 mM KCl**		**100 mM KCl**		**200 mM KCl**	
	WT	**R781C**	**WT**	**R781C**	**WT**	**R781C**
10-20	0%	0%	0%	0%	0%	0%
20-30	0%	0%	0%	0%	1.6%	0%
30-35	0%	0%	0%	0%	4.8%	0%
35-45	0%	0%	0%	0%	4.7%	5.4%
40-45	0%	0%	**12.2%**	0%	**37.3%**	**26.9%**
45-50	0%	0%	**64.4%**	0%	**43.4%**	**51.8%**
50-55	0%	2%	9.6%	**33%**	4.5%	2%
55-60	**27.3%**	**84.3%**	4.9%	**58.1%**	1.5%	1.2%
60-65	**44.7%**	7.5%	2.3%	4.5%	0.5%	0.4%
65-70	12.7%	0.7%	1.3%	2.4%	0.6%	0.3%
70-75	5.2%	1.2%	0.8%	0.6%	0.3%	0%
75-80	1%	0.4%	1%	1.3%	0.2%	0%
80-85	2.5%	0.5%	0.5%	0%	0.7%	0.2%
85-90	1%	0.6%	0.3%	0%	0%	0.2%

Table 3.5: Oligomeric state analysis for the isolated wild type AAA2 module and AAA2-R781C (R781C).

The predominant species at 100 mM KCl shifted towards lower molecular weights, when compared to that of 25 mM KCl measurements. At 100 mM KCl concentration, for the wild type AAA2 module, 75% of the protein was present between 45-55 kDa range. The peak portion of

the chromatogram yielded an average molar mass of 51 kDa, which consists of 110 µg of 115 µg total protein analyzed. For AAA2-R781C, 91% of the protein remained in 50-60 kDa range. Like the wild type isolated AAA2 module, the peak portion of AAA2-R781C chromatogram yielded an average molar mass of 55 kDa, which consisted of 90 µg of 120 µg total protein injected. These observations pointed towards a possible mixture of monomers and dimers.

However, at 200 mM KCl concentration both the proteins largely yielded molar masses closer to a theoretical monomer. For the wild type AAA2 module, 80% of the protein was present in the range of 40-50 kDa; whereas, nearly 79% of AAA2-R781C was in the same range. The peak portion of the chromatogram yielded an average molar mass of 45 kDa, which consists of 115 µg of 120 µg total protein analyzed for the wild type isolated AAA2 module. For AAA2-R781C, the peak portion of the chromatogram yielded an average molar mass of 45.8 kDa, which consists of 113 µg of 120 µg total protein analyzed. All these observations are mostly in agreement with previously reported information on the oligomeric state of the isolated AAA2 module (Beinker et al., 2005 and Werbeck et al., 2009). Experiments performed here showed that at low ionic strength, in the absence of nucleotides, both the wild type AAA2 module and AAA2-R781C yield molar masses representative of a dimer. In other words, at ionic strength where ADP binding experiments were performed (3.1.2.2), both the wild type AAA2 module and AAA2-R781C can assemble into a dimer.

3.1.2.6 ADP binding to the isolated AAA2 module in the presence the isolated AAA2 module carrying P-loop mutation.

The following studies were done to address two major questions. What is the oligomeric state of the isolated AAA2 module at protein concentration of 0.5 µM, where ADP binding was studied? Is the conformational change occurring in SD2, upon ADP binding to the isolated AAA2 module, either intra-subunit or inter-subunit? Mutations in the P-loop of the nucleotide binding domain of the AAA2 module (AAA2-K601Q) results in altered nucleotide binding and hydrolysis properties. K601Q mutation in the AAA2 module of the full-length $ClpB_{Tth}$ resulted in loss of chaperone activity, and a 100 fold reduction in ATP hydrolysis (Schlee et al., 2001). This mutant impairs ADP binding-mediated conformational changes in $ClpB_{Tth}$. This is evident by the absence of oligomer dissociation upon ADP binding. This mutation appears to impair the

ability of $ClpB_{Tth}$ to distinguish between ATP and ADP, where it formed similar amount of hexamers both in the presence of ATP and ADP. ATP and ADP binding was not drastically affected due to the K601Q mutation; however, when compared to wild type $ClpB_{Tth}$ and P-loop mutant of AAA1 module (K204Q), affinity for MANT-ADP and MANT-2'd-ADP was lowered by two orders of magnitude. This observation implies that the nucleotide bound at the nucleotide binding domain of the AAA2 module plays a key role in nucleotide-mediated association or dissociation of $ClpB_{Tth}$. This makes it an excellent candidate for studying the nature of conformational change occurring in SD2 upon ADP binding to the isolated AAA2 module.

3.1.2.7 Binding of AAA2-K601Q to the isolated AAA2 module.

Although, the protein used in these experiments is AAA2-R781C*$^{Alexa\ 532}$, it will be referred to as wild type; since, the introduced single-cysteine mutation has no effect on functionality of the AAA2 module (Section 3.1.1). Addition of 0.5 µM AAA2-K601Q to 0.5 µM AAA2-R781C*$^{Alexa\ 532}$ resulted in a decrease, in the emission intensity of the Alexa 532 label attached to SD2 of the isolated AAA2 module (Fig 3.12A). The fluorescence emission decrease observed here might be indicative of a hetero-dimeric complex formation between the wild type and P-loop mutant AAA modules.

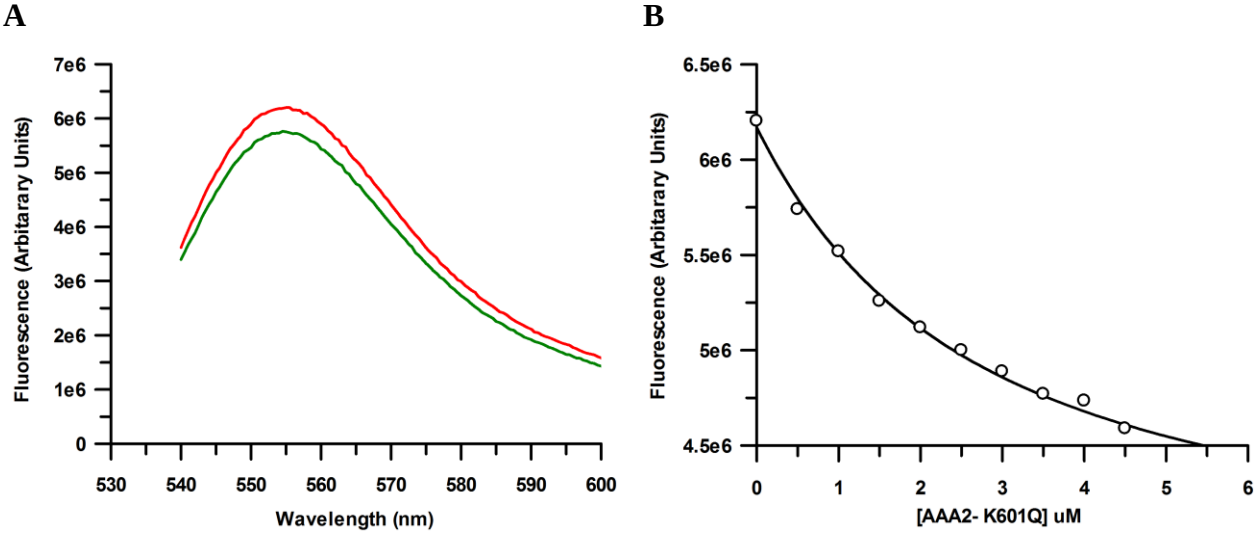

Fig 3.12: Titration of AAA2-K601Q to AAA2-R781C*$^{Alexa\ 532}$. Upon excitation at 528 nm, fluorescence of the Alexa 532 label was monitored at 555 nm, in a buffer containing 50 mM HEPES-NaOH pH 7.5, 50 mM KCl, 5 mM MgCl2 at 25°C. **(A)** Fluorescence of the Alexa 532 label attached to the α-helical small domain (SD2) in the AAA2 module before (Red) and after (Green) addition of AAA2-K601Q at 25°C. **(B)** Fluorescence emission intensity decrease of the Alexa 532 label was plotted against AAA2-K601Q concentration. Solid line indicates the fit obtained upon analysis using the quadratic equation.

Addition of increasing amounts of AAA2-K601Q further decreased the fluorescence emission intensity of Alexa 532 label. AAA2-K601Q was added, in 0.5 µM increments, to make wild type and P-loop mutant complexes of 1:1, 1:2, 1:3…. 1:10 stoichiometries. Fluorescence emission amplitude for each titration was plotted against the concentration of AAA2-K601Q (Fig 3.12B). Data analysis with quadratic equation yielded a K_D of 2.3 (±0.35) µM. This value indicates that, at 0.5 µM protein concentration, the chances for the AAA2 module to exist as a dimer are fairly good (≈15%).

3.1.2.8 Titration of AAA2-K601Q to the ADP bound isolated AAA2 module

Titration of AAA2-K601Q to AAA2-R781C*$^{Alexa\ 532}$ in the presence of ADP was performed to understand the nature of ADP-induced conformational changes (Methods 2.4.4). Hypothetically, if the conformational change in SD2 is inter-subunit, then a shift of wild type AAA2 module homo-dimer equilibrium towards a wild type and P-loop mutant hetero-dimer should have a reinstating effect on the emission intensity decreased due to the prior addition of ADP. If the conformational change in SD2 is intra-subunit, then the presence of a nucleotide binding domain with P-loop mutation in the neighboring subunit should not alter the emission intensity.

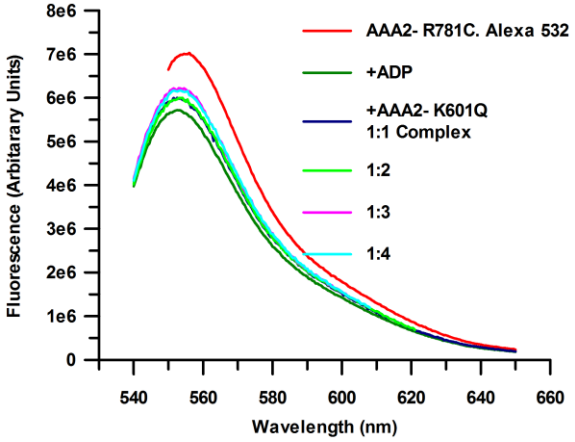

Fig 3.13: Titration of AAA2-K601Q to AAA2-R781C*$^{Alexa\ 532}$ in the presence of ADP. Fluorescence of the Alexa 532 label attached to the α-helical small domain (SD2) in the AAA2 module before and after addition of ADP and increasing amounts of AAA2-K601Q. Upon excitation at 528 nm, fluorescence of the Alexa 532 label was monitored at 555 nm, in a buffer containing 50 mM HEPES-NaOH pH 7.5, 50 mM KCl, 5 mM MgCl2 at 25°C.

Addition of ADP to AAA2-R781C*$^{Alexa\ 532}$ as already shown resulted in decreased Alexa 532 fluorescence (Fig 5.13). Addition of 0.5 µM of AAA2-K601Q to this mixture resulted in an emission intensity increase of the Alexa 532 label. Addition of increasing amounts of AAA2-

K601Q (0.5 µM increments) further increased the signal (Fig 3.13). Here, the effect of 1:1, 1:2, 1:3 and 1:4 stoichiometric complexes of the wild type and P-loop mutant AAA2 modules were studied.

The fluorescence intensity lost due to the ADP addition was recovered partially by adding increasing amounts of AAA2-K601Q. This could mean that the presence of the P-loop mutation in the neighboring subunit can affect the conformation of SD2 of the previous AAA2 module. In turn, this could also imply that the conformational change observed due to ADP binding could be an inter-subunit conformational change. If the presence of an altered P-loop does affect the conformation of the neighboring AAA2 module, then it should also have the same influence on the affinity for ADP binding to the isolated AAA2 module. In other words, if the Alexa 532 fluorescence decrease is due to an inter-subunit conformational change upon ADP binding, then the presence of one altered P-loop in the dimer should decrease the affinity of ADP to the isolated AAA2 module dimer. To address this question, the following experiments were performed.

3.1.2.9 Titration of ADP to AAA2-K601Q and the isolated AAA2 module complex

Titration of ADP to 1:1 and 1:2 stoichiometric complexes of the wild type and P-loop mutant AAA2 modules were done. First increasing amounts of ADP (0.02 to 1000 µM) were titrated to a 1:1 stoichiometric complex of the wild type and P-loop mutant AAA2 modules (0.5 µM AAA2-R781C*$^{\text{Alexa 532}}$ and 0.5 µM AAA2-K601Q) (Fig 3.14A). Fluorescence of the Alexa 532 label attached to AAA2-R781C decreased with the addition of increasing amounts of ADP. The fluorescence emission amplitude, when plotted against ADP concentration, yielded a rectangular hyperbola. Data analysis using the biphasic binding model yielded two dissociation constants of K_D1: 0.7 µM and K_D2: 621 µM (Methods 2.4.4 and Appendix A) (Fig 3.14A).

Likewise, titration of ADP to 1:2 stoichiometric complexes of the wild type and P-loop mutant AAA2 modules were performed (0.5 µM AAA2-R781C*$^{\text{Alexa 532}}$ and 1 µM AAA2-K601Q) (Fig 3.14B). Fluorescence emission amplitude, when plotted against ADP concentration, yielded a rectangular hyperbola. Data analysis with biphasic binding model did not yield a good fit with the simulated curve and yielded two dissociation constants of K_D1: 1.05µM and K_D2: 630 µM.

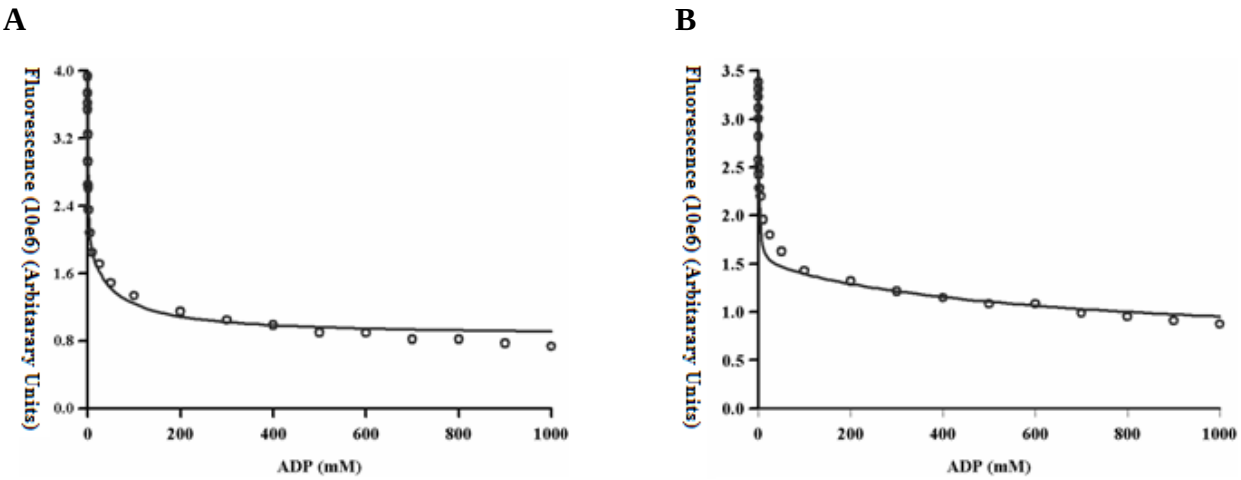

Fig 3.14: Titration of ADP to 1:1 and 1:2 complex of AAA2-R781C*$^{Alexa\ 532}$ and AAA2-K601Q. Upon excitation at 528 nm, fluorescence of the Alexa 532 label was monitored at 555 nm, in a buffer containing 50 mM HEPES-NaOH pH 7.5, 50 mM KCl, 5 mM MgCl2. Fluorescence emission intensity decrease of the Alexa 532 label attached to the isolated AAA2 module upon addition of increasing amounts of ADP was plotted against ADP concentration.
(A) Titration of ADP to 1:1 complex of AAA2-R781C*$^{Alexa\ 532}$ and AAA2-K601Q. Solid line represents the fit obtained upon data analysis using the biphasic binding model. **(B)** Titration of ADP to 1:2 complex of AAA2-R781C*$^{Alexa\ 532}$ and AAA2-K601Q. Solid line represents the fit obtained upon data analysis using the biphasic binding model.

Protein/ Complex	**K_D1 [ADP] µM**	**K_D2 [ADP] µM**
AAA2-R781C*$^{Alexa\ 532}$ (Fluorescence Titration)	0.6	145
AAA2-R781C (Isothermal calorimetric Titration)	0.66	---
AAA2-R781C*$^{Alexa\ 532}$ and AAA2-K601Q 1:1 Complex (Fluorescence Titration)	0.7	621
AAA2-R781C*$^{Alexa\ 532}$ and AAA2-K601Q 1:2 Complex (Fluorescence Titration)	1.05	630

Table 3.6: High and low affinity K_D values calculated for ADP binding to AAA2 module with R781C mutation. Fluorescence titration experiments were performed at an AAA2-R781C*$^{Alexa\ 532}$ concentration of 0.5 µM; whereas, isothermal calorimetric titration was performed at an AAA2-R781C concentration of 10 µM. For experiments with ADP binding to AAA2-R781C*$^{Alexa\ 532}$ in the presence of AAA2-K601Q protein concentration of 0.5 µM of each protein in the case of 1:1 complex was used. For 1:2 complex 0.5 µM AAA2-R781C*$^{Alexa\ 532}$ and 1 µM AAA2-K601Q was used.

3.1.3 Studies on nucleotide binding to the AAA2 module in the absence of the α-helical small domain 2.

Experiments done so far have hinted at an inter-subunit conformational change in the isolated AAA2 module, upon ADP binding. The following experiments were done to study the effect of deletion of SD2 on the isolated AAA2 module. For that purpose an SD2 deletion variant of the isolated AAA2 module was prepared (AAA2ΔSD2) (Fig 3.15). Binding of AAA2ΔSD2 to the isolated SD2 was also assessed to study whether covalent linkage is essential for oligomer formation.

A

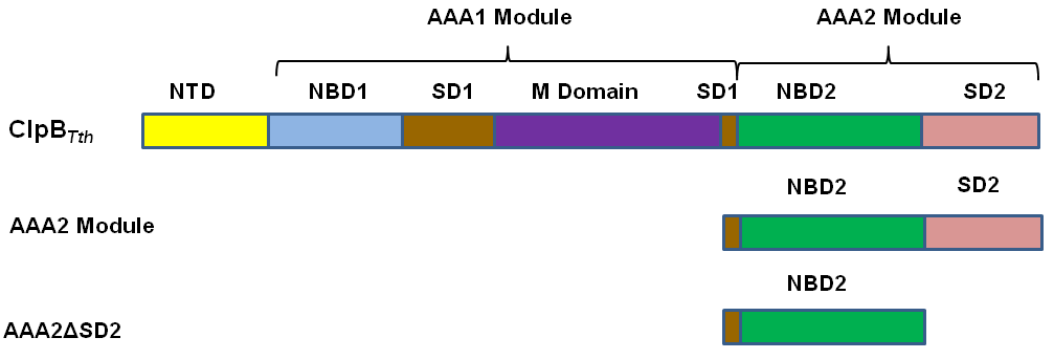

B

Fig 3.15: The isolated AAA2 module of ClpB$_{Tth}$ with SD2 deletion. (A) A Schematic depicting domain organization in AAA2ΔSD2 (ClpB 520-758). The isolated AAA2 module of ClpB$_{Tth}$ consists of the nucleotide binding domain 2 (NBD2) and the α-helical small domain 2 (SD2) and a part of the α-helical small domain 1 (SD1). In AAA2ΔSD2 the α-helical small domain 2 (SD2) is deleted (AA 759-854). **(B)** A ribbon representation of AAA2ΔSD2, featuring NBD2 in green and part of SD1 in brown. Structural data were obtained from PDB entry 1QVR (Lee et al., 2003) and rendered using Pymol software.
NTD (AA 1-152), NBD1 (AA 153-331), SD1 (AA 332-400 and 519-535), M domain (AA 401-518), NBD2 (AA 536-758) and SD2 (759-854)

3.1.3.1 Purification of AAA2ΔSD2.

AAA2ΔSD2 was prepared by introducing a stop codon after amino acid 758 (Methods 2.2). The AAA2ΔSD2 protein was purified using immobilized metal ion affinity chromatography and gel permeation chromatography (Methods 2.3). Quality of the purified AAA2ΔSD2 was assessed by 10% poly-acrylamide gel electrophoresis. Purified AAA2ΔSD2 was analyzed for bound nucleotide using HPLC-based reverse phase chromatography (Methods 2.3.4). Comparison of the chromatogram to standard nucleotides indicated that AAA2ΔSD2 is nucleotide-free (Data not shown).

3.1.3.2 Oligomeric state analysis of AAA2ΔSD2.

To study the effect of SD2 deletion on the isolated AAA2 module, oligomeric state of AAA2ΔSD2 was analyzed using gel permeation chromatography coupled with multi-angle light scattering. Experiments were performed on AAA2ΔSD2 and pre-incubated complex of AAA2ΔSD2 and isolated SD2. Measurements were performed both in the presence and absence of 1mM ATP, and molar mass analysis was performed using the manufacturer's software (ASTRA Version 5.1.4.3).

The predominant species present in the peak region of the AAA2ΔSD2 chromatogram corresponded to a molar mass of approximately 33 kDa (Fig 3.16). This is close to the theoretical molar mass for monomeric AAA2ΔSD2 (28.5 kDa). The molar mass distribution analysis revealed that 100% of the injected protein was present in a range between 30-35 kDa.

Pre-incubated equimolar mixtures of AAA2ΔSD2 and isolated SD2 eluted in two separate peaks. The first peak corresponded with the molar mass obtained for AAA2ΔSD2, indicting no complex formation (Fig 3.16 and Table 3.7). Molar mass analysis yielded 34.5 kDa for the predominant species in the first peak of the chromatogram. Predominant species in the second peak of the chromatogram yielded a molar mass of 12.4 kDa, which is close to the theoretical monomeric mass of the isolated SD2. Molar mass distribution analysis revealed that 35% of the injected protein is present in the range of 10-12 kDa, which is possibly isolated SD2; whereas, 65% of the injected protein was present in the range between 30-35 kDa, indicative of AAA2ΔSD2.

Addition of 1 mM ATP did not have any effect on the outcome where, neither a peak shift nor a change in the obtained molar mass has been observed (Fig 3.16 and Table 3.7). Complex formation between isolated AAA2ΔSD2 and isolated SD2 can be excluded due to the absence of a shift in the AAA2ΔSD2 peak and no change in obtained molar masses. These results suggested that the deletion of SD2 results in loss of oligomer formation in the isolated AAA2 module.

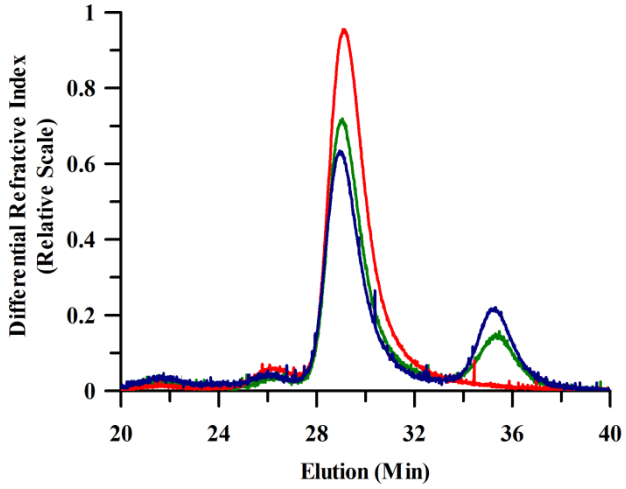

Fig 3.16: Oligomeric state analysis for AAA2ΔSD2. Elution profile of isolated AAA2ΔSD2 (Red), AAA2ΔSD2+ SD2 complex (Green) and AAA2ΔSD2+ SD2 complex in the presence of 1mM ATP (Blue).

Protein/ Complex	Predominant oligomeric species
AAA2ΔSD2	Monomer
AAA2ΔSD2+SD2	Monomers of both the proteins
AAA2ΔSD2+SD2+ATP	Monomers of both the proteins

Table 3.7: Oligomeric state analysis for AAA2ΔSD2.

3.1.3.3 Nucleotide binding and hydrolysis in AAA2ΔSD2.

Fluorescent nucleotide Mant-ADP binds to the isolated AAA2 module with a K_D of 0.07 µM (Beinker et al., 2005). To study the effect of deletion of the α-helical small domain on nucleotide binding properties of AAA2ΔSD2, binding of ADP was studied. Isothermal titration calorimetric experiments were performed (Methods 2.5.1). ADP titration was performed by adding 100 µM ADP to 10 µM AAA2ΔSD2 in 29 injections of 10 µL each at 25°C. This titration did not result in any heat exchange, suggesting the absence of complex formation (Fig 3.17). Data obtained

was not adequate to calculate thermodynamic parameters and binding constants. This observation points towards the lack of nucleotide binding due to deletion of SD2 in AAA2 module.

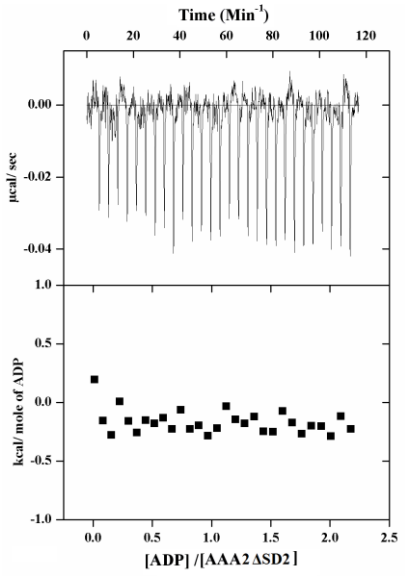

Fig 3.17: Binding of ADP to AAA2ΔSD2. The upper part of the figure features thermodynamics of the heat release due to the addition of ADP to AAA2ΔSD2 at 25°C. The lower part of the figure shows a plot of the heat release and the molar ratio of ADP and AAA2ΔSD2.

To study the effect of deletion of SD2 on ATPase activity of the isolated AAA2 module, ATP hydrolysis was studied under steady-state conditions (Methods 2.4.2). No hydrolysis of ATP was detected for ATP concentration ranging from 0.02 to 2 mM for AAA2ΔSD2 (Data not shown). Addition of isolated SD2 to AAA2ΔSD2 in all the above experiments did not have any impact on the outcome of the experiments conducted (Data not shown). Data obtained indicated that the deletion of SD2 results in loss nucleotide binding and hydrolysis, in the AAA2 module.

3.1.3.4 Refolding of denatured α-Glucosidase by AAA2ΔSD2.

To study the effect of SD2 deletion, refolding experiments were conducted for a mixture containing equimolar amounts of isolated AAA1 module, AAA2ΔSD2 and isolated SD2 (AAA1+AAA2ΔSD2+SD2) (Methods 2.4.3.1). Refolding of heat denatured α-Glucosidase by the AAA1+AAA2ΔSD2+SD2 complex was compared to the AAA1+AAA2 complex. As expected, the AAA1+AAA2 complex refolded heat denatured α-Glucosidase to nearly 15% of its native activity after incubation at 55°C for 120 min. However, AAA1+AAA2ΔSD2+SD2 recovered only 3% of α-Glucosidase native activity, which is similar to that observed for the

DnaK$_{Tth}$ system alone (Fig 3.18 and Table 3.8). This indicates the loss of chaperone activity due to the deletion of SD2 in the isolated AAA2 module.

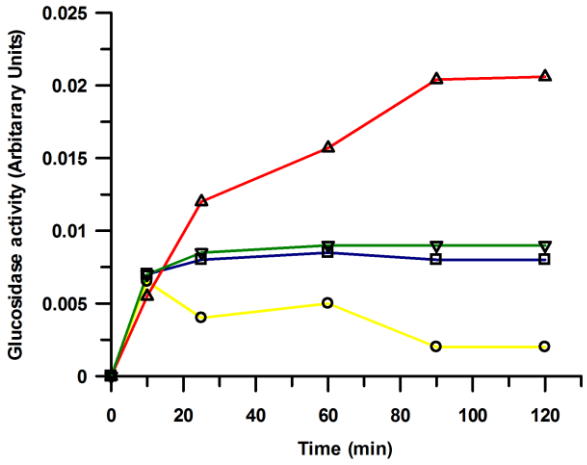

Fig 3.18: Chaperone activity. Refolding of heat denatured α-Glucosidase by the reconstituted complex of AAA1+AAA2ΔSD2+SD2 (Green) was compared with the reconstituted complex of wild type AAA1 and AAA2 (Red). α-Glucosidase, upon denaturation at 75°C for 10 min, was subjected to refolding at 55°C for 120 min in the presence of 1.0 µM reconstituted complex, 1.6 µM DnaK$_{Tth}$, 0.4 µM DnaJ$_{Tth}$ and 0.4 µM GrpE$_{Tth}$. Activity of refolded α-Glucosidase at various time points during the refolding reaction was plotted against time (min). The blue and yellow lines represent activity of α-Glucosidase after refolding in the presence of DnaK$_{Tth}$ system alone and no chaperones respectively.

Protein	**Fraction of refolded α-Glucosidase (%)**
AAA1+AAA2	15
AAA1+AAA2ΔSD2+SD2	2-3
DnaK$_{Tth}$ system alone	2-3

Table 3.8: Refolding yields of heat denatured α-Glucosidase by AAA2ΔSD2. Catalysis of cleavage of the glycosidic bond in p-nitrophenyl-α-D-glucopyranoside by refolded α-Glucosidase was quantified and expressed as fraction of its native activity regained. Native activity refers to the activity of α-Glucosidase prior to heat denaturation.

3.1.4 Studies on the effect of rigidity in the conformation of the α-helical small domain on ClpB$_{Tth}$.

Experiments thus far, have suggested that the deletion of SD2 in the isolated AAA2 module results in loss of oligomerization, nucleotide binding, hydrolysis and refolding of heat denatured substrate proteins. The following experiments were performed to demonstrate the significance of SD2 motion and flexibility.

A

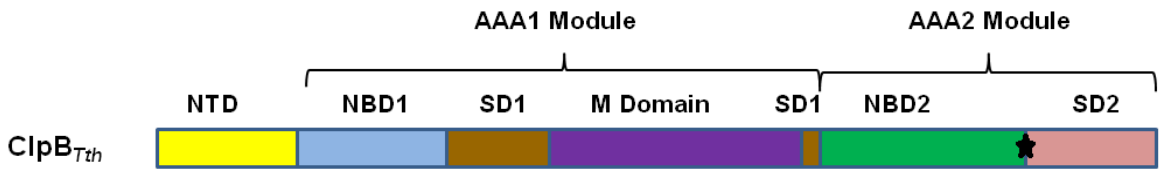

B

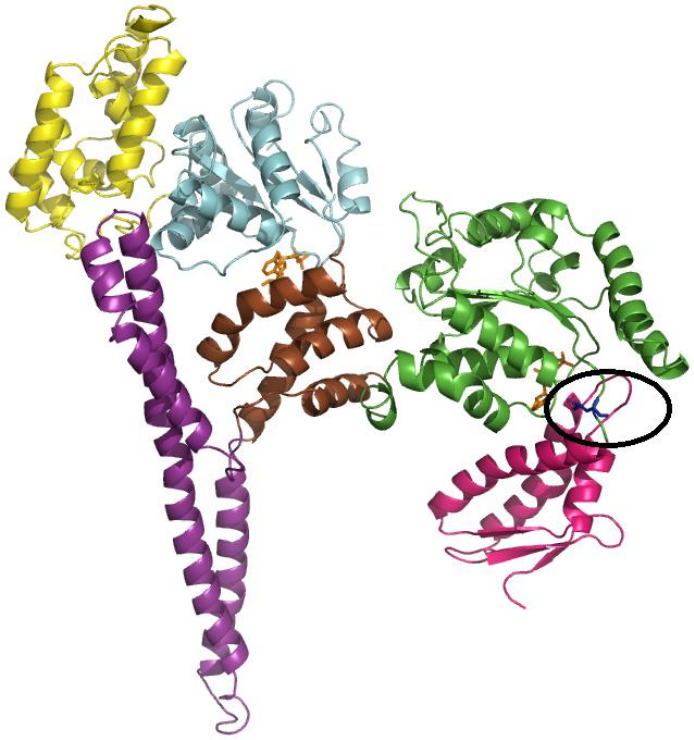

Fig 3.19: ClpB-L757P. (A) A Schematic depicting L757P mutation in full-length ClpB$_{Tth}$. Black asterisk indicates the location of the mutation. **(B)** A ribbon representation of ClpB$_{Tth}$ with location of L757P mutation circled. Leucine 757 is highlighted in blue in stick representation. Structural data were obtained from PDB entry 1QVR (Lee et al., 2003) and rendered using Pymol software. Bound AMP-PNP molecules are highlighted in orange, in stick representation.
NTD- Yellow (AA 1-152), NBD1- Blue (AA 153-331), SD1- Brown (AA 332-400 and 519-535), M domain- Violet (AA 401-518), NBD2- Green (AA 536-758) and SD2- Pink (759-854)

To achieve this, leucine at position 757 was mutated to proline in full-length $ClpB_{Tth}$ (Fig 3.19). Leucine 757 is on a loop connecting SD2 and nucleotide binding domain in an AAA2 module. Mutating it to a proline is expected to confer conformational rigidity, which in turn might disrupt motion in SD2.

3.1.4.1 Purification of ClpB-L757P mutant.

ClpB-L757P was purified using immobilized metal ion affinity and gel permeation chromatography (Methods 2.3). Protein precipitation occurred at several stages during the purification. Quality of the purified protein was quite low, as assessed by 10% poly-acrylamide gel electrophoresis. Purified ClpB-L757P was analyzed for nucleotide content using HPLC based reverse phase chromatography (Methods 2.3.4). Comparison with the chromatograms of standard nucleotides indicated that ClpB-L757P has no bound nucleotide (Data not shown).

3.1.4.2 ATPase and refolding properties of ClpB-L757P.

The effect of proline mutation on the ATPase activity of $ClpB_{Tth}$ was studied under steady-state conditions (Methods 2.4.2). If the introduced proline has resulted in rigidity, in the movement of SD2, then ClpB-L757P should be inactive in ATP hydrolysis. No ATPase activity was observed for ClpB-L757P mutant at ATP concentrations ranging from 0.02 to 2 mM (Data not shown).

Refolding of heat denatured α-Glucosidase by ClpB-L757P was investigated, to study the effect of proline mutation on chaperone activity of $ClpB_{Tth}$ (Methods 2.4.3.1). L757P mutation resulted in complete loss of refolding ability in $ClpB_{Tth}$ (Fig 3.20). Wild type $ClpB_{Tth}$ along with the $DnaK_{Tth}$ system refolded heat denatured α-Glucosidase to 30% of its native activity. Whereas, ClpB-L757P resulted in approximately 2-3% activity, which is similar to that observed for $DnaK_{Tth}$ system alone. Both the above experiments suggest loss of ATPase and chaperone activity upon introduction of proline in the loop connecting SD2 to the nucleotide binding domain of the AAA2 module of $ClpB_{Tth}$. The effect of proline mutation on the oligomeric properties of $ClpB_{Tth}$ could not be assessed owing to the highly unstable protein.

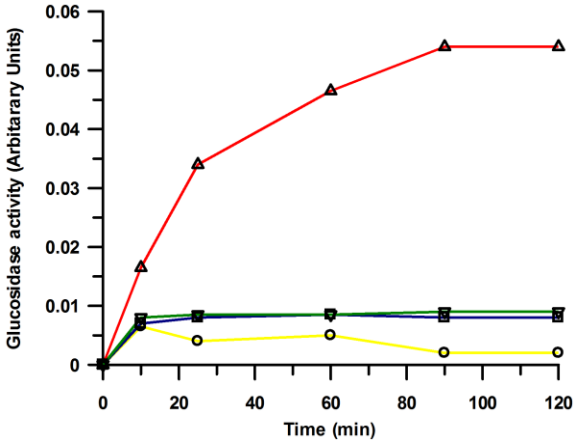

Fig 3.20: Chaperone activity. Refolding of heat denatured α-Glucosidase by ClpB-L757P (Green) was compared wild type $ClpB_{Tth}$ (Red). α-Glucosidase, upon denaturation at 75°C for 10 min, was subjected to refolding at 55°C for 120 min in the presence of 1.0 µM $ClpB_{Tth}$ (WT or L757P), 1.6 µM $DnaK_{Tth}$, 0.4 µM $DnaJ_{Tth}$, and 0.4 µM $GrpE_{Tth}$. Activity of refolded α-Glucosidase at various time points during the refolding reaction was plotted against time (min). The blue and yellow lines represent activity of α-Glucosidase after refolding in the presence of $DnaK_{Tth}$ system alone and no chaperones respectively.

Protein	**Fraction of Refolded α-Glucosidase (%)**
Wild type $ClpB_{Tth}$	30
ClpB-L757P	2-3
$DnaK_{Tth}$ system alone	2-3

Table 3.9: Refolding yields of heat denatured α-Glucosidase by ClpB-L757P. Catalysis of cleavage of the glycosidic bond in p-nitrophenyl-α-D-glucopyranoside by refolded α-Glucosidase was quantified and expressed as fraction of its native activity regained. Native activity refers to activity of α-Glucosidase prior to heat denaturation.

3.2 Studies on reconstituted complex of the isolated AAA modules of $ClpB_{Tth}$.

$ClpB_{Tth}$ features two AAA modules, both of them bind and hydrolyze ATP, and in doing so communicate with each other. The isolated AAA2 module has an elevated rate in ATP hydrolysis, but upon reconstitution with isolated AAA1 module, the complex follows typical features of wild type $ClpB_{Tth}$. This suggests a unique allosteric mechanism for optimal function. Following experiments were performed to understand this complex formation, in more detail.

3.2.1 FRET studies to understand complex formation between the isolated AAA modules.

Fluorescence resonance energy transfer experiments were performed to study the interaction between the AAA modules in $ClpB_{Tth}$. Influence of the presence of the acceptor (AAA2-R781C*$^{Alexa\ 532}$) on the donor (AAA1-A434C*$^{Alexa\ 488}$) emission spectrum was studied at 25°C. AAA1-A434C$^{*Alexa\ 488}$ (donor) was excited at 488 nm, and emission was monitored at 528 nm. Very little or no change was observed in the intensity of the donor emission spectrum in the presence of the acceptor indicating little or no interaction between the two AAA modules (Fig 3.21).

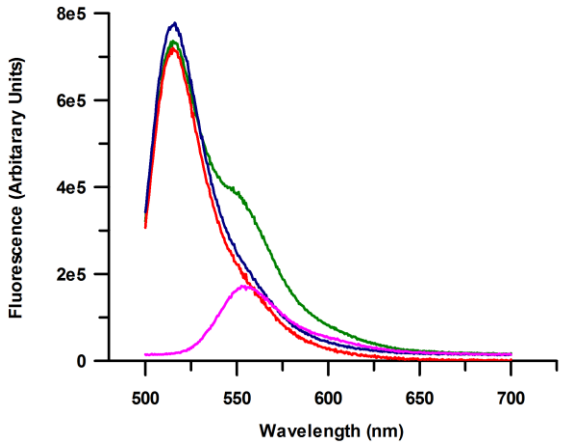

Fig 3.21: Fluorescence resonance energy transfer at 25^{0}C. In blue and fuchsia are emission spectra of AAA1-A434C$^{*Alexa\ 488}$ (Donor) and AAA2-R781C$^{*Alexa\ 532}$ (Acceptor), respectively, in a buffer containing 50 mM HEPES-NaOH pH 7.5, 50 mM KCl, 5 mM MgCl2. Emission spectrum of the Alexa 488 label attached to AAA1-A434C was measured upon excitation at 488 nm. Emission spectra of the Alexa 532 label attached to AAA2-R781C was measured upon excitation at 528 nm. In green is the emission spectrum of a complex of AAA1-A434C$^{*Alexa\ 488}$ and AAA2-R781C$^{*Alexa\ 532}$ (FRET pair). In red is the emission spectrum of FRET pair after subtraction of acceptor emission spectrum.

Since $ClpB_{Tth}$ is a thermophilic protein, FRET experiments were performed at elevated temperatures to observe effective energy transfer. First, the effect of elevated temperature (25-45°C) on excitation and emission maxima of the fluorescent labels was studied. Emission and excitation scans for both AAA1-A434C*$^{Alexa\ 488}$ and AAA2-R781C*$^{Alexa\ 532}$ were performed (Fig 3.22 A, B, C and D). No effect of increased temperature could be observed on excitation and emission maxima for Alexa 488 and Alexa 532 labels. Hence, energy transfer experiments were performed at 45°C. However, a general trend of a decrease in fluorescence intensity for Alexa 488 and an increase for Alexa 532 could be observed with increasing temperature.

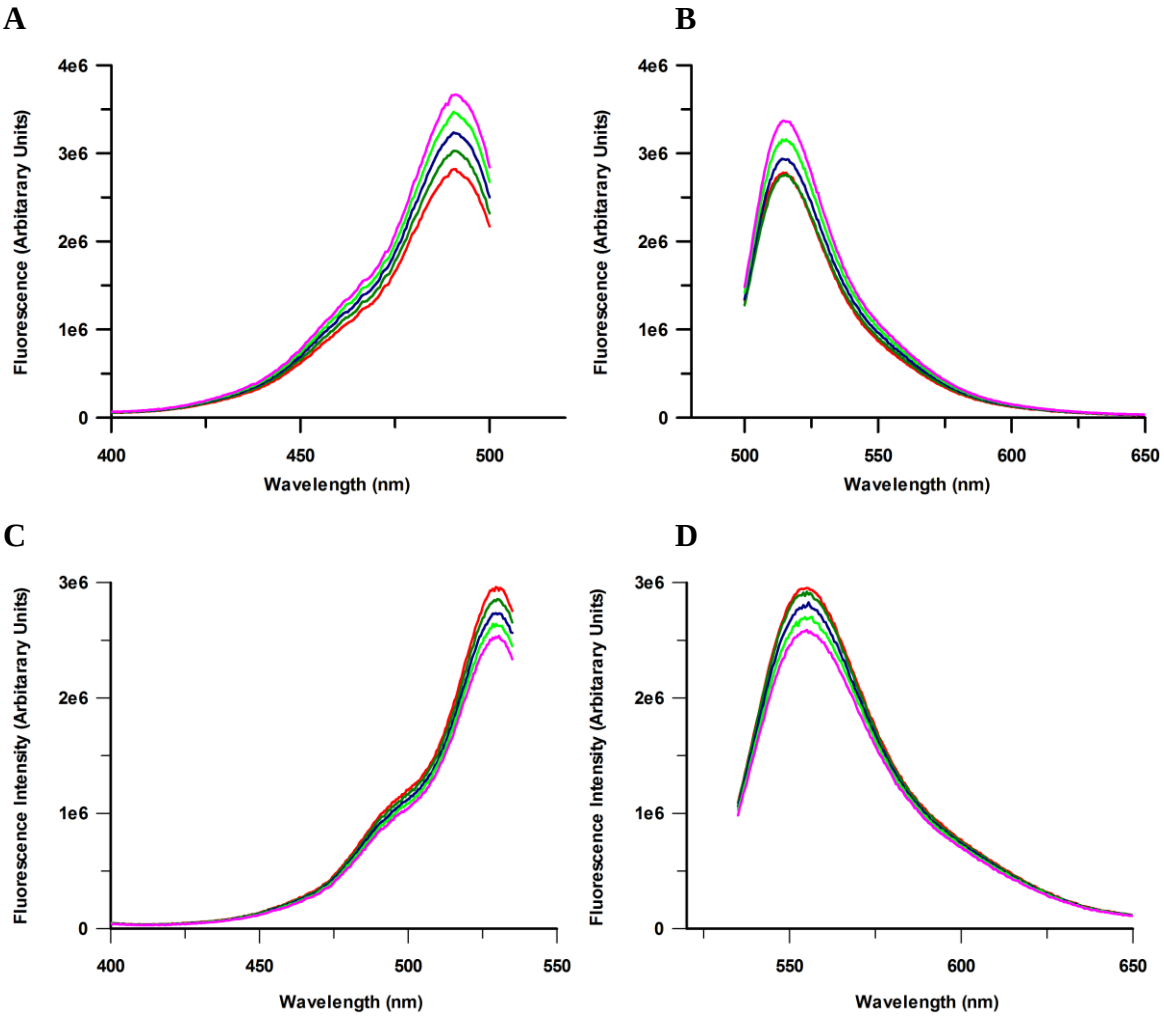

Fig 3.22: Effect of temperature on excitation and emission maxima of AAA1-A434C*$^{Alexa\ 488}$ and AAA2 R781C*$^{Alexa\ 532}$. 25°C - Fuchsia, 30°C - Lime, 35°C - Blue, 40°C - Green and 45°C – Red. **(A)** Excitation spectra of the Alexa 488 label attached to AAA1-A434C, at an emission maximum of 532 nm. **(B)** Emission spectra of the Alexa 488 label attached to AAA1-A434C, at an excitation maximum of 488 nm. **(C)** Excitation spectra of the Alexa 532 label attached to AAA2-R781C, at an emission maximum of 555 nm. **(D)** Emission spectra of the Alexa 532 label attached to AAA2-R781C, at an excitation maximum of 528 nm.

Interestingly, at 45°C presence of the acceptor resulted in an increase, in acceptor emission (Fig 3.23). These experiments hinted at temperature dependence in their interaction.

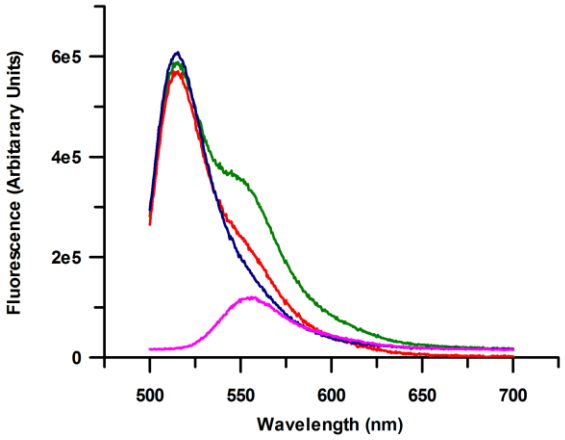

Fig 3.23: Fluorescence resonance energy transfer at 45°C. In blue and fuchsia are emission spectra of AAA1-A434C*$^{Alexa\ 488}$ (Donor) and AAA2-R781C*$^{Alexa\ 532}$ (Acceptor), respectively. Emission spectrum of the Alexa 488 label attached to AAA1-A434C was measured upon excitation at 488 nm. Emission spectra of the Alexa 532 label attached to AAA2-R781C was measured upon excitation at 528 nm. In green is the emission spectrum of a complex of AAA1-A434C*$^{Alexa\ 488}$ and AAA2-R781C$^{*Alexa\ 532}$ (FRET pair). In red is the emission spectrum of FRET pair after subtraction of acceptor emission spectrum.

3.2.3 ITC studies to investigate complex formation between the AAA modules of $ClpB_{Tth}$.

To understand the communication between the AAA modules from a thermodynamic point of view, experiments were performed to study binding between the isolated AAA modules. Although this complex formation is not physiologically relevant, binding between the AAA modules 1 and 2 was studied to gain insights into the nature of their communication. To determine the affinity and other thermodynamic parameters involved in the binding of the two AAA modules isothermal titration calorimetry experiments were performed.

Binding was studied at 25°C by titrating 97.2 μM AAA1 module to 9.39 μM AAA2 module in 29 injections of 10 uL each in a buffer containing 50 mM HEPES NaOH pH 7.5, 100 mM KCl, 5mM MgCl2 (Fig 3.24A) which yielded a very small heat exchange with each titration. Data analysis with a single site binding model yielded an association constant of 3.2 $x10^7$ M^{-1} and obtained ΔH, TΔS and stoichiometry of binding are shown (Table 3.10). Although the calculated stoichiometry of binding of 0.83 is close to the expected 1:1, the data obtained had a high error owing to the poorly fitted curve. Varying molar ratios of the reactants did not have any positive effect on the quality of the final titration curve (Data not shown).

To obtain a satisfactory titration curve, temperature of the experiment was changed to 45°C. Binding of 90 μM AAA1 module to 10 μM AAA2 module resulted in a pronounced heat exchange in the ITC experiment (Fig 3.24B). Data analysis using a single site binding equation yielded an association constant of around 1.4 $x10^8$ M^{-1}. Calculated dissociation constant and ΔG and obtained ΔH, TΔS and stoichiometry of binding are listed (Table 3.10). The stoichiometry of binding 0.78:1 is close to the expected 1:1 binding, the deviation possibly due to error in protein concentration estimation.

A **B**

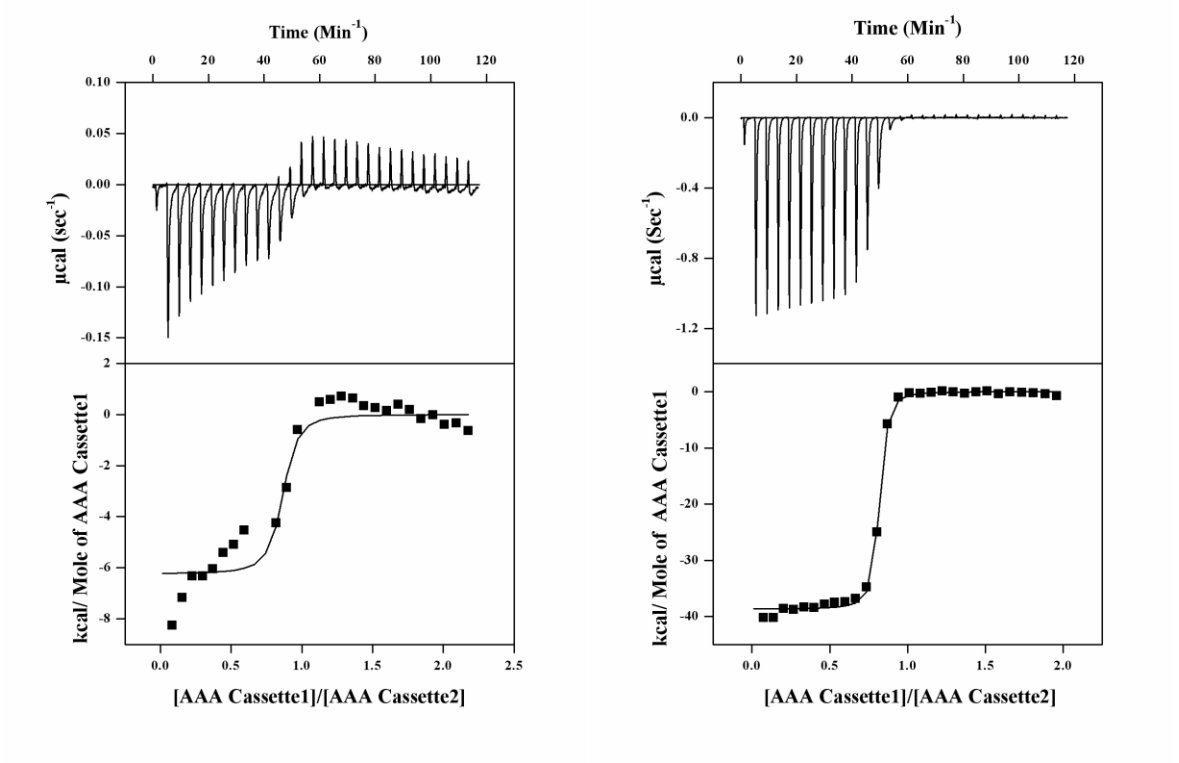

Fig 3.24: (A) Isothermal Titration Calorimetry at 25°C. The upper part of the figure features thermodynamics of heat release due to the addition of the AAA1 module to the AAA2 module at 25°C. The lower part of the figure shows a plot of heat release and molar ratio of the AAA1 module and the AAA2 module. Fitting the data with a one site binding model yielded a stoichiometry of 0.8 and an association constant of 3.2 X 10^7 M^{-1}. (**B) Isothermal Titration Calorimetry at 45°C.** The upper part of the figure features thermodynamics of heat release due to the addition of the AAA1 module to the AAA2 module at 45 ^{0}C. The lower part of the figure shows a plot of heat release and molar ratio of the AAA1 module and the AAA2 module. Fitting the data with a one site binding model yielded a stoichiometry of 0.7 and an association constant of 1.4 X 10^8 M^{-1}.

Temperature	K_D	N	ΔH (kcal/mol)	TΔS (kcal/mol)	ΔG (kcal/mol)
25°C	31 nM	0.83	-6.2	3.9	-10.1
45°C	7 nM	0.78	-38.7	-27	-11.7

Table 3.10: Table for thermodynamic parameters for complex formation between the isolated AAA modules at 25°C and 45°C.

3.3 Mutagenesis studies to decipher communication between the AAA modules in $ClpB_{Tth}$.

To understand heterotypic communications (between non-identical AAA modules of the same subunit) in $ClpB_{Tth}$ hexamer with minimal perturbation, examination of the interface between AAA modules was undertaken. Based on the published crystal structure (Lee et al., 2003), amino acids interacting at the interface were mutated to either alanine or an uncharged counterpart. Mutant proteins were examined for deviations in characteristic features like, (a) Nucleotide-dependent oligomerization (b) Refolding of heat denatured substrate proteins (c) Steady-state ATP hydrolysis.

3.3.1 Studies on interface mutant proteins in $ClpB_{Tth}$.

3.3.1.1 Crystal structure analysis of the interface between the AAA modules in $ClpB_{Tth}$.

For site directed mutagenesis, amino acids interacting at the interface between the AAA1 and AAA2 modules of $ClpB_{Tth}$ (PDB File: 1QVR Mol A) was analyzed using LIGPLOT (Methods 2.7). A total of 22 amino acids from the AAA1 module and 6 amino acids from the AAA2 module were predicted to be interacting at the interface (Fig 3.25A). Amino acids present at the interface belonged to SD1 and NBD1 of the AAA1 module and NBD2 of the AAA2 module (Fig 3.25B). There are in total 7 hydrogen bonds involving 13 different amino acids whereas, 16 amino acids are involved in hydrophobic interactions. Out of the 29 amino acids, four residues are strictly conserved between $ClpB_{Tth}$, $ClpB_{E\ coli}$ and $Hsp104_{Yeast}$ (Y371, I526, V521, and A360). The importance of each amino acid was investigated by replacing it with alanine to remove interactions arising from atoms after the β carbon. A substitution with uncharged counterpart was done in the case of charged amino acids that form hydrogen bonds. Glutamic acid was replaced with glutamine, to remove the hydrogen bond formed by the carboxyl oxygen in the side chain. Aromatic amino acid such as tyrosine was mutated to phenylalanine to infer the importance of hydrogen bond formed by the phenyl oxygen. Hydrogen bonds formed by polar, uncharged amino acids like serine were studied by replacing it with alanine. Importance of all the 7 hydrogen bonds was tested by mutating at least one of the partners (E545, E528, E523, R355, S357, Y371, and H369). Hydrophobic amino acids isoleucine 529 and valine 521 were also mutated to alanine separately (Table 3.11).

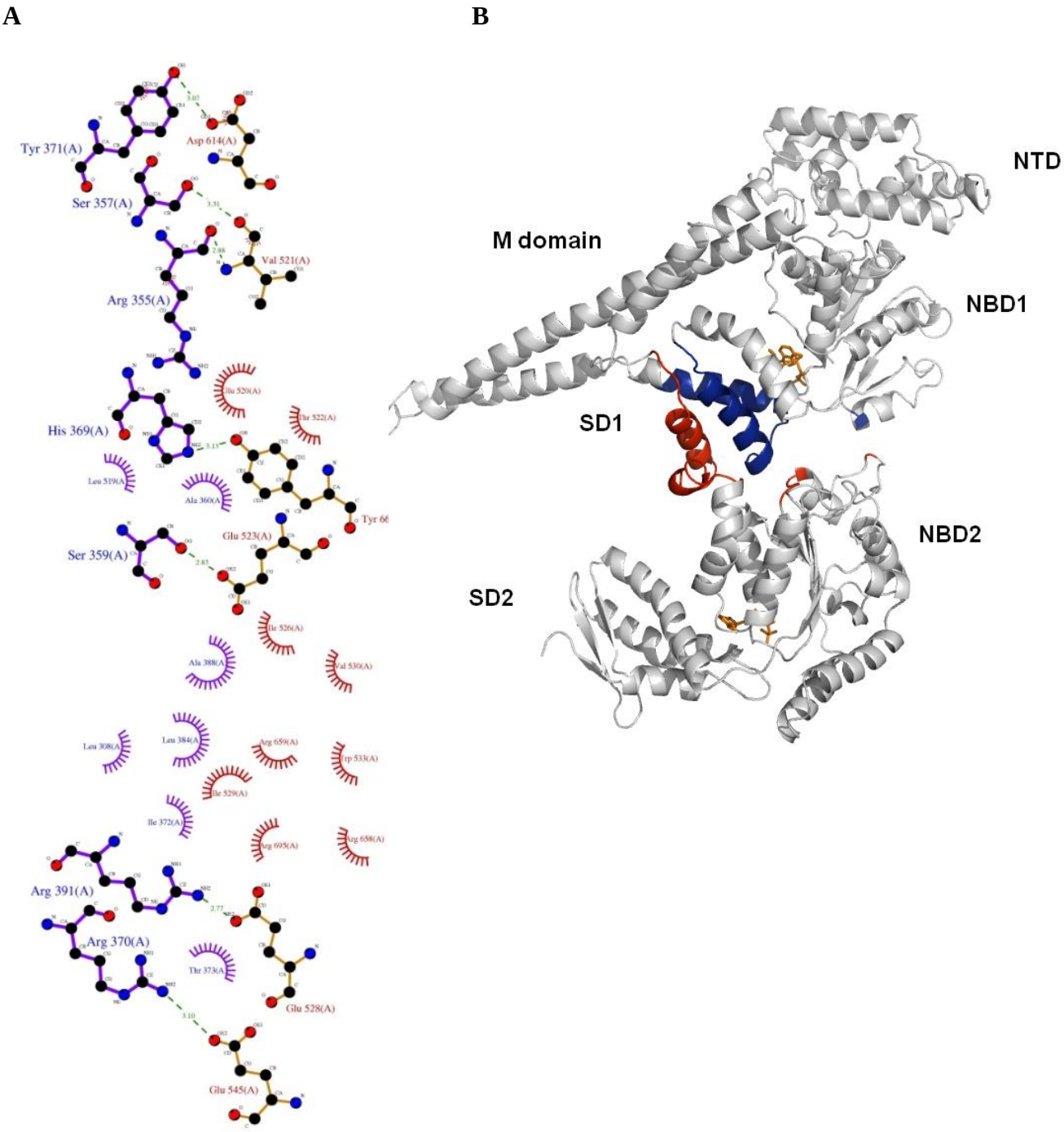

Fig 3.25: Interface between the AAA modules in ClpB$_{Tth}$. (A) In the figure are amino acid residues interacting at the interface between the AAA modules of ClpB$_{Tth}$. In blue are the residues of ClpB$_{Tth}$ from AA 1-519 and in red are the residues from AA 520-854. **(B)** A Ribbon representation of ClpB$_{Tth}$ with areas that form the interface between the AAA modules highlighted in color (Blue: AAA1 module and Red: AAA2 module). Structural data were obtained from PDB entry 1QVR (Lee et al., 2003) and rendered using Pymol software. Bound AMP-PNP molecules are highlighted in orange in stick representation.
NTD (AA 1-152), NBD1 (AA 153-331), SD1 (AA 332-400 and 519-535), M domain (AA 401-518), NBD2 (AA 536-758) and SD2 (759-854)

Amino Acid	Type of interaction	Substitution
I529	Hydrophobic Interaction	A
V521	Hydrophobic Interaction	A
E545	Hydrogen Bond #1	Q
E528	Hydrogen Bond #2	Q
E523	Hydrogen Bond #3	Q
H369	Hydrogen Bond #4	A
R355	Hydrogen Bond #5	A
S357	Hydrogen Bond #6	A
Y371	Hydrogen Bond #7	F

Table 3.11: List of amino acids selected for mutagenesis.

3.3.1.2 Purification of the interface mutants of ClpB$_{Tth}$.

Both wild type ClpB$_{Tth}$ and the interface mutants were purified using immobilized metal ion affinity chromatography and gel permeation chromatography (Methods 2.3.3). ClpB-H369A precipitated during purification resulting in no purified protein. The purity of wild type ClpB$_{Tth}$ and the interface mutant proteins was assessed by 10% poly-acrylamide gel electrophoresis. Purified proteins were analyzed for the type and amount of intrinsic nucleotide by HPLC based reverse phase chromatography (Methods 2.3.4). Neither wild type ClpB$_{Tth}$ nor any of the interface mutants revealed any intrinsic nucleotide upon comparison with the chromatograms of standard nucleotides (Data not shown).

3.3.1.3 ATP hydrolysis properties of the interface mutants of ClpB$_{Tth}$.

ATP hydrolysis by ClpB$_{Tth}$ follows sigmoidal kinetics under multi turnover conditions (0.02 to 2 mM ATP), signifying the importance of communication between both the AAA modules (Parsell et al., 1994; Schirmer et al., 2001; Schlee et al., 2001). Hence, the influence of interface mutations on the ATPase activity of ClpB$_{Tth}$ was studied here (Methods 2.4.2). For wild type ClpB$_{Tth}$, the plot of obtained rate constants versus Mg*ATP concentration when analyzed with the Hill equation yielded a k_{cat} of 2.81 ±0.07 min^{-1}, a Hill coefficient of 4.79 ±0.48 and a K_m value of 0.36 ±0.008 mM ATP (Fig 3.26). The k_{cat} value obtained here is in agreement with 2.65 min^{-1} reported for wild type ClpB$_{Tth}$ (Schlee et al., 2001), but slightly lower than 3.9 min^{-1}

reported in a separate study for the same protein (Beinker et al., 2002). These changes cannot be attributed to changes in protein purification protocols, since both the studies mentioned above have followed similar purification protocols. These deviations could probably arise from changes in total active protein from one purification batch to the other, or possible stimulation due to higher impurity content (aggregated or misfolded proteins).

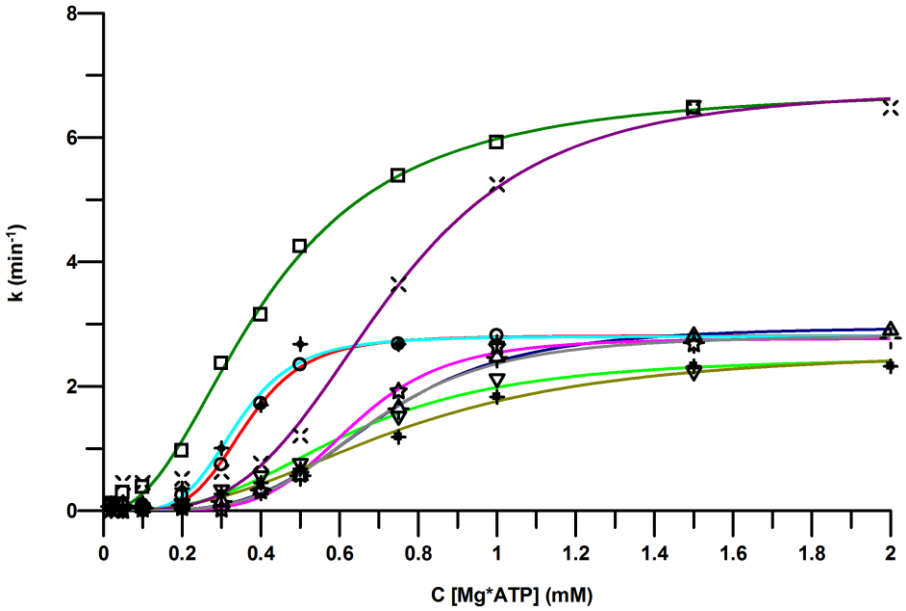

Fig 3.26: ATP hydrolysis by the interface mutants. Steady-state ATPase activity of 10 µM wild type $ClpB_{Tth}$ and the interface mutants was measured at 25°C using ATP regenerative system. The obtained rate constants were plotted against Mg*ATP concentration. The solid line represents data fitted with the Hill equation.
Wild type $ClpB_{Tth}$ (Red), I529A (Green), V521A (Navy), E545Q (Lime), E528Q (Fuchsia), E523Q (Aqua), S357A (Olive), R355A (Purple) Y371F (Gray)

Protein	k_{cat} (min^{-1})	K_m (mM)	n
$ClpB_{Tth}$	2.81 ±0.07	0.36 ±0.008	4.79 ±0.48
I529A	6.80 ±0.21 ↑	0.41 ±0.01 ↑	2.23 ±0.17↓
V521A	2.95 ±0.06	0.69 ±0.01 ↑	4.06 ±0.28
E545Q	2.47 ±0.13	0.62 ±0.03 ↑	2.93 ±0.32↓
E528Q	2.77 ±0.06	0.63 ±0.01 ↑	4.80 ±0.50
E523Q	2.80 ±0.10	0.34 ±0.01	4.80 ±0.30
R355A	5.40 ±0.22 ↑	0.60 ±0.02 ↑	4.20 ±0.48
S357A	2.60 ±0.12	0.75 ±0.04 ↑	2.58 ±0.24↓
Y371F	2.82 ±0.06	0.68 ±0.01 ↑	4.25 ±0.31

Table 3.12: ATPase activity of the interface mutants.

All the interface mutants tested were active in ATP hydrolysis, under steady-state conditions (Fig 3.26) (Table 3.12). E523Q mutation resulted in no change in all the kinetic parameters obtained, when compared to wild type $ClpB_{Tth}$. However, the rest of the interface mutants showed minor deviations from values obtained for wild type $ClpB_{Tth}$, most commonly an increase in the K_m value. V521A, E545Q, E528Q, E523Q, and Y371F resulted in similar turnover numbers when compared with wild type $ClpB_{Tth}$, but I529A and R355A mutants yielded higher turnover numbers. The Hill coefficient value remained the same as that obtained for wild type $ClpB_{Tth}$ in most of the interface mutants tested, except I529A, S357A and E545Q. I529A is the only mutation that resulted in an alteration, in all the kinetic parameters of ATP hydrolysis.

3.3.1.4 Oligomeric state analysis of the interface mutants of $ClpB_{Tth}$.

Experiments on ATP hydrolysis by the interface mutants revealed that changes at the interface, in most cases, translated to a reduction in the affinity for ATP (Table 3.12). Since hexamer formation, in $ClpB_{Tth}$, is nucleotide- and ionic strength-dependent, any changes for affinity towards nucleotides, might translate into changes in the oligomeric profile. Hence, the effect of the interface mutations on the ability of $ClpB_{Tth}$ to form ionic strength- and nucleotide-dependent oligomers was tested. Experiments were performed using gel permeation chromatography coupled with multi-angle light scattering measurements (Methods 2.6). Molar mass distribution analysis was performed using manufacturer's software (ASTRA Version 5.1.4.3 Wyatt Tech Corp.). Ionic strength dependent oligomer formation was studied at two different KCl concentrations (100mM and 200mM). Nucleotide-dependent oligomer formation was studied in the presence of 0.5mM ADP or ATP.

At 100 mM KCl concentration, 85% of wild type $ClpB_{Tth}$ was in the molar mass range of 330-420 kDa (Tetramer). The peak portion of the chromatogram, which accounted for half of the injected protein, yielded a molar mass of 371 kDa (Fig 3.27A and Table 3.13). E545Q mutation was the only interface mutation that showed molar masses in the range of hexamers (28% in the range of 500-600 kDa) at 100 mM KCL concentration (Fig 3.27A and Table 3.13). For the mutants E528Q, R355A and Y371F peak portion of the chromatograms (40% of injected protein) corresponded with a molar mass of 371 kDa, 332 kDa and 330 kDa (tetramer) respectively, which is similar to that observed for wild type $ClpB_{Tth}$ (Table 3.13). However, E528Q mutation

also resulted in elevated amounts (41%) of oligomers in the range of 420-510 kDa compared to 0.2% observed for wild type $ClpB_{Tth}$ (Fig 3.27A and Table 3.13). For the remaining interface mutants, the predominant species in molar mass distribution analysis remained mostly in the range of 240-330 kDa (Trimer). For I529A (300 kDa), V521A (320 kDa) and E523Q (300 kDa) peak portions of the chromatograms corresponded to a molar mass in lower 300s indicating a shift towards trimers (Table 3.13).

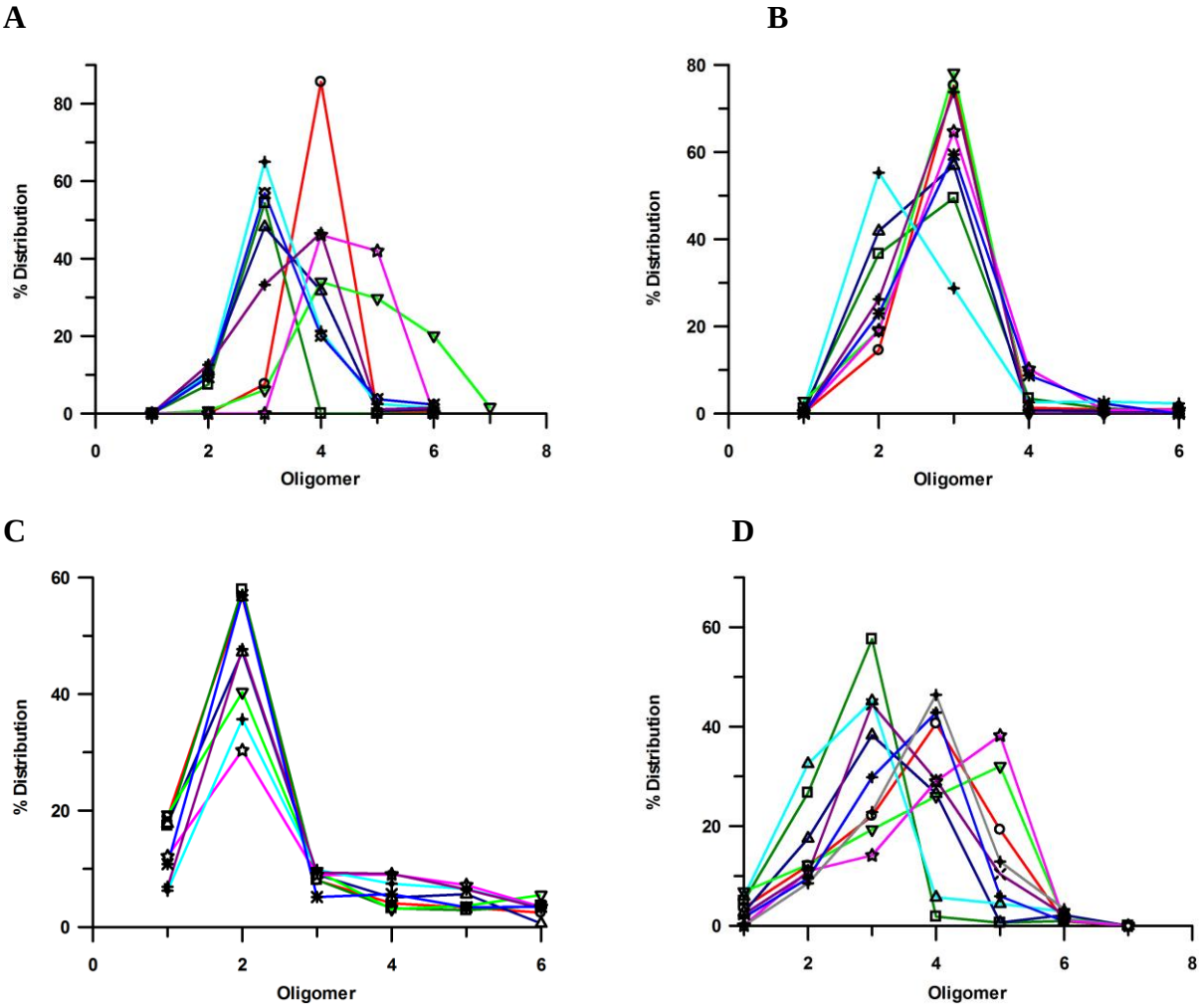

Fig 3.27: Oligomeric state of wild type $ClpB_{Tth}$ and the interface mutants. Fractional distribution of various molar mass species obtained for wild type ClpB and the interface mutants.
(A) In buffer containing 50 mM Tris-HCl pH 7.5, 100 mM KCl and 5 mM MgCl2.
(B) In buffer containing 50 mM Tris-HCl pH 7.5, 200 mM KCl and 5 mM MgCl2.
(C) In buffer containing 50 mM Tris-HCl pH 7.5, 100 mM KCl, 5 mM MgCl2 and 0.5 mM ADP.
(D) In buffer containing 50 mM Tris-HCl pH 7.5, 100 mM KCl, 5 mM MgCl2 and 0.5 mM ATP.
Wild type $ClpB_{Tth}$ (Red), I529A (Green), V521A (Navy), E545Q (Lime), E528Q (Fuchsia), E523Q (Aqua), S357A (Blue), R355A (Purple), Y371F (Gray)

M. Wt (kDa)	WT	I529A	V521A	E545Q	E528Q	E523Q	R355A	S357A	Y371F
80-150 (M)	0	0.04	0	0	0	0	0	0	0.07
150-240 (D)	0	7.47	10.89	0.71	0	9.96	12.55	9.37	12.28
240-330 (Tr)	7.55	**54.33**	**48.16**	6.06	0	**64.96**	**33.22**	**56.9**	**40.72**
330-420 (Te)	**85.64**	29.81	**31.66**	**33.94**	**46.08**	**21.17**	**46.63**	**20.05**	**39.12**
420-510 (P)	0.20	1.20	0.65	**29.70**	**41.98**	2.48	1.04	3.69	1.07
510-600 (H)	0.58	1.69	1.08	**20.07**	0.04	1.43	1.45	2.30	1.31

Table 3.13: Distribution of various molar mass species for wild type $ClpB_{Tth}$ and the interface mutants. M: Monomer; D: Dimer; Tr: Trimer; Te: Tetramer; P: Pentamer; H: Hexamer. All the numbers shown here are % of the total protein injected.

At 200 mM KCl, for wild type $ClpB_{Tth}$, molar mass distribution analysis revealed that 75% of the injected protein was in the range of 240-330 kDa, suggesting the predominant species to be a trimer (Fig 3.27B and Table 3.14). The peak portion of the chromatogram yielded a molar mass of 293 kDa. E545Q mutation showed a similar oligomeric profile like the wild type protein with 78% of the injected protein in the range of 240-330 kDa, suggesting a trimer. E528Q, R355A and Y371F mutants also predominantly formed trimers with 65%, 73% and 67% of the injected masses in the range of 240-330 kDa respectively. Interface mutants I529A, V521A and E523Q formed a mixture of trimers and dimers, with E523Q forming maximum amount of dimers (55%).

M. Wt (kDa)	WT	I529A	V521A	E545Q	E528Q	E523Q	R355A	S357A	Y371F
80-150 (M)	0.19	1.15	0	2.83	0.26	1.36	0	0	0.72
150-240 (D)	14.51	**36.59**	**41.86**	19.06	**19.06**	**55.23**	**26.25**	22.94	**24.04**
240-330 (Tr)	**75.26**	**49.44**	**56.88**	**78.11**	**64.73**	**28.75**	**73.75**	59.39	**67.62**
330-420 (Te)	1.34	3.42	0.70	0	10.21	2.56	0	8.74	1.41
420-510 (P)	0.94	1.19	0.57	0	0.79	2.74	0	2.27	1.70
510-600 (H)	0.95	0.66	0.00	0	0.86	2.34	0	0	1.89

Table 3.14: Distribution of various molar mass species for wild type $ClpB_{Tth}$ and the interface mutants. M: Monomer; D: Dimer; Tr: Trimer; Te: Tetramer; P: Pentamer; H: Hexamer. All the numbers shown here are % of the total protein injected.

In the presence of 0.5 mM ADP molar mass distribution analysis resulted in the following observations. Wild type $ClpB_{Tth}$ predominantly formed dimers with 56% of the injected protein

present in the range of 150-240 kDa. Most of the interface mutants studied did not show any substantial difference in molar masses obtained, when compared with wild type $ClpB_{Tth}$ (Fig 3.27C and Table 3.15). However, Y371F mutation resulted in an increased amount of trimers, with a higher fraction of injected protein in a molar mass range between 240-330 kDa.

M. Wt (kDa)	WT	I529A	V521A	E545Q	E528Q	E523Q	R355A	S357A	Y371F
80-150 (M)	**18.87**	**17.40**	**17.73**	**19.28**	**12.13**	6.23	6.91	**10.80**	2.22
150-240 (D)	**56.65**	**57.91**	**47.22**	**40.30**	**30.33**	**35.65**	**47.70**	**56.95**	**37.46**
240-330 (Tr)	8.01	8.08	9.01	9.56	8.93	**9.81**	**9.33**	5.15	**37.62**
330-420 (Te)	4.05	3.19	5.04	3.06	9.02	7.42	9.13	5.62	7.54
420-510 (P)	3.35	2.90	5.62	3.62	7.17	6.52	6.42	3.39	2.07
510-600 (H)	2.45	3.65	0.60	5.48	3.48	3.27	3.24	3.48	1.42

Table 3.15: Distribution of various molar mass species for wild type $ClpB_{Tth}$ and the interface mutants. M: Monomer; D: Dimer; Tr: Trimer; Te: Tetramer; P: Pentamer; H: Hexamer. All the numbers shown here are % of the total protein injected.

Wild type $ClpB_{Tth}$ in the presence of 0.5 mM ATP formed a wide range of oligomers (Tetramers (22%), Pentamers (40%) and Hexamers (19%)) (Fig 3.27D and Table 3.16). All the interface mutants studied showed no loss of ATP-dependent oligomer formation, with E545Q and E528Q mutants showing a tendency to form more pentamers (32% and 38% respectively) compared to wild type $ClpB_{Tth}$ (19%). I529A, V521A, E528Q, R355A and Y371F formed relatively lower order oligomers when compared to wild type $ClpB_{Tth}$ (Table 3.16).

M. Wt (kDa)	WT	I529A	V521A	E545Q	E528Q	E523Q	R355A	S357A	Y371F
80-150 (M)	3.63	4.98	2.71	6.82	0.02	5.89	2.31	1.69	0.30
150-240 (D)	12.03	**26.7**	**17.54**	12.22	10.98	**32.54**	10.59	9.52	8.50
240-330 (Tr)	**22.05**	**57.6**	**38.29**	**19.32**	**14.12**	**45.19**	**44.50**	**29.83**	**22.83**
330-420 (Te)	**40.65**	1.82	**26.54**	**26**	**29.01**	5.72	**29.28**	**42.84**	**46.39**
420-510 (P)	**19.29**	0.58	0.63	**32.04**	**38.21**	4.4	10.35	5.92	12.86
510-600 (H)	0.88	0.94	2.16	1.37	1.09	2.81	2.18	0.86	3.34

Table 3.16: Distribution of various molar mass species for wild type $ClpB_{Tth}$ and the interface mutants. M: Monomer; D: Dimer; Tr: Trimer; Te: Tetramer; P: Pentamer; H: Hexamer. All the numbers shown here are % of the total protein injected.

Data obtained for ATP measurements most possibly represents the lower limits for oligomer formation, due to ATP hydrolysis properties of $ClpB_{Tth}$. The introduction of point mutations at the interface between AAA modules in $ClpB_{Tth}$ does not appear to have any drastic effects on its ability to form ionic strength- and nucleotide-dependent oligomers (Table 3.17). The mutations, which resulted in reduced affinity for ATP in ATP hydrolysis, did not alter nucleotide-dependent oligomer formation. However, the interface mutant I529A which resulted in deviations in all the kinetic parameters formed slightly lower order oligomers, when compared to wild type $ClpB_{Tth}$ (Table 3.17). E528Q mutation, which did not show any deviation from wild type in the ATP hydrolysis assay also showed formation of oligomers of lower order.

	Predominant Oligomeric state			
Mutation	**100 mM KCl**	**200 mM KCl**	**ATP**	**ADP**
WT	Tetramer	Trimer	Tetramer	Dimer
I529A	Trimer	Trimer	Trimer	Dimer
V521A	Trimer	Trimer	Trimer	Dimer
E545Q	Tetra/ Penta	Trimer	Pentamer	Dimer
E528Q	Tetra/ Penta	Trimer	Pentamer	Dimer
E523Q	Trimer	Dimer	Trimer	Dimer
R355A	Tetramer	Trimer	Tetramer	Dimer
Y371F	Tetramer	Trimer	Tetramer	Dimer
S357A	Tetramer	Trimer	Tetramer	Dimer

Table 3.17: Predominant oligomeric species for wild type $ClpB_{Tth}$ and the interface mutants.

3.3.1.5 Refolding of denatured α-Glucosidase and Lactate dehydrogenase by the interface mutants of $ClpB_{Tth}$.

Allostery in ATP hydrolysis, by $ClpB_{Tth}$ has always been shown to be essential for its ability to refold heat denatured substrate proteins. If heterotypic allostery between the AAA modules during nucleotide hydrolysis is essential for chaperone activity, then the interface mutants (I529A, R355A, E545Q) with the altered Hill coefficient should have altered refolding abilities. Hence, all the interface mutants were tested for their ability to refold heat denatured α-Glucosidase and Lactate dehydrogenase (LDH), in two separate assays.

All the interface mutants were active in refolding of both α-Glucosidase and LDH and followed refolding kinetics similar to wild type $ClpB_{Tth}$ (Fig 3.28). In refolding of heat denatured α-Glucosidase, wild type $ClpB_{Tth}$ yielded 30% of native activity (Table 3.18). Interface mutants E528Q and V521A resulted in slightly higher refolding yields compared to wild type $ClpB_{Tth}$, whereas R355A showed a slightly lower yield (Table 3.18). I529A, E545Q, E523Q and Y371F resulted in refolding yields very close to that of wild type $ClpB_{Tth}$ (Table 3.18).

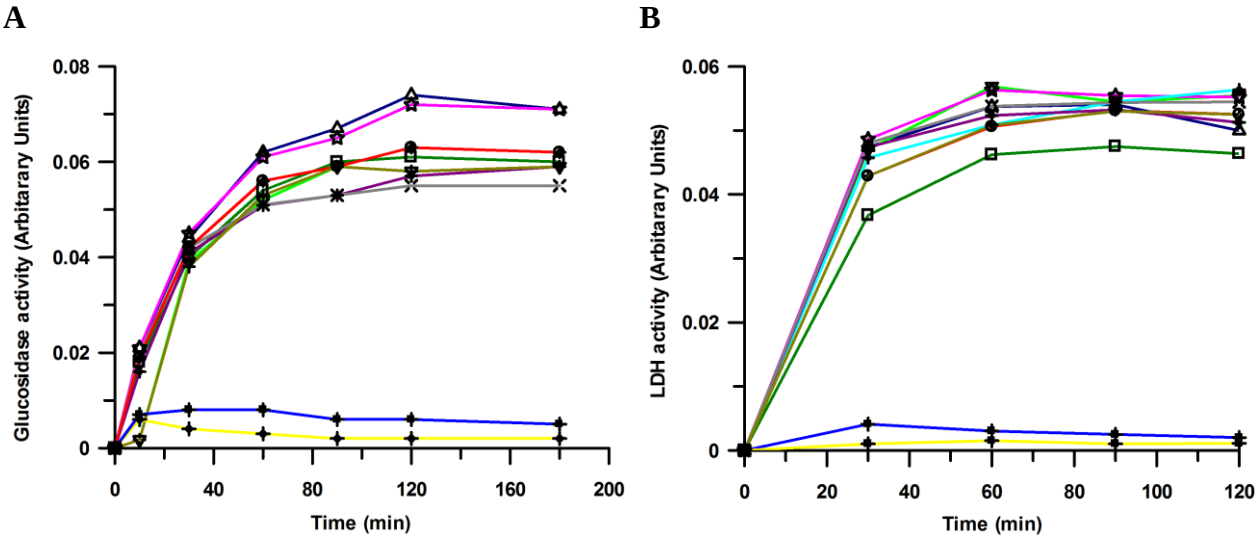

Fig 3.28: Refolding of heat denatured substrate proteins by the interface mutants of $ClpB_{Tth}$.
(A) Refolding of heat denatured α-Glucosidase by wild type $ClpB_{Tth}$ and the interface mutants. α-Glucosidase, upon denaturation at 75°C for 10 min, was subjected to refolding at 55°C in the presence of 1.0 µM $ClpB_{Tth}$ (Wild type or Interface mutant), 1.6 µM $DnaK_{Tth}$, 0.4 µM $DnaJ_{Tth}$, and 0.4 µM $GrpE_{Tth}$. **(B)** Refolding of heat denatured Lactate dehydrogenase by WT $ClpB_{Tth}$ and the interface mutants. Lactate dehydrogenase, upon denaturation at 80°C for 30 min, was subjected to refolding at 55°C for 120 min in the presence of 1.0 µM $ClpB_{Tth}$ (Wild type or Interface mutant), 1.6 µM $DnaK_{Tth}$, 0.4 µM $DnaJ_{Tth}$, and 0.4 µM $GrpE_{Tth}$.
Wild type $ClpB_{Tth}$ (Red), I529A (Green), V521A (Navy), E545Q (Lime), E528Q (Fuchsia), E523Q (Aqua), S357A (Olive), R355A (Purple), Y371F (Gray)
Activity of refolded α-Glucosidase at various time points during the refolding reaction was plotted against time (min). The blue and yellow lines represent activity of (A) α-Glucosidase and (B) LDH after refolding in the presence of $DnaK_{Tth}$ system alone and no chaperones respectively.

In refolding of heat denatured LDH, wild type $ClpB_{Tth}$ yielded 60% of native activity. Interface mutants I529A, R355A and V521A resulted in slightly lower refolding yields, whereas, E545Q, E528Q, E523Q and Y371F resulted in slightly higher refolding yields (Table 3.18). The results of refolding assays suggest that changes in ATP hydrolysis properties of $ClpB_{Tth}$, due to mutations at the interface between AAA modules, did not alter its refolding ability significantly. The mutations (I529A, E545Q and S357A) that reduced the Hill coefficient did not have any effect on refolding capacity of $ClpB_{Tth}$.

Mutation	α-Glucosidase assay	LDH assay
WT	100	100
I529A	96.77	88.46
V521A	114.51	96.15
E545Q	95.16	106.73
E528Q	114.51	106.15
E523Q	100	108.46
R355A	88.70	98.46
Y371F	95.16	104.61
S357A	95.16	100.96

Table 3.18: Refolding yields of the interface mutants. Catalysis of cleavage of the glycosidic bond in p-nitrophenyl-α-D-glucopyranoside by refolded α-Glucosidase, and catalysis of conversion of pyruvate to lactate by refolded LDH was quantified, and expressed as a fraction of its native activity regained. Native activity refers to the activity of α-Glucosidase or LDH prior to heat denaturation. The yield in refolding of α-Glucosidase or Lactate dehydrogenase by wild type $ClpB_{Tth}$ was taken as 100%, to which all the interface mutants were compared.

I529A mutant was the only protein that resulted in alterations in all the kinetic parameters of ATP hydrolysis (Results 3.3.1.3). Reduction in affinity towards ATP did not affect its ability to form higher order oligomers. Reduction in the Hill coefficient did not affect its chaperone activity (Results 3.3.1.5). Hence this mutation was studied in more detail in the following experiments.

3.3.2 Effect of I529A mutation on the isolated AAA2 module.

Although, amino acid isoleucine at position 529 is present on SD1 of the AAA1 module, it is located on the section of SD1 (AA 520-535) which is a part of the isolated AAA2 module construct (AA 520-854). The Hill coefficient obtained for I529A mutant (2.23 ±0.17) is similar to that of reported for the isolated AAA2 module (2.08 ±0.21) (Beinker et al., 2005). Hence, experiments were conducted to confirm whether I529A mutation has indeed been affecting the intended interface. If the decreased Hill coefficient value is due to impaired heterotypic allostery between the AAA modules of same subunit, then introduction of the I529A mutation (AAA2-I529A) should not have any effect on homotypic allostery exhibited by the isolated AAA2 module (Fig 3.29).

A

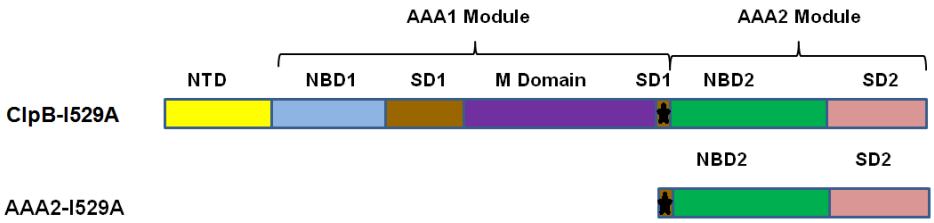

B

Fig 3.38: Structure of AAA2-I529A. (A) A Schematic depicting I529A mutation in the isolated AAA2 module of $ClpB_{Tth}$ (AAA2-I529A). Black asterisk indicates the location of the mutation.
(B) A ribbon representation of the isolated AAA2 module with I529A mutation highlighted in blue. NBD2 is shown in green and SD2 in pink; whereas, the part of SD1 (AA 519-535) that features I529A mutation is shown in brown. Structural data were obtained from PDB entry 1QVR (Lee et al., 2003) and rendered using Pymol software. Bound AMP-PNP molecule is highlighted in orange, in stick representation.
NTD- Yellow (AA 1-152), NBD1- Blue (AA 153-331), SD1- Brown (AA 332-400 and 519-535), M domain- Violet (AA 401-518), NBD2- Green (AA 536-758) and SD2- Pink (759-854)

3.3.2.1 Purification of AAA2-I529A.

Purified AAA2-I529A was assessed to be 95% pure using 10% poly acrylamide gel electrophoresis. AAA2-I529A was then analyzed for intrinsic nucleotide content using HPLC based reverse phase chromatography. AAA2-I529A protein was found to be nucleotide-free upon comparison with the chromatograms of standard nucleotides (Data not shown).

3.3.2.2 ATP hydrolysis properties of AAA2-I529A.

The ATPase activity of AAA2-I529A was measured and compared to the full-length I529A mutant and the wild type isolated AAA2 module (Methods 2.4.2). Upon analysis using the Hill equation, AAA2-I529A yielded a k_{cat} of 7.97 ±0.67 min^{-1}, which is close to that reported for the wild type isolated AAA2 module (6.9 min^{-1}) and also to that shown by full-length I529A (6.8 ±0.21 min^{-1}) (Fig 3.30). Introduction of the I529A mutation in the isolated AAA2 module did not affect its affinity towards ATP. The K_m value obtained for AAA2-I529A (0.83 ±0.07 mM) is similar to that reported for the wild type isolated AAA2 module (0.76 ±0.04 mM). Similarly, the Hill coefficient value obtained for AAA2-I529A (2.66 ±0.38) is also similar to the one reported for the wild type isolated AAA2 module (2.08 ±0.21) (Table 3.19). This, in turn, is also similar to that obtained for full-length I529A (2.23 ±0.17), suggesting that I529A mutation in full-length $ClpB_{Tth}$ is, in fact, affecting the interface between the AAA modules within the subunit.

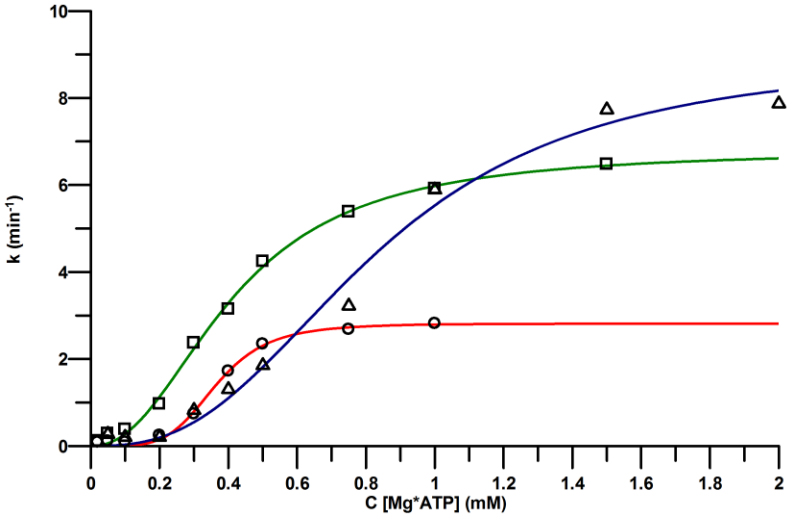

Fig 3.30: Steady-state ATPase activity. Steady-state ATPase activity of 10 µM wild type $ClpB_{Tth}$, interface mutant I529A and AAA2-I529A were measured at 25°C using ATP regenerative system. The obtained rate constants were plotted against Mg*ATP concentration. The solid line represents data fitted with the Hill equation. Wild type $ClpB_{Tth}$ (Red), I529A (Green) AAA2-I529A (Blue)

Protein	k_{cat} (min^{-1})	K_m (mM)	n
Wild type $ClpB_{Tth}$	2.81 ±0.07	0.36 ±0.008	4.79 ±0.48
ClpB I529A	6.80 ±0.21	0.41 ±0.01	2.23 ±0.17
AAA2-I529A	7.97 ±0.67	0.83 ±0.07	2.66 ±0.38

Table 3.19: ATPase activity of AAA2-I529A. Wild type $ClpB_{Tth}$ values are shown for comparison.

3.3.2.3 Refolding of denatured α-Glucosidase by AAA2-I529A.

The influence of I529A mutation on the ability of the isolated AAA2 module to form a functional complex with the isolated AAA1 module was assessed. A mixture of equimolar amounts of the wild type isolated AAA1 module and AAA2-I529A was prepared and its ability to refold heat denatured α-Glucosidase was studied and compared to the complex of wild type isolated AAA1 and AAA2 modules. Both the complexes refolded heat denatured α-Glucosidase to 15% of its native activity (Fig 3.31). Isolated AAA2-I529A alone did not show any refolding (Data not shown). This result suggests that the I529A mutation has no effect on the AAA2 module's ability to form a functional higher order complex upon reconstitution with the isolated AAA1 module.

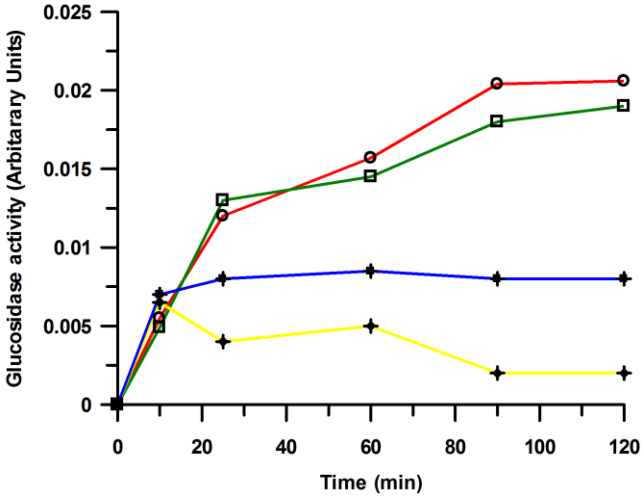

Fig 3.31: Chaperone activity. Refolding of heat denatured α-Glucosidase by the reconstituted complex of AAA1 module and AAA2-I529A (Green) was compared with the reconstituted complex of wild type AAA1 and AAA2 modules (Red). α-Glucosidase, upon denaturation at 75°C for 10 min, was subjected to refolding at 55°C for 120 min in the presence of 1.0 µM reconstituted complex, 1.6 µM $DnaK_{Tth}$, 0.4 µM $DnaJ_{Tth}$ and 0.4 µM $GrpE_{Tth}$. Activity of refolded α-Glucosidase at various time points during the refolding reaction was plotted against time (min). The blue and yellow lines represent activity of α-Glucosidase after refolding in the presence of $DnaK_{Tth}$ system alone and no chaperones respectively.

3.3.3 Effect of Guanidinium Chloride on ClpB$_{Tth}$ wild type and I529A.

The likelihood of contaminating ATPases and/or kinases coming from purification for I529A mutant, which might have given rise to the increased turnover numbers was investigated. For this purpose, studies on the effect of GdmCl on ClpB$_{Tth}$ ATPase were conducted. It was reported that, at very low concentrations (10 mM), GdmCl reduced the turnover in ATP hydrolysis of Hsp104$_{Yeast}$, by 50% (Grimminger et al., 2004). The effect was shown to be due to the specific action of Guanidinium ions on the nucleotide bound form of hexameric Hsp104$_{Yeast}$. The effect is specific to Hsp104$_{Yeast}$ ATPase, but not other ATPases like Na^+K^+ATPase. If GdmCl reduced ClpB$_{Tth}$ ATPase activity, a decrease of a similar extent should also be observed for the I529A mutant. This will hold true only when the high turnover observed in the ATPase activity of I529A is due to the mutation but not contamination.

3.3.3.1 Effect of Guanidinium chloride on ATP hydrolysis properties of wild type ClpB$_{Tth}$ and I529A.

To investigate the effect of GdmCl on ClpB$_{Tth}$ and I529A, ATPase assay was performed under steady-state conditions in the presence of 10 mM GdmCl (Methods 2.4.2). At ATP concentration of 1 mM, the turnover number of wild type ClpB$_{Tth}$ was reduced by 60% due to 10 mM GdmCl (Fig 3.32). However, at higher ATP concentration the turnover of ATP reached close to the normal levels. Along with a decreased turnover in ATPase activity, the presence of GdmCl also reduced the Hill coefficient from 4.79 to 1.76 (Table 3.20). The affinity for ATP decreased in the presence of GdmCl, where the K_m value increased from 0.36 to 0.84 mM ATP.

For I529A, at the ATP concentration of 1 mM, a 60% decrease in turnover was observed (Fig 3.32). Unlike wild type ClpB$_{Tth}$, the presence of GdmCl did not change the affinity for ATP, but the Hill coefficient decreased from 2.23 to 0.98. The decrease in turnover, in the presence of 10 mM GdmCl, for wild type ClpB$_{Tth}$ and I529A were of the same magnitude. This result indicates that the high turnover of I529A is most probably due to the mutation at the interface, and not due to any contaminating highly active ATPases.

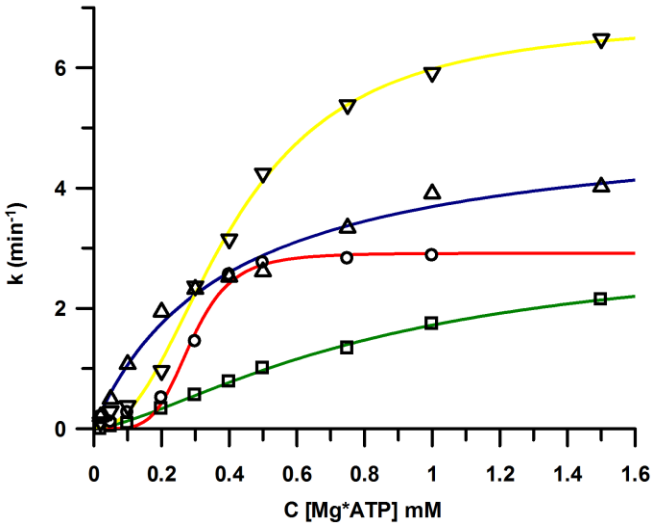

Fig 3.32: Steady-state ATPase activity. Steady-state ATPase activity of 10 µM wild type $ClpB_{Tth}$ and I529A, in the presence and absence of 10 mM GdmCl, was measured at 25°C using ATP regenerative system. The obtained rate constants were plotted against Mg*ATP concentration. The solid line represents data fitted with the Hill equation. Wild type $ClpB_{Tth}$ (Red), Wild type $ClpB_{Tth}$ +GdmCl (Green), I529A (Yellow), I529A +GdmCl (Blue)

Protein	k_{cat} (Min $^{-1}$)	K_m (mM)	n
Wild type $ClpB_{Tth}$	2.81 ±0.07	0.36 ±0.008	4.79 ±0.48
Wild type $ClpB_{Tth}$ + GdmCl	3.06 ±0.21	0.84 ±0.09	1.46 ±0.08
ClpB I529A	6.80 ±0.21	0.41 ±0.01	2.23 ±0.17
ClpB I529A+ GdmCl	5.19 ±0.64	0.40 ±0.11	0.98 ±0.14

Table 3.20: ATPase activity of $ClpB_{Tth}$ and I529A in the presence of 10 mM GdmCl.

3.3.3.2 Effect of Guanidinium chloride on refolding of denatured α-Glucosidase by wild type $ClpB_{Tth}$ and I529A.

The presence of Guanidinium chloride not only altered turnover in ATP hydrolysis by $ClpB_{Tth}$, but also affected the Hill coefficient. This observation provided a platform to study the importance of allosteric communications in chaperone activity of $ClpB_{Tth}$. If allosteric communications between the AAA modules, within each subunit of $ClpB_{Tth}$, are essential for its chaperone activity, then the presence of GdmCl should have a negative effect on chaperone activity by $ClpB_{Tth}$. This scenario will be similar to that observed in the case of I529A, where the mutation at the interface resulted in reduced Hill coefficient, but did not affect chaperone activity. Before studying the effect of GdmCl on chaperone activity of $ClpB_{Tth}$, its effect on the

substrate protein α-Glucosidase was investigated. Activity of α-Glucosidase was measured both in the presence and absence of 10 mM GdmCl before and after heat denaturation (Fig 3.33A). Activity of native α-Glucosidase (prior to heat denaturation) decreased by 22% due to the presence of 10 mM GdmCl. The presence of GdmCl did not have any effect on activity of heat denatured α-Glucosidase, since the protein has already lost all of its activity due to heat shock.

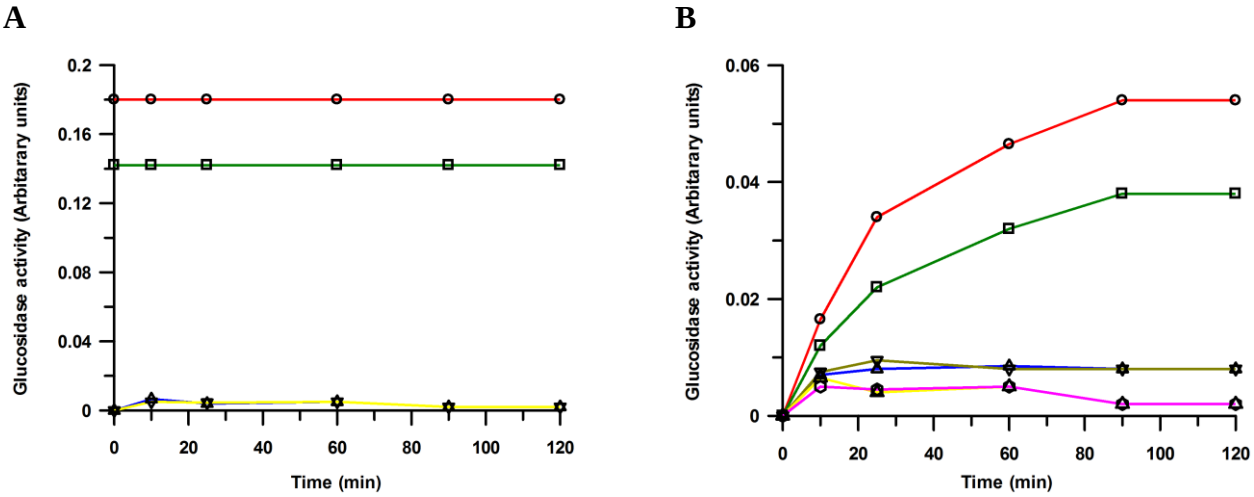

Fig 3.33: (A) Effect of 10 mM GdmCl on α-Glucosidase. Activity of α-Glucosidase prior to denaturation was measured in the presence (Green) and absence (Red) of 10 mM GdmCl. Activity of α-Glucosidase at various time points during the incubation was plotted against time (min). The blue and yellow lines represent activity of α-Glucosidase after heat denaturation in the presence and absence of 10 mM GdmCl respectively. **(B) Chaperone activity.** Refolding of heat denatured α-Glucosidase by wild type $ClpB_{Tth}$ both in the presence (Green) and absence (Red) of 10 mM GdmCl. α-Glucosidase, upon denaturation at 75°C for 10 min, was subjected to refolding at 55°C for 120 min in the presence of 1.0 µM $ClpB_{Tth}$ (WT), 1.6 µM $DnaK_{Tth}$, 0.4 µM $DnaJ_{Tth}$, and 0.4 µM $GrpE_{Tth}$. Activity of refolded α-Glucosidase at various time points during the refolding reaction was plotted against time (min). The blue and olive lines represent activity of α-Glucosidase after refolding with $DnaK_{Tth}$ system alone in the presence and absence of 10 mM GdmCl respectively. The yellow and fuchsia lines represent activity of α-Glucosidase after heat denaturation in the presence and absence of 10 mM GdmCl respectively.

The effect of 10 mM GdmCl on refolding of heat denatured α-Glucosidase by wild type $ClpB_{Tth}$ was studied. Wild type $ClpB_{Tth}$ resulted in 30% of α-Glucosidase native activity after refolding at 55 ^{0}C for 120 Min, whereas, in the presence of 10 mM GdmCl it resulted in 24% of α-Glucosidase native activity (Fig 3.33B). The minor difference in refolding yield is due to the effect of GdmCl on the stability of α-Glucosidase itself (Fig 3.33A). The presence of GdmCl did not influence the chaperone activity of $ClpB_{Tth}$, although it affected sigmoidal kinetics in ATPase activity. Based on this observation, it can be concluded that allosteric communications between the AAA modules in $ClpB_{Tth}$ may not be as essential, as initially assumed, for chaperone activity of ClpB from Thermus thermophlius.

4. DISCUSSION

4.1 Nucleotide-mediated conformational changes in the AAA modules of $ClpB_{Tth}$: Their role in inter-subunit communication and oligomer dissociation.

The two tandem AAA modules, in $ClpB_{Tth}$, interact in a complex nucleotide-dependent manner to achieve oligomerization, nucleotide hydrolysis and ultimately chaperone activity. Nucleotide-dependent oligomer formation is not only important for ATP hydrolysis but also essential for chaperone activity in $ClpB_{Tth}$. ATP induces higher order oligomer formation, whereas ADP drives the equilibrium towards lower order (Schlee et al., 2001). However, the mechanism through which different nucleotides affect oligomer formation and dissociation, and the individual domains and conformational changes involved still remains elusive. To break down the inherent complexity of the system, nucleotide-mediated conformational changes in the isolated AAA modules of $ClpB_{Tth}$ were attempted to study. The conformational changes through which the M domain of the AAA1 module and SD2 of the AAA2 module affect the nucleotide-dependent oligomeric state have been investigated. To achieve this, nucleotide binding to fluorescently labeled single-cysteine mutants of the isolated AAA modules was investigated.

At first, similarity of the cysteine mutants to the wild type proteins was confirmed. Both the single-cysteine mutants were similar to their wild type counterparts in oligomerization, ATP hydrolysis and their ability to form a functional protein, upon reconstitution (Results 3.1.1). The isolated AAA1 module with cysteine mutation remained monomeric like its wild type counterpart and showed no ATP hydrolysis (Results 3.1.1.3 and 3.1.1.4). The isolated AAA2 module with cysteine mutation hydrolyzed ATP and displayed oligomer formation like its wild type counterpart (Results 3.1.1.3 and 3.1.1.4). Both the cysteine mutants, upon reconstitution, refolded heat denatured substrate proteins indicating no loss of chaperone activity (Results 3.1.1.5). Experiments on nucleotide binding to the fluorescently labeled isolated AAA modules and experiments on the wild type isolated AAA2 module and wild type $ClpB_{Tth}$ (full-length) have resulted in the following observations:

1. ADP binding to the isolated AAA2 module resulted in an inter-subunit conformational change and followed biphasic binding with two different affinities.

2. Experiments using mixture of the wild type and the P-loop mutant AAA2 modules confirmed dimer formation, and that inter-subunit communication takes place in SD2 upon ADP binding at the neighboring AAA2 module.
3. Deletion of SD2 in the wild type isolated AAA2 module resulted in complete loss of oligomerization, nucleotide binding and hydrolysis and its ability to form a functional complex upon reconstitution with the isolated AAA1 module. A mutation conferring conformational rigidity at the loop connecting SD2 and NBD2 in the AAA2 module, in full-length $ClpB_{Tth}$, resulted in unstable protein and complete loss of function.
4. Homotypic allostery present between the AAA2 modules plays a key role in ADP-mediated oligomer dissociation. This occurs via inter-subunit conformational changes in SD2.
5. Addition of ATP to the isolated AAA1 module did not appear to result in any change, in the conformation of the M domain.

4.1.1 Mode of ADP binding and associated conformational changes in SD2 of the AAA2 module.

Addition of ATP and ADP both resulted in decrease of the fluorescence signal of the label located on SD2 of the isolated AAA2 module (Results 3.1.2.2). The signal decrease may represent a change in conformation or movement of SD2 (most probably away from the protein core) in the isolated AAA2 module. The reason for this similarity is most probably due to ATP hydrolysis by the isolated AAA2 module. In both the cases, signal changes observed are probably due to ADP binding since the isolated AAA2 module hydrolyzes ATP at a rate of 6.9/ min. In addition, fluorescence titration experiments showed that ADP binding to the isolated AAA2 module follows a biphasic mode implying two types of binding sites (Results 3.1.2.3). However, a similar observation could not be made in the isothermal titration calorimetric measurements (Results 3.1.2.4). The dissociation constant obtained was very close to the one obtained for high affinity binding. Even though, binding of ADP to the lower affinity site was actually occurring during the titration, the heat exchange was probably not significant enough to be detected. Alternately, low affinity value obtained for the second binding site is probably too low to be measured by ITC measurements.

More insights were gained into possible biphasic binding of ADP to the AAA2 module upon examination of the $ClpB_{Tth}$ crystal structure. In $ClpB_{Tth}$, nucleotides bind at the interface between the nucleotide binding domains of the neighboring AAA modules (Lee et al., 2003). Within the lower ring (formed by the AAA2 modules), SD2 of each AAA2 module orients itself towards the nucleotide binding domain of the neighboring AAA2 module and appears to form an interface (Results Fig 3.1). This interface formation could be observed in most known structures of the AAA family proteins suggesting functional relevance. To understand this structural information in the context of experiments performed and observations made, a ribbon representation of the AAA2 module dimer was used (Fig 4.1). Though this is a structure of $ClpB_{Tth}$ bound with AMP-PNP molecules, it works, as a good platform, to understand conformational changes occurring in the isolated AAA2 module upon ADP binding. AMP-PNP was shown to support function in Clp/Hsp100 proteins; hence, this structure represents a functionally relevant form (Lee et al., 2003; Shorter and Lindquist 2004; Lee et al., 2007). Since it is not hydrolyzed by $ClpB_{Tth}$, this structure probably represents an early ATP hydrolysis state.

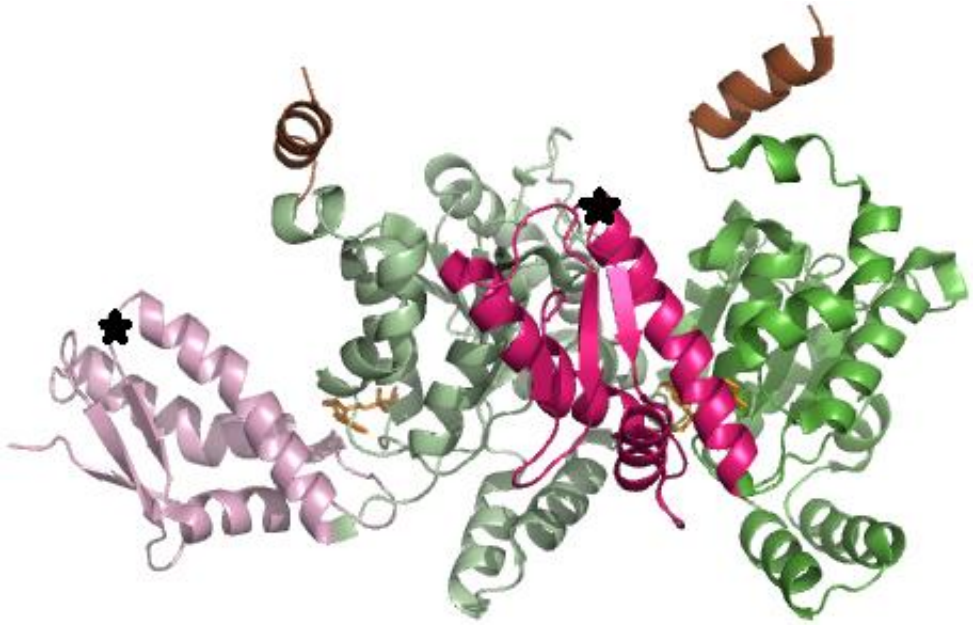

Fig 4.1: Structure of the isolated AAA2 module dimer (ribbon representation). Structural data were obtained from PDB entry 1QVR (Lee et al., 2003) and rendered using Pymol software. In green (dark and pale), are the nucleotide binding domains (NBD2) of the neighboring AAA2 modules, and in pink (dark and pale) are the α-helical small domains (SD2). In brown is a section of SD1 (AA 520-535) which is a part of the isolated AAA2 module construct. SD2 of each AAA2 module forms a tight interface with NBD2 of the neighboring AAA2 module. Nucleotides (stick representation in orange) are bound at the interface between the neighboring nucleotide binding domains. Black asterisks indicate the locations where Alexa Flour dyes were placed.

Addition of ADP reduced the fluorescence signal of the label attached to SD2 of the isolated AAA2 module (Results 3.1.2.2). This could imply a conformational change in SD2 of the AAA2 module upon ADP binding at its nucleotide binding domain as mentioned before. The structure of the dimeric AAA2 module shows the proximity of each SD2 to the nucleotide binding domain of the neighboring AAA2 module (Fig 4.1). Binding of ADP at the nucleotide binding domain of each AAA2 module could result in a conformational change either in its SD2 (intra-subunit) or the SD2 of the neighboring AAA2 module (inter-subunit). It is not only the relative orientation of SD2 that supports an inter-subunit conformational change but also the position of the fluorescence label on SD2 itself. The Alexa 532 label is attached to Cys781 (R781C) of SD2 in the isolated AAA2 module, which is positioned quite close to the nucleotide binding domain of the neighboring AAA2 module. All these observations point towards the possibility for an inter-subunit conformational change in the AAA2 module, upon ADP binding.

Two binding sites with dissimilar affinity in ADP binding and inter-subunit conformational changes are possible, only if the isolated AAA2 module exists as dimer. Oligomeric state analysis of the isolated AAA2 module pointed towards a dimer in the ionic strength at which ADP binding experiments were conducted (Results 3.1.2.5). Dissimilar affinities observed in ADP binding could be due to the difference between the affinity of ADP to dimeric and monomeric AAA2 module. A dimeric AAA2 module also explains the discrepancy between the fluorescence titration and the isothermal titration calorimetry results (Results 3.1.2.3 and 3.1.2.4). A high total amount of protein per ADP used in ITC experiments might have resulted in a large amount of dimeric protein left for the ADP to bind even at the end of the titration. The stoichiometry value of 0.5 indicated that ADP bound to the dimeric form of the isolated AAA2 module and that in the case of ITC experiments only binding to a high affinity site could be occurring.

4.1.2 P-loop mutation affected ADP binding and associated conformational changes.

Experiments were performed using the isolated AAA2 module carrying P-loop mutation (K601Q) to test the possibility of inter-subunit conformational changes occurring in SD2 upon ADP binding. The P-loop mutation results in a change in the nucleotide-dependence for

oligomerization (ADP and ATP both promoted hexamer formation), but does not eliminate nucleotide binding (Schlee et al., 2001). Addition of the isolated AAA2 module carrying a P-loop mutation to ADP bound fluorescently labeled wild type isolated AAA2 module, resulted in increase of fluorescence signal of the label present on SD2 of the isolated AAA2 module (Results 3.1.2.8). This increase may represent a change in the conformation of SD2 (towards the protein core), essentially reversing the effect of ADP. This confirms that the conformational change observed in SD2 upon ADP binding is an inter-subunit conformational change. In other words, in an isolated AAA2 module dimer, ADP binding at one AAA2 module may result in a conformational change in SD2 of the neighboring AAA2 module. The biphasic nature in the binding of ADP to the isolated AAA2 module was further confirmed by using the isolated AAA2 module carrying P-loop mutation (Results 3.1.2.9). ADP titration to the isolated AAA2 module in the presence of increasing amounts of the P-loop mutant AAA2 module resulted in changes, in the high affinity phase of ADP binding. However, no substantial change was observed for the low affinity phase.

Furthermore, experiments done on binding of the isolated P-loop mutant AAA2 module to the wild type isolated AAA2 module revealed that complex formation was spontaneous with a K_D of 2.3 µM (Results 3.1.2.7). This titration resulted in hetero-dimer formation between the wild type and P-loop mutant AAA2 modules and the obtained K_D is indicative of possible dimeric species at conditions where ADP binding experiments were performed.

4.1.3 Importance of the presence and flexibility of SD2 of the AAA2 module.

The isolated AAA2 module forms dimers at low ionic strength (Results 3.1.2.5). It also forms functional higher order oligomers upon reconstitution with the isolated AAA1 module (Results 3.1.1.3). The SD2 deletion variant of the isolated AAA2 module (AAA2ΔSD2) lost its ability to perform refolding of heat denatured substrate proteins upon reconstitution with the AAA1 module (Results 3.1.3.4). Addition of the isolated SD2 was not sufficient for complex formation with the isolated AAA1 module and subsequent chaperone activity. Loss of function can be attributed to loss of nucleotide-mediated oligomerization in AAA2ΔSD2. AAA2ΔSD2 lost its ability to bind ADP or bind and hydrolyze ATP (Results 3.1.3.3). AAA2ΔSD2 remained monomeric both in the presence and absence of ATP. Addition of the isolated SD2 did not alter

the outcome of oligomerization experiments, and complex formation was not observed (Results 3.1.3.2). All these results demonstrated that not only the presence of the SD2 is important for oligomer formation and chaperone activity by $ClpB_{Tth}$, but also its covalent linkage to the rest of the protein.

Substitution of a leucine with proline in the loop connecting NBD2 and SD2 in each AAA2 module, in full-length $ClpB_{Tth}$, resulted in an unstable protein with complete loss of activity (Both ATPase and Chaperone activity) (Results 3.1.4). Presence of proline at position 757 seems to be detrimental for $ClpB_{Tth}$ stability. This mutation was intended to induce conformational rigidity to SD2, thereby influencing nucleotide-mediated inter-subunit conformational changes. Oligomerization in ClpB/Hsp104 proteins is a prerequisite for ATPase activity and chaperone activity. Oligomeric state of $ClpB_{Tth}$ carrying proline mutation could not be assessed due to its unstable nature. Nevertheless, complete lack of nucleotide binding and hydrolysis in the ATPase assay suggested loss of oligomerization. Although affirmative evidence has not been obtained in this case, proline mutation experiments hinted at the importance of the flexibility of SD2.

4.1.4 ADP-mediated inter-subunit conformational changes: Implications for oligomer dissociation in $ClpB_{Tth}$.

The importance of the AAA2 module in nucleotide-dependent oligomerization has been observed in studies where mutations in the P-loop of the second AAA module resulted in oligomerization defects (Kim et al., 1998; Schirmer et al., 1998; Schlee et al., 2001; Barnett et al., 2002; Mogk et al., 2003). More specifically, the role of SD2 has been demonstrated in studies where SD2 deletion resulted in loss of chaperone activity (Barnett et al., 2000; Mogk et al., 2003; Tkach et. al., 2004). In most known AAA family protein structures, sensor-2 arginine (R806 in $ClpB_{Tth}$–SD2) projects from one AAA module in to the nucleotide binding site of the next AAA module and its mutation is known to affect nucleotide binding and hydrolysis and consequently the oligomeric state of the protein (Neuwald et al., 1999; Hattendorf and Lindquist 2002b; Barnett et al., 2002; Mogk et al., 2003). Loss of function due to the deletion of SD2 from the AAA2 module has always been attributed to loss of the above mentioned interactions, but lack of more details always hampered further understanding. Results obtained in this study have contributed to the understanding of the role of SD2 in oligomeric state of $ClpB_{Tth}$.

Oligomeric state analysis reported in this study revealed that at low ionic strength, in the absence of nucleotides, the isolated AAA2 module exists as a dimer (Results 3.1.2.6). Additionally, oligomeric state analysis that has been previously reported showed that in the presence of either ATP or ADP, and at low ionic strength, the isolated AAA2 module exists as a mixture of monomers and dimers (Beinker et al., 2005). Considering both the above observations and the ATP hydrolysis properties of the isolated AAA2 module (6.9 ATP/ min) (Results 3.1.1.4), it can be safely concluded that the monomer-dimer mixture is due to either ATP hydrolysis or ADP binding. In other words, binding of ADP to the AAA2 module might result in dissociation of the dimer. This could happen through an inter-subunit communication-mediated conformational change in SD2 of the AAA2 module. The inter-subunit conformational change occurring in SD2, upon ADP binding, perhaps results, in exposure of the buried interface between the nucleotide binding domains of the neighboring AAA2 modules (Fig 4.1). This might facilitate nucleotide release and/or exchange. That means the type of nucleotide occupying the nucleotide binding domain of the AAA2 module might play a significant role in determining the oligomeric state of $ClpB_{Tth}$.

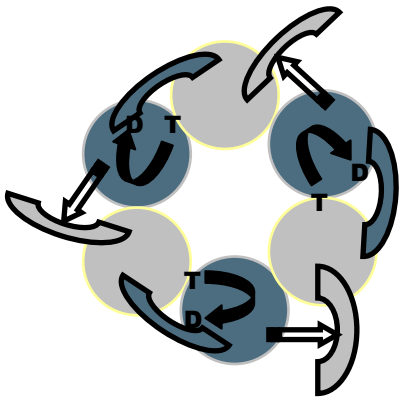

Fig 4.2: Schematic representing ADP-mediated conformational changes. D: ADP; T: ATP. Circles represent the nucleotide binding domains (NBD2) and lids represent the α-helical small domains (SD2) of the lower ring formed by the AAA2 modules. SD2 of the each AAA2 module orients itself towards the NBD2 of the neighboring AAA2 module. Upon ATP hydrolysis in the neighboring NBD2, the preceding SD2 undergoes a conformational change, which moves away from the protein core. Filled (Black) arrows represent ATP hydrolysis and formation of ADP. Unfilled arrows represent the movement of SD2 away from the protein core.

From a functional point of view, ATP hydrolysis forms ADP at the nucleotide binding domain of the AAA2 module. This ADP formation at each AAA2 module could result in a conformational change, in the SD2 of its neighboring AAA2 module (Fig 4.2). This in turn might result in the

dissociation of the $ClpB_{Tth}$ oligomer. However, in the case of full-length $ClpB_{Tth}$ hexamer this might be more complicated due to the presence of more AAA modules (6 AAA1 and 6 AAA2). Since the exact mechanism through which all the 12 AAA modules communicate with each other is not clear, it is very difficult to speculate on how ADP-mediated dissociation occurs. An inter-subunit conformational change can also explain ADP-mediated oligomer dissociation in $ClpB_{Tth}$ as observed in several studies. Dynamic coupling between subunits in $ClpB_{Tth}$ was shown to be occurring at time scales comparable to rates of ATP hydrolysis (Werbeck et al., 2008). Partial threading of substrate proteins through the central channel of ClpB also involves the dynamic nature of ClpB oligomers. Dissociation of ClpB oligomers has been shown to be important for release of partially threaded polypeptide chains (Haslberger et al., 2008). Opening of the lower ring has also been suggested as a possible mechanism for translocation of substrates through the central channel and for release of substrate at the distal end of the ring (Lee et al., 2007).

Rigid body movement of the α-helical small domain during the nucleotide hydrolysis cycle has been reported for other AAA proteins like HslU, ABC transporter proteins (MJ1267 and GlcV), NSF and ClpX (Wang et al., 2001, Karpowich et al., 2001, Verdon et al., 2003, Lenzen et al., 1998, Glynn et al., 2009). Studies on crystal structures of the nucleotide bound ABC transporter proteins (AAA family) revealed a 13° outward movement of the α-helical small domain from ATP bound to ADP bound state upon γ-phosphate release (Karpowich et al., 2001). Significant structural changes were not observed in the lower ring of $ClpB_{Tth}$ hexamer in various nucleotide states in the recently published EM reconstruction (Lee et al., 2007), which is probably due to the low resolution in the lower ring part of the protein.

Inter-subunit interactions, especially between AAA2 modules, have been reported to play an important role in the chaperone activity of $Hsp104_{Yeast}$. AAA2 module carrying P-loop mutation displayed oligomerization defects, which were overcome by high protein concentration. ATP hydrolysis was recovered to nearly 60-80% of the wild type protein, which indicates that allosteric inter-subunit interactions between the AAA2 modules in the lower ring are crucial to ATP hydrolysis and chaperone activity (Schirmer et al., 2001). Even though over expression of $Hsp104_{Yeast}$ was never reported being detrimental to cellular activity, over expression of Hsp104 protein carrying P-loop mutation in the AAA2 module along with the wild type protein inhibited

cell growth (Schirmer et al., 2001). This observation hints at the importance of inter-subunit communication between the AAA2 modules for oligomeric state determination. All the arginine-finger mutants in $Hsp104_{Yeast}$ failed to oligomerize in the absence of nucleotides except the one in the AAA2 module. However, here it was assigned to inter-subunit arginine-finger interactions between the M domain and the AAA2 module of the neighboring subunit (Wendler et al., 2007). Presence of homotypic allostery (between the neighboring AAA2 modules) in the isolated AAA2 module signified by a Hill coefficient of 2.08 also points towards a possible inter-subunit communication during nucleotide hydrolysis (Beinker et al., 2005).

4.1.5 Binding of ATP to the AAA1 module did not elicit a conformational change in the M domain.

M domain mobility during ATP hydrolysis has been studied quite extensively in $ClpB_{Tth}$ and its homologues. Deletion of the M domain or the mutations, that render the M domain immobile, have been shown to remove chaperone activity in ClpB/Hsp104 proteins; however, with no influence on oligomerization (Kedzierska et al., 2003; Lee et al., 2003 Mogk et al., 2003; Schirmer et al., 2004; Lee et al., 2005 Watanabe et al., 2005). All these studies point towards a highly mobile M domain. However, similar observations could not be made here in the case of the isolated AAA1 module, both in the presence and absence of the isolated AAA2 module. Addition of ATP to the isolated AAA1 module did not result in any detectable fluorescence change of the label present on the M domain, indicating a possible lack of change in conformation (Results 3.1.2.1). This can be explained by a lack of ATP binding/ hydrolysis in this construct (Results 3.1.1.4). Even though, oligomer formation is expected, addition of the isolated AAA2 module did not alter the outcome of ATP binding experiment (Results 3.1.2.1). No change of the fluorescence signal upon reconstitution with the AAA2 module, which results in functional protein, is puzzling. One reason could be the lack of covalent linkage between the two AAA modules. Another reason simply could be due to wrong placement of the fluorescence label on the M domain, which might not be sensitive to the conformational changes occurring, if any. Lack of signal changes, upon addition of ATP and the isolated AAA2 module to the isolated AAA1 module, hampered further investigation of the importance of M domain motion in nucleotide-dependent oligomeric state of $ClpB_{Tth}$. However, this outcome reiterates the complexity of the system and the need for more sensitive measurements.

4.2 Complex formation between the isolated AAA modules of $ClpB_{Tth}$: Role of temperature.

This part of the work focuses on complex formation between the isolated AAA modules of $ClpB_{Tth}$. Fluorescence resonance energy transfer measurements for the fluorescently labeled isolated AAA modules hinted at temperature dependence in complex formation and communication between AAA modules in $ClpB_{Tth}$ (Results 3.2.1). This is not surprising, due to thermophilic nature of the protein. Isothermal titration calorimetric measurements provided conclusive evidence about the nature of complex formation between the isolated AAA modules (Results 3.2.2). Pronounced heat release and better binding curve at higher temperatures indicated a similar temperature dependency in complex formation and communication. Increase in temperature did not affect the actual binding affinity. However, the error for data obtained for 25°C was high.

At 25°C and 45°C, the calculated free energy of binding (ΔG) remains negative, indicating the spontaneity of the association reaction. At both the temperatures, the association reaction was enthalpy driven with a high entropic contribution at 45°C. The negative entropy value obtained at 45°C does not necessarily mean that there is no change in hydration of the interface, upon association of the two AAA modules. Data obtained show the temperature dependence of thermodynamic parameters for the complex formation. The obvious dependence of ΔH on temperature indicates a temperature-dependent ΔCp. This probably indicates temperature-dependent conformational changes occurring in AAA modules and a change in their vibrational content during complex formation.

4.3 Allosteric communications between the AAA modules of $ClpB_{Tth}$: Implications for chaperone activity.

Homotypic and heterotypic allosteric communications between the AAA modules play an important role in function of ClpB/Hsp104 proteins (Kim et al 1998; Schlee et al., 2001; Schirmer et al., 2001; Watanabe et al., 2001; Hattendorf and Lindquist 2002; Barnett et al., 2002; Mogk et al., 2003). This study was aimed at understanding the heterotypic allostery between the AAA modules of $ClpB_{Tth}$ by altering the respective interface. Studies were performed by mutating interface residues and analyzing mutants for altered behavior. Experiments were also performed to study allostery-defective condition in $ClpB_{Tth}$.

All the mutant proteins except for mutation where histidine at 369 has been substituted with alanine were structurally stable (Results 3.3.12). Mutation resulting in loss of the hydrogen bond between histidine 369 and tyrosine 661 (H369A) resulted in highly unstable protein. Lack of stable protein hindered further investigation. However, all the other interface mutants were structurally stable and nucleotide-free after purification (Results 3.3.1.2); investigation of these resulted in the following observations:

1. Most of the interface mutants tested showed a decrease in the affinity towards ATP in ATPase assays. But that did not translate into altered oligomerization profile or chaperone activity.
2. Interface mutants I529A and R355A showed increased turnover in the ATPase assay.
3. Interface mutants I529A, E545Q and S357A showed a reduced Hill coefficient in ATPase assays. But, changes in sigmoidal behavior did not result in loss of chaperone activity.
4. Presence of GdmCl also reduced the Hill coefficient in ATPase assay for $ClpB_{Tth}$, but with no affect on chaperone activity.
5. Heterotypic allostery between the AAA modules does not seem to be absolutely essential for chaperone activity in $ClpB_{Tth}$.

Mutant	Predominant oligomeric state			ATPase activity			Chaperone activity	
	ATP	No Nuc	ADP	k_{cat} (min^{-1})	K_m (mM)	n	α-Gluc	LDH
WT	Tetramer	Tetramer	Dimer	2.81	0.36	4.79	100	100
I529A	Trimer	Trimer	Dimer	6.80↑	0.41↑	2.23↓	96	88
V521A	Trimer	Trimer	Dimer	2.95	0.69↑	4.06	114	96
E545Q	Pentamer	Tet/Pent	Dimer	2.47	0.62↑	2.93↓	95	106
E528Q	Pentamer	Tet/Pent	Dimer	2.77	0.63↑	4.80	114	106
E523Q	Trimer	Trimer	Dimer	2.80	0.34	4.80	100	108
R355A	Tetramer	Tetramer	Dimer	5.40↑	0.60↑	4.20	88	98
Y371F	Tetramer	Tetramer	Dimer	2.82	0.68↑	4.25	95	104
S357A	Tetramer	Tetramer	Dimer	2.60	0.75↑	2.58↓	95	100
H369A	NA	NA	NA	NA	NA	NA	NA	NA

Table 4.1: Properties of the interface mutants. Predominant Oligomeric state: Monomer (80-150 kDa), Dimer (150-240 kDa), Trimer (240-330 kDa), Tetramer (330-420 kDa), Pentamer (420-510 kDa). Tet/Pent indicates a mixture of tetramers and pentamers. Oligomeric state analysis was performed in the presence of 0.5 mM ATP or ADP or no nucleotide (No Nuc). ATPase activity: ↑ indicates an increase compared to the wild type protein (WT); whereas, ↓ indicates a decrease compared to the wild type protein. Chaperone activity: The yield in refolding of α-Glucosidase or Lactate dehydrogenase by the wild type $ClpB_{Tth}$ was taken as 100%, to which all the interface mutants were compared.

4.3.1 Decreased affinity due to the interface mutations did not alter oligomeric state or chaperone activity of $ClpB_{Tth}$ significantly.

Mutations at the interface between the AAA1 and AAA2 modules affected ATP hydrolysis properties in $ClpB_{Tth}$. All the mutant proteins were functional in ATPase assay, however, displayed an interesting array of deviations from the wild type protein. Based on the results obtained, it appears that none of the hydrogen bonds forming at the interface seem to be essential for ATP hydrolysis in $ClpB_{Tth}$ (E545Q, E528Q, E523Q, R355A, Y371F, and S357A). The most widely affected aspect in the ATPase assay was the affinity for ATP, as evident by a decrease in the obtained K_m values. Except E523Q, all the interface mutants displayed decreased K_m, by a factor of 2 (Table 4.1 and Results 3.3.1.3). It is not clear whether it was binding of ATP to the AAA1 or AAA2 module that was affected or probably both to a certain extent. This observation reiterated the importance of heterotypic communications between the AAA modules for ATP binding, in $ClpB_{Tth}$.

Change in the affinity towards ATP did not translate into change in kinetics and yield, in refolding assays. The interface mutants V521A, E545Q, E528Q, S357A, and R355A with decreased affinity towards ATP displayed different properties in refolding assays. In α-Glucosidase refolding assay, E528Q and V521A showed higher activity, whereas, the R355A mutant showed lower activity and the E545Q and Y371F mutants are similar to that of the wild type $ClpB_{Tth}$. Although E523Q mutation did not alter ATPase properties of $ClpB_{Tth}$, it resulted in slightly higher refolding yield, in the LDH assay.

None of the interface mutants which showed decreased affinity towards ATP had any significant loss in oligomer formation (Results 3.3.1.4). Interface mutants I529A and V521A showed slightly decreased affinity for ATP in ATP hydrolysis (Table 4.1). These mutants formed oligomers of slightly lower order when compared to the wild type $ClpB_{Tth}$ at both the salt concentrations measured and also in the presence of ADP. On the contrary, E523Q mutation, which followed the wild type in all kinetic parameters, also showed slightly lower order oligomer formation. Decrease in affinity for ATP did not appear to translate into lower order oligomer formation; since, the mutations E545Q and E528Q which also displayed decreased affinity for ATP, formed relatively higher order oligomers, when compared to the wild type (Table 4.1). This probably indicates that although nucleotide binding influences the type of oligomers formed, slight changes in affinity for ATP might not translate to loss of oligomer formation.

It is interesting to note that most of the interface mutants which showed slightly altered oligomerization properties are the ones with mutations in the second part of SD1 (AA 519-535, after the M domain insertion) (I529A, V521A, E523Q and E528Q). None of the mutants (R355A, Y371F and S357A), which are present in the first part of SD1 (AA 332-400, before the M domain insertion), showed any difference in the oligomerisation profile, when compared to the wild type. E545Q with slightly higher order oligomer formation features this mutation in the second AAA module. Further studies on nucleotide binding to the interface mutants are required to obtain dissociation constants (K_D), which is a more accurate measure for affinity than K_m.

4.3.2 Increased turnover due to the interface mutations in $ClpB_{Tth}$ did not affect its chaperone activity.

Mutations at the interface between the AAA modules of $ClpB_{Tth}$ also altered turnover number in ATP hydrolysis. I529A (3 times) and R355A (2.5 times) yielded higher turnover numbers when compared with the wild type $ClpB_{Tth}$ (Results 3.3.1.3 and Table 4.1). Except for these two mutants, all the others showed no significant change in the rate of ATP hydrolysis, when compared to that of wild type $ClpB_{Tth}$ values obtained in this study.

In the case of interface mutants, increased turnover coincided with lowered affinity for ATP in ATP hydrolysis. The reverse does not hold true; interface mutants with decreased affinity towards ATP did not show increased turnover. One possible explanation is that in mutants with higher turnover (I529A and R355A) affinity of ATP binding is altered at the AAA2 module. Since, the AAA2 module is the site with a high rate of hydrolysis any change in affinity to ATP might result in pronounced effect on rate of ATP hydrolysis. For mutants with no change in turnover, affinity at the AAA1 module might be affected. Since, the AAA1 module is the site for lower turnover, subtle changes in affinity might not affect the rate of ATP hydrolysis. Increased turnover in ATP hydrolysis did not affect oligomer formation or yield in refolding of heat denatured substrate proteins by $ClpB_{Tth}$ (Results 3.3.1.4 and 3.3.1.5). Both I529A and R355A were active in refolding heat denatured α-Glucosidase and LDH. In oligomerization studies I529A mutant showed slightly lower order oligomer formation, compared to the wild type, whereas R355A mutants had no deviation from the wild type (Table 4.1).

Increased turnover in $ClpB_{Tth}$ has already been reported in the case of the isolated AAA2 module where it hydrolyzes ATP 3 times faster than wild type $ClpB_{Tth}$ (Beinker et al., 2005). This increased turnover of the isolated AAA2 module (AA 520-854) (6.9 min^{-1}) was closer to that obtained for ClpBΔN (7.9 min^{-1}) (Beinker et al., 2005); which in turn is lower than a previously reported value of 5.5 min^{-1} for ClpBΔN (Beinker et al., 2002). One has to consider that the ATP hydrolysis properties (especially the k_{cat} value) of $ClpB_{Tth}$ reported seems to be slightly different from various studies. So, alterations in protein preparation and/or total active protein cannot be

excluded as the reason for higher turnover observed for interface mutants I529A and R355A in this study.

4.3.3 Decrease in the Hill coefficient in ATP hydrolysis due to the interface mutations did not result in loss of chaperone activity in $ClpB_{Tth}$.

Interface mutants I529A, E545Q and S357A showed a reduction in the Hill coefficient. Although, increased turnover was observed in mutants only from the AAA1 module (I529A and R355A), decrease in the Hill coefficient was not confined to either AAA1 or AAA2 module (I529A and S357A: AAA1 module; E545Q: AAA2 module) (Table 4.1). Both S357A and E545Q were functional in refolding heat denatured substrate proteins, with yields close to that observed for wild type $ClpB_{Tth}$ (Results 3.3.1.3 and 3.3.1.5 and Table 4.1). I529A mutant showed lowest amount of refolding in LDH assay as mentioned before (Table 4.1). Interestingly, in the case of I529A mutation the decreased Hill coefficient was accompanied by increased turnover (Results 3.3.1.3 and Table 4.1). Similar to turnover number, as mentioned above, the Hill coefficient obtained for $ClpB_{Tth}$ seem to vary from various studies. The Hill coefficient obtained in this study is slightly higher than 3.1 reported earlier (Schlee et al., 2001).

The isolated AAA2 module hydrolyzes ATP in a sigmoidal manner, with a Hill coefficient of 2.08 indicating homotypic allostery between the neighboring AAA2 modules. Further studies on the isolated AAA2 module with mutation I529A revealed that this mutation has no effect on the homotypic allostery present between the AAA2 modules. Introduction of I529A mutation in the isolated AAA2 module did not affect its ATP hydrolysis properties (Results 3.3.2.2). It has also not affected the ability of the isolated AAA2 module to form a functional complex, upon reconstitution, with the isolated AAA1 module. The complex of AAA2 module carrying I529A mutation and isolated wild type AAA1 module showed a similar amount of refolding like the complex between the wild type isolated AAA1 and AAA2 modules (Results 3.3.2.3).

4.3.4 Presence of GdmCl resulted in loss of sigmoidal behavior in ATP hydrolysis with no effect on chaperone activity, in $ClpB_{Tth}$.

The possibility of contamination by highly active ATPases or kinases has been excluded as a reason for higher turnover of the I529A mutant. This was achieved by making use of the effect of specific inhibition of $ClpB_{Tth}$ ATPase by GdmCl. The presence of 10 mM GdmCl reduced the rate of ATP turnover, affinity for ATP binding and reduced the Hill coefficient in $ClpB_{Tth}$. At 1 mM ATP concentration, the presence of GdmCl reduced both wild type $ClpB_{Tth}$ and I529A ATPase turnover by 60% (Results 3.3.3.1). Uncompetitive inhibition of the Hsp104-ATP complex has been suggested as the reason for this specific inhibition of $Hsp104_{Yeast}$ ATPase by GdmCl (Grimminger et al., 2005). This explains the decreased K_m value observed for wild type $ClpB_{Tth}$, although not to the same extent like the turnover number. Interestingly, the k_{cat} was recovered at a higher ATP concentration suggesting competitive inhibition. This difference in mode of inhibition by GdmCl might be due to some fundamental difference between the thermophilic $ClpB_{Tth}$ and the mesophillic $Hsp104_{Yeast}$. However, presence of GdmCl did not affect the K_m value for ATP hydrolysis by I529A (Results 3.3.3.1); probably due to the altered interface between the AAA modules, which has already resulted in reduced affinity towards ATP (Results 3.3.1.3 and Table 4.1).

Nevertheless, ATP hydrolysis by $ClpB_{Tth}$ in the presence of GdmCl revealed the effect of GdmCl on allosteric communications between the AAA modules. The Hill coefficient value was reduced to 1.76 from 4.79, probably effecting both homotypic and heterotypic allostery present between the AAA modules of $ClpB_{Tth}$. The influence of GdmCl on homotypic allostery is further supported by its effect on the I529A mutant with altered heterotypic allostery. Presence of GdmCl in ATPase assay buffer further reduced the Hill coefficient from 2.23 to 0.98 perhaps indicating loss of homotypic allostery present between the AAA2 modules.

Effect of GdmCl on allostery in ATP hydrolysis, on the other hand, was not reported in the case of $Hsp104_{Yeast}$ ATPase. Since the structural basis for allosteric communications between the AAA modules in $ClpB_{Tth}$ is not very clear, it is difficult to speculate on the exact mechanism through which GdmCl exerts this effect. In the case of $Hsp104_{Yeast}$, aspartic acid at position 184 (at position 170 in $ClpB_{Tth}$), has been shown to be essential for GdmCl inactivation (Jung et al.,

2002). Further studies involving substitution of aspartic acid at position 170 might prove to be helpful in understanding the effect GdmCl has on $ClpB_{Tth}$.

4.3.5 Are allosteric communications between the AAA modules in $ClpB_{Tth}$, more important for catalytic effectiveness than mere chaperoning?

The effect of GdmCl on allostery provided a platform for studying the allostery-defective situation in wild type $ClpB_{Tth}$ with a minimum or no structural changes to the protein. Presence of GdmCl did not change the yield in refolding of heat denatured α-Glucosidase (Results 3.3.3.2). Considering this and no loss of refolding activity in I529A, S357A, E545Q mutants (with altered heterotypic allostery), it appears that cooperativity in ATP hydrolysis, which signifies allosteric communication between the AAA modules may not be essential for chaperone activity. These allosteric communications may not also play a direct role in interaction of $ClpB_{Tth}$ with $DnaK_{Tth}$ and its co-chaperones.

Heterotypic allosteric communications between the AAA modules are most probably present for controlling the AAA2 module's higher ATP turnover by the AAA1 module. The isolated AAA2 module hydrolyzes ATP at a rate higher than WT $ClpB_{Tth}$. The increased turnover was not present when both the isolated AAA modules were reconstituted (Beinker et al., 2005). This also coincided with an increase in the Hill coefficient from 2.08 reported for the isolated AAA2 module to 3.3 reported for the reconstituted complex. This pointed out at the effect of heterotypic allosteric communications between the AAA modules coming into play upon reconstitution. In the absence of the AAA1 module, the isolated AAA2 module shows ATP hydrolysis properties similar to the I529A mutant. So in case of I529A, the mutation appears to omit, the affect AAA1 module has on AAA2 module, where the protein shows higher turnover and lowered Hill coefficient. Lowering of the ATP hydrolysis in one AAA module by the other through inter-domain communications is probably required for coordination of the pace of various domain movements. This can play a role while the polypeptide chain is being threaded through the central channel, or the M domain is exerting a molecular crowbar like force.

Asymmetric deceleration of ATP hydrolysis was shown in $Hsp104_{Yeast}$ and $ClpB_{Ecoli}$, in the presence of a mixture of ATP and ATPγS (Doyle et al., 2007). The presence of ATPγS reduced

ATPase activity of the AAA2 module in $Hsp104_{Yeast}$ and either module in $ClpB_{Ecoli}$, upon which both proteins elicited refolding activity without DnaK/Hsp70 system. Similar speculations have been made for $Hsp104_{Yeast}$; the cavity side placement of the M domain with atypically arranged AAA modules in $Hsp104_{Yeast}$ puts its helix 3 in contact with the AAA1 module and the N-terminal domain, whereas helices 1 and 2 contact the AAA2 module. Mutating helix 2 arginine 495 resulted in increased ATPase activity (3 fold). This could also be due to loss of allosteric communications between the AAA modules, although in this case mediated through the M domain interactions. Mutation of conserved arginines in $Hsp104_{Yeast}$ resulted in significant loss of disaggregation activity except in the case of R495, which was thought to be playing a role in communication between the AAA modules via the M domain. This mutant retained 30% of the wild type activity, indicating that the heterotypic allosteric communications between the AAA modules play a role in controlling and coordinating ATP hydrolysis, to match polypeptide threading through the central channel or whatever it takes to disaggregate (Wendler et al., 2007).

Although, loss of AAA1 module's control on ATP hydrolysis at AAA2 module might not make the protein dysfunctional, it most probably increases turnover in ATP hydrolysis. A high turnover in ATP hydrolysis did not translate into a higher yield in refolding of heat denatured substrate proteins (Table 4.1). On the contrary, mutants with a higher turnover showed slightly lower refolding yields (I529A in LDH assay and R355A in α-Glucosidase assay). Mutants with a change in the Hill coefficient but not turnover (E545Q and S357A) resulted in the similar refolding yield to wild type $ClpB_{Tth}$ (Table 4.1). It is interesting to note that, although, the R355A mutant displayed unchanged Hill coefficient increased turnover was enough to slightly lower its refolding yield. Both the interface mutants I529A and R355A did not show slightly lower refolding yield in both the assays studied. Developing refolding assays with more sensitivity to subtle changes in ATPase properties of $ClpB_{Tth}$ might be necessary to gain more evidence. However, it appears that altered heterotypic communication between the AAA modules in $ClpB_{Tth}$ might have resulted in increased ATP hydrolysis at the AAA2 module's nucleotide binding domain. Since the absence of allosteric communications is not making $ClpB_{Tth}$ dysfunctional, it could be suggested that this is probably nature's way of introducing catalytic effectiveness in a molecular motor. It will be a terrible waste of energy if the refolding process uses more ATP than a new protein biosynthesis cycle.

4.4 Outlook

The work reported in this thesis deals with the investigation of homotypic and heterotypic allosteric communications in ClpB from Thermus thermophilus. $ClpB_{Tth}$ is an AAA ATPase that converts ATP hydrolysis to mechanical work. The main goal of this work was to study the process with which it occurs, various domains and the conformational changes involved. $ClpB_{Tth}$ is a hexameric protein with two AAA modules per subunit, which makes studying nucleotide-mediated conformational changes a daunting task. However, studies reported in this work on the isolated AAA modules have resulted in gaining insights into homotypic allosteric communications in the lower ring of $ClpB_{Tth}$. Although the results suggested at the importance of the motion of α-helical small domain 2, conclusive evidence could not be obtained. Further biochemical and biophysical studies on the flexibility of this domain and its motion may give information about the importance of the α-helical small domain 2 in the nucleotide-mediated conformational changes. Further studies on understanding movements of various domains during the ATP hydrolysis cycle might provide information regarding the protein's mode of action. Biphasic nucleotide binding to the AAA2 module and inter-domain communication between neighboring subunits provided hints for a possible basis for nucleotide-mediated oligomer dissociation. Obtaining high resolution structural information on hexameric $ClpB_{Tth}$ at various nucleotide states might help to visualize the domain motions and nucleotide-mediated conformational changes. Complex formation between the isolated AAA2 modules could be detected in fluorescence energy transfer and isothermal titration calorimetry measurements. Further work to study nucleotide-mediated conformational changes that occur in $ClpB_{Tth}$ using the isolated AAA modules might prove insightful.

Heterotypic allosteric communications in $ClpB_{Tth}$ were studied by altering the interface between the non-identical AAA modules gave interesting insights. Refolding assays, with higher sensitivity, need to be developed to understand the effects of subtle changes in ATPase properties on the chaperone activity of $ClpB_{Tth}$. Importance of heterotypic allosteric communications can be further investigated using double mutants carrying the interface mutations and Walker A mutations in either AAA module. Also, the effect of GdmCl can be further investigated by studying its role in oligomer formation and dissociation.

6. REFERENCE

Abravaya K, Myers MP, Murphy SP, Morimoto RI. The human heat shock protein hsp70 interacts with HSF, the transcription factor that regulates heat shock gene expression. Genes Dev. 1992 Jul; 6(7):1153-64.

Acebrón SP, Martín I, del Castillo U, Moro F, Muga A. DnaK-mediated association of ClpB to protein aggregates. A bichaperone network at the aggregate surface. FEBS Lett. 2009 Sep 17;583(18):2991-6.

Agashe VR, Guha S, Chang HC, Genevaux P, Hayer-Hartl M, Stemp M, Georgopoulos C, Hartl FU, Barral JM. Function of trigger factor and DnaK in multidomain protein folding: increase in yield at the expense of folding speed. Cell 2004 Apr 16; 117(2):199-209.

Barnett ME, Zolkiewska A, Zolkiewski M. Structure and activity of ClpB from Escherichia coli. Role of the amino-and -carboxyl-terminal domains. J Biol Chem. 2000 Dec 275(48):37565-71.

Barnett ME, Zolkiewski M. Site-directed mutagenesis of conserved charged amino acid residues in ClpB from Escherichia coli. Biochemistry. 2002 Sep 17;41(37):11277-83.

Barnett ME, Nagy M, Kedzierska S, Zolkiewski M. The amino-terminal domain of ClpB supports binding to strongly aggregated proteins. J Biol Chem. 2005 Oct 14;280(41):34940-5. Epub 2005 Aug 2.

Bercovich JA, Grinstein S, Zorzopulos J. Effect of DNA concentration on recombinant plasmid recovery after blunt-end ligation. Biotechniques. 1992 Feb;12(2):190, 192-3.

Beinker P, Schlee S, Groemping Y, Seidel R, Reinstein J. The N terminus of ClpB from Thermus thermophilus is not essential for the chaperone activity. J Biol Chem. 2002 Dec 6; 277(49):47160-6.

Beinker P, Schlee S, Auvula R, Reinstein J. Biochemical coupling of the two nucleotide binding domains of ClpB: covalent linkage is not a prerequisite for chaperone activity. J Biol Chem. 2005 Nov 11;280(45):37965-73.

Beuron F, Maurizi MR, Belnap DM, Kocsis E, Booy FP, Kessel M, Steven AC. At sixes and sevens: characterization of the symmetry mismatch of the ClpAP chaperone-assisted protease. J Struct Biol. 1998 Nov; 123(3):248-59.

Bochtler M, Hartmann C, Song HK, Bourenkov GP, Bartunik HD, Huber R. The structures of HsIU and the ATP-dependent protease HsIU-HsIV. Nature. 2000 Feb 17; 403(6771):800-5.

Bösl B, Grimminger V, Walter S. Substrate binding to the molecular chaperone Hsp104 and its regulation by nucleotides. J Biol Chem. 2005 Nov 18;280(46):38170-6. Epub 2005 Aug 31.

Bradford MM. A rapid and sensitive method for the quantitation of microgram quantities of protein utilizing the principle of protein-dye binding. Anal Biochem. 1976 May 7;72:248-54.

Browlee 1969 Brownlee,G.G. & Sanger,F. Chromatography of 32P-labelled oligonucleotides on thin layers of DEAE-cellulose. *Eur. J. Biochem.* 11, 395-399 (1969).

Buchberger A, Theyssen H, Schröder H, McCarty JS, Virgallita G, Milkereit P, Reinstein J, Bukau B. Nucleotide-induced conformational changes in the ATPase and substrate binding domains of the DnaK chaperone provide evidence for interdomain communication. J Biol Chem. 1995 Jul 14; 270(28):16903-10.

Bukau B, Horwich AL. The Hsp70 and Hsp60 chaperone machines. Cell 1998 Feb 6; 92(3):351-66.

Bullock DW, Webb AJ, Duerden BI, Rotimi VO. Bacteraemia due to a rifampicin-resistant strain of Bacteroides fragilis. J Clin Pathol. 1981 Jan;34(1):87-9.

Bult CJ, White O, Olsen GJ, Zhou L, Fleischmann RD, Sutton GG, Blake JA, FitzGerald LM, Clayton RA, Gocayne JD, Kerlavage AR, Dougherty BA, Tomb JF, Adams MD, Reich CI, Overbeek R, Kirkness EF, Weinstock KG, Merrick JM,Glodek A, Scott JL, Geoghagen NS, Venter JC. Complete genome sequence of the methanogenic archaeon, Methanococcus jannaschii. Science. 1996 Aug 23;273(5278):1058-73

Carter 1993 Carter,M.J. & Milton,I.D. An inexpensive and simple method for DNA purifications on silica particles. *Nucleic Acids Res.* 21, 1044 (1993).

Cashikar AG, Schirmer EC, Hattendorf DA, Glover JR, Ramakrishnan MS, Ware DM, Lindquist SL. Defining a pathway of communication from the C-terminal peptide binding domain to the N-terminal ATPase domain in a AAA protein Mol Cell. 2002 Apr; 9(4):751-60.

Chernoff YO, Lindquist SL, Ono B, Inge-Vechtomov SG, Liebman SW. Role of the chaperone protein Hsp104 in propagation of the yeast prion-like factor [psi+]. Science. 1995 May 12; 268(5212):880-4.

Cohen 1972 Cohen,S.N., Chang,A.C. & Hsu,L. Nonchromosomal antibiotic resistance in bacteria: genetic transformation of Escherichia coli by R-factor DNA. *Proc. Natl. Acad. Sci. U. S. A* 69, 2110-2114 (1972).

Diemand AV, Lupas AN. Modeling AAA+ ring complexes from monomeric structures. J Struct Biol. 2006 Oct; 156(1):230-43.

Dobson CM. Protein misfolding, evolution and disease. Trends Biochem Sci. 1999 Sep; 24(9):329-32.

Dougan DA, Mogk A, Zeth K, Turgay K, Bukau B. AAA+ proteins and substrate recognition, it all depends on their partner in crime. FEBS Lett. 2002 Oct 2; 529(1):6-10.

Doyle SM, Hoskins JR, Wickner S. Collaboration between the ClpB AAA+ remodeling protein and the DnaK chaperone system. Proc Natl Acad Sci U S A. 2007 Jul 3;104(27):11138-44. Epub 2007 Jun 1.

Doyle SM, Shorter J, Zolkiewski M, Hoskins JR, Lindquist S, Wickner S. Asymmetric deceleration of ClpB or Hsp104 ATPase activity unleashes protein-remodeling activity. Nat Struct Mol Biol. 2007 Feb;14(2):114-22. Epub 2007 Jan 28.

Ellis RJ. Macromolecular crowding: obvious but underappreciated. Trends Biochem Sci. 2001 Oct; 26(10):597-604.

Ellis RJ. Protein folding: inside the cage. Nature. 2006 Jul 27;442(7101):360-2.

Fenton WA, Horwich AL. GroEL-mediated protein folding. Protein Sci. 1997 Apr; 6(4):743-60.

Ferbitz L, Maier T, Patzelt H, Bukau B, Deuerling E, Ban N. Trigger factor in complex with the ribosome forms a molecular cradle for nascent proteins. Nature. 2004 Sep 30; 31(7008):590-6.

Fersht AR. Fidelity of DNA replication in vitro. Adv Exp Med Biol. 1984;179:525-33.

Flaherty KM, DeLuca-Flaherty C, McKay DB. Three-dimensional structure of the ATPase fragment of a 70K heat-shock cognate protein. Nature 1990 346: 623-628

Glasel 1995 Glasel,J.A. Validity of nucleic acid purities monitored by 260nm/280nm absorbance ratios. *Biotechniques* 18, 62-63 (1995).

Glover JR, Lindquist S. Hsp104, Hsp70, and Hsp40: a novel chaperone system that rescues previously aggregated proteins. Cell. 1998 Jul 10; 94(1):73-82.

Glynn SE, Martin A, Nager AR, Baker TA, Sauer RT. Structures of asymmetric ClpX hexamers reveal nucleotide-dependent motions in a AAA+ protein-unfolding machine. Cell. 2009 Nov 13;139(4):744-56.

Goldberg ME. Investigating protein conformation, dynamics and folding with monoclonal antibodies.Trends Biochem Sci. 1991 Oct; 16(10):358-62.

Goloubinoff P, Mogk A, Zvi AP, Tomoyasu T, Bukau B. Sequential mechanism of solubilization and refolding of stable protein aggregates by a bichaperone network. Proc Natl Acad Sci U S A. 1999 Nov 3; 96(24):13732-7.

Grimminger V, Richter K, Imhof A, Buchner J, Walter S. The prion curing agent guanidinium chloride specifically inhibits ATP hydrolysis by Hsp104. J Biol Chem. 2004 Feb 27;279(9):7378-83.

Bösl B, Grimminger V, Walter S. Substrate binding to the molecular chaperone Hsp104 and its regulation by nucleotides. J Biol Chem. 2005 Nov 18;280(46):38170-6. Epub 2005 Aug 31.

Hanson PI, Whiteheart SW. AAA+ proteins: have engine, will work. Nat Rev Mol Cell Biol. 2005 Jul;6(7):519-29.

Harrison CJ, Hayer-Hartl M, Di Liberto M, Hartl F, Kuriyan J. Crystal structure of the nucleotide exchange factor GrpE bound to the ATPase domain of the molecular chaperone DnaK. Science. 1997 Apr 18;276(5311):431-5.

Hartl FU, Hayer-Hartl M. Molecular chaperones in the cytosol: from nascent chain to folded protein. Science. 2002 Mar 8; 295(5561):1852-8.

Haslberger T, Weibezahn J, Zahn R, Lee S, Tsai FT, Bukau B, Mogk A. M domains couple the ClpB threading motor with the DnaK chaperone activity. Mol Cell. 2007 Jan 26;25(2):247-60.

Haslberger T, Zdanowicz A, Brand I, Kirstein J, Turgay K, Mogk A, Bukau B. Protein disaggregation by the AAA+ chaperone ClpB involves partial threading of looped polypeptide segments. Nat Struct Mol Biol. 2008 Jun;15(6):641-50. Epub 2008 May 18.

Hattendorf DA, Lindquist SL. Cooperative kinetics of both Hsp104 ATPase domains and interdomain communication revealed by AAA sensor-1 mutants. EMBO J. 2002 Jan 15;21(1-2):12-21.

Hattendorf DA, Lindquist SL. Analysis of the AAA sensor-2 motif in the C-terminal ATPase domain of Hsp104 with a site-specific fluorescent probe of nucleotide binding. Proc Natl Acad Sci U S A. 2002 Mar 5;99(5):2732-7. Epub 2002 Feb 26.

Herrmann JM, Neupert W. Protein transport into mitochondria. Curr.Opin.Microbiol. 2000 3:210-214

Ho SN, Hunt HD, Horton RM, Pullen JK, Pease LR. Site-directed mutagenesis by overlap extension using the polymerase chain reaction. Gene. 1989 Apr 15;77(1):51-9.

Hoskins JR, Doyle SM, Wickner S. Coupling ATP utilization to protein remodeling by ClpB, a hexameric AAA+ protein. Proc Natl Acad Sci U S A. 2009 Dec 29;106(52):22233-8. Epub 2009 Nov 25.

Ibba M, Söll D. Quality control mechanisms during translation.Science. 1999 Dec 3;286(5446):1893-7.

Ishikawa T, Beuron F, Kessel M, Wickner S, Maurizi MR, Steven AC. Translocation pathway of protein substrates in ClpAP protease.Proc Natl Acad Sci U S A. 2001 Apr 10;98(8):4328-33.

Jung G, Jones G, Masison DC. Amino acid residue 184 of yeast Hsp104 chaperone is critical for prion-curing by guanidine, prion propagation, and thermotolerance. Proc Natl Acad Sci U S A. 2002 Jul 23;99(15):9936-41. Epub 2002 Jul 8.

Kedzierska S, Akoev V, Barnett ME, Zolkiewski M. Structure and function of the middle domain of ClpB from Escherichia coli. Biochemistry. 2003 Dec 9;42(48):14242-8.

Kim KI, Woo KM, Seong IS, Lee ZW, Baek SH, Chung CH. Mutational analysis of the two ATP-binding sites in ClpB, a heat shock protein with protein-activated ATPase activity in Escherichia coli. Biochem J. 1998 Aug 1;333 (Pt 3):671-6.

Kim KI, Cheong GW, Park SC, Ha JS, Woo KM, Choi SJ, Chung CH. Heptameric ring structure of the heat-shock protein ClpB, a protein-activated ATPase in Escherichia coli. J Mol Biol. 2000 Nov 10; 303(5):655-66.

King RW, Deshaies RJ, Peters JM, Kirschner MW. How proteolysis drives the cell cycle.Science. 1996 Dec 6; 274(5293):1652-9.

Krzewska J, Langer T, Liberek K. Mitochondrial Hsp78, a member of the Clp/Hsp100 family in Saccharomyces cerevisiae, cooperates with Hsp70 in protein refolding.FEBS Lett. 2001 Jan 26; 489(1):92-6.

Laemmli UK. Cleavage of structural proteins during the assembly of the head of bacteriophage T4. Nature. 1970 Aug 15; 227(5259):680-5.

Lee S, Sowa ME, Watanabe YH, Sigler PB, Chiu W, Yoshida M, Tsai FT. The structure of ClpB: a molecular chaperone that rescues proteins from an aggregated state. Cell. 2003 Oct 17; 115(2):229-40.

Lee S, Hisayoshi M, Yoshida M, Tsai FT. Crystallization and preliminary X-ray crystallographic analysis of the Hsp100 chaperone ClpB from Thermus thermophilus. Acta Crystallogr D Biol Crystallogr. 2003 Dec;59(Pt 12):2334-6.

Lee S, Sowa ME, Choi JM, Tsai FT. The ClpB/Hsp104 molecular chaperone-a protein disaggregating machine.J Struct Biol. 2004 Apr-May; 146(1-2):99-105.

Lee S, Choi JM, Tsai FT. Visualizing the ATPase cycle in a protein disaggregating machine: structural basis for substrate binding by ClpB. Mol Cell. 2007 Jan 26;25(2):261-71.

Lenzen CU, Steinmann D, Whiteheart SW, Weis WI. Crystal structure of the hexamerization domain of N-ethylmaleimide-sensitive fusion protein. Cell. 1998 Aug 21;94(4):525-36.

Li D, Zhao R, Lilyestrom W, Gai D, Zhang R, DeCaprio JA, Fanning E, Jochimiak A, Szakonyi G, Chen XS. Structure of the replicative helicase of the oncoprotein SV40 large tumour antigen. Nature. 2003 May 29;423(6939):512-8.

Lum R, Tkach JM, Vierling E, Glover JR. Evidence for an unfolding/threading mechanism for protein disaggregation by Saccharomyces cerevisiae Hsp104. J Biol Chem. 2004 Jul 9;279(28):29139-46. Epub 2004 May 5.

Mackay RG, Helsen CW, Tkach JM, Glover JR. The C-terminal extension of Saccharomyces cerevisiae Hsp104 plays a role in oligomer assembly. Biochemistry. 2008 Feb 19;47(7):1918-27. Epub 2008 Jan 16.

Mayer MP, Rüdiger S, Bukau B. Molecular basis for interactions of the DnaK chaperone with substrates. Biol Chem. 2000 Sep-Oct; 381(9-10):877-85.

Mayer MP, Schröder H, Rüdiger S, Paal K, Laufen T, Bukau B. Multistep mechanism of substrate binding determines chaperone activity of Hsp70.Nat Struct Biol. 2000 Jul; 7(7):586-93.

McCarty JS, Buchberger A, Reinstein J, Bukau B. The role of ATP in the functional cycle of the DnaK chaperone system.J Mol Biol. 1995 May 26; 249(1):126-37.

Mayhew M, da Silva AC, Martin J, Erdjument-Bromage H, Tempst P, Hartl FU. Protein folding in the central cavity of the GroEL-GroES chaperonin complex.Nature. 1996 Feb 1; 379(6564):420-6.

Mayhew M, Hartl FU.Lord of the rings: GroES structure. Science. 1996 Jan 12; 271(5246):161-2.

Menz RI, Walker JE, Leslie AG. Structure of bovine mitochondrial F(1)-ATPase with nucleotide bound to all three catalytic sites: implications for the mechanism of rotary catalysis. Cell. 2001 Aug 10;106(3):331-41.

Michelsen 1995 Michelsen,B.K. Transformation of Escherichia coli increases 260-fold upon inactivation of T4 DNA ligase. *Anal. Biochem.* 225, 172-174 (1995).

Minton AP. Implications of macromolecular crowding for protein assembly. Curr Opin Struct Biol. 2000 Feb;10(1):34-9.

Minton AP. Protein folding: Thickening the broth. Curr Biol. 2000 Feb 10; 10(3):R97-9.

Mogk A, Tomoyasu T, Goloubinoff P, Rüdiger S, Röder D, Langen H, Bukau B. Identification of thermolabile Escherichia coli proteins: prevention and reversion of aggregation by DnaK and ClpB.EMBO J. 1999 Dec 15; 18(24):6934-49.

Mogk A, Deuerling E, Vorderwülbecke S, Vierling E, Bukau B. Small heat shock proteins, ClpB and the DnaK system form a functional triade in reversing protein aggregation.Mol Microbiol. 2003 Oct;50(2):585-95.

Mogk A, Schlieker C, Friedrich KL, Schönfeld HJ, Vierling E, Bukau B. Refolding of substrates bound to small Hsps relies on a disaggregation reaction mediated most efficiently by ClpB/DnaK.J Biol Chem. 2003 Aug 15;278(33):31033-42.

Mogk A, Schlieker C, Strub C, Rist W, Weibezahn J, Bukau B. Roles of individual domains and conserved motifs of the AAA+ chaperone ClpB in oligomerization, ATP hydrolysis, and chaperone activity.J Biol Chem. 2003 May 16;278(20):17615-24.

Mosser DD, Ho S, Glover JR. Saccharomyces cerevisiae Hsp104 enhances the chaperone capacity of human cells and inhibits heat stress-induced proapoptotic signaling.Biochemistry. 2004 Jun 29; 43(25):8107-15.

Motohashi K, Watanabe Y, Yohda M, Yoshida M. Heat-inactivated proteins are rescued by the DnaK.J-GrpE set and ClpB chaperones.Proc Natl Acad Sci U S A. 1999 Jun 22; 96(13):7184-9.

Neuwald AF, Aravind L, Spouge JL, Koonin EV. AAA+: A class of chaperone-like ATPases associated with the assembly, operation, and disassembly of protein complexes. Genome Res. 1999 Jan; 9(1):27-43.

Nicola AV, Chen W, Helenius A. Co-translational folding of an alphavirus capsid protein in the cytosol of living cells. Nat Cell Biol. 1999 Oct; 1(6):341-5.

Netzer WJ, Hartl FU. Recombination of protein domains facilitated by co-translational folding in eukaryotes. Nature. 1997 Jul 24;388(6640):343-9.

Ogura T, Wilkinson AJ. AAA+ superfamily ATPases: common structure--diverse function. Genes Cells. 2001 Jul;6(7):575-97.

Ogura T, Whiteheart SW, Wilkinson AJ. Conserved arginine residues implicated in ATP hydrolysis, nucleotide-sensing, and inter-subunit interactions in AAA and AAA+ ATPases. J Struct Biol. 2004 Apr-May;146(1-2):106-12.

Ortega J, Singh SK, Ishikawa T, Maurizi MR, Steven AC. Visualization of substrate binding and translocation by the ATP-dependent protease, ClpXP. Mol Cell. 2000 Dec; 6(6):1515-21.

Parsell DA, Kowal AS, Singer MA, Lindquist S. Protein disaggregation mediated by heat-shock protein Hsp104.Nature. 1994 Dec 1; 372(6505):475-8.

Parsell DA, Kowal AS, Lindquist S. Saccharomyces cerevisiae Hsp104 protein. Purification and characterization of ATP-induced structural changes. J. Biol. Chem. 1994 Feb 11; 269(6):4480-7.

Pellecchia M, Montgomery DL, Stevens SY, Vander Kooi CW, Feng HP, Gierasch LM, Zuiderweg ER. Structural insights into substrate binding by the molecular chaperone DnaK. Nat Struct Biol. 2000 Apr; 7(4):298-303.

Perrin V, Régulier E, Abbas-Terki T, Hassig R, Brouillet E, Aebischer P, Luthi-Carter R, Déglon N. Neuroprotection by Hsp104 and Hsp27 in lentiviral-based rat models of Huntington's disease. Mol Ther. 2007 May;15(5):903-11. Epub 2007 Mar 20.

Pfanner N. Who chaperones nascent chains in bacteria? Curr Biol. 1999 Oct 7; 9(19):R720-4.

Queitsch C, Hong SW, Vierling E, Lindquist S.Heat shock protein 101 plays a crucial role in thermotolerance in Arabidopsis. Plant Cell. 2000 Apr; 12(4):479-92.

Sanchez Y, Taulien J, Borkovich KA, Lindquist S. Hsp104 is required for tolerance to many forms of stress. EMBO J. 1992 Jun; 11(6):2357-64.

Schatz G, Dobberstein B Common principles of protein translocation across membranes. Science. 1996 Mar 15; 271(5255):1519-26

Schirmer EC, Glover JR, Singer MA, Lindquist S. HSP100/Clp proteins: a common mechanism explains diverse functions. Trends Biochem Sci. 1996 Aug; 21(8):289-96.

Schirmer EC, Queitsch C, Kowal AS, Parsell DA, Lindquist S. The ATPase activity of Hsp104, effects of environmental conditions and mutations. J Biol Chem. 1998 Jun 19;273(25):15546-52.

Schirmer EC, Ware DM, Queitsch C, Kowal AS, Lindquist SL. Subunit interactions influence the biochemical and biological properties of Hsp104. Proc Natl Acad Sci U S A. 2001 Jan 30;98(3):914-9.

Schirmer EC, Homann OR, Kowal AS, Lindquist S. Dominant gain-of-function mutations in Hsp104p reveal crucial roles for the middle region. Mol Biol Cell. 2004 May;15(5):2061-72. Epub 2004 Feb 20.

Schlee S, Groemping Y, Herde P, Seidel R, Reinstein J. The chaperone function of ClpB from Thermus thermophilus depends on allosteric interactions of its two ATP-binding sites. J Mol Biol. 2001 Mar 2; 306(4):889-99.

Schlee S, Reinstein J. The DnaK/ClpB chaperone system from Thermus thermophilus. Cell Mol Life Sci. 2002 Oct; 59(10):1598-606.

Schlee S, Beinker P, Akhrymuk A, Reinstein J. A chaperone network for the resolubilization of protein aggregates: direct interaction of ClpB and DnaK. J Mol Biol. 2004 Feb 6; 336(1):275-85.

Schlieker C, Weibezahn J, Patzelt H, Tessarz P, Strub C, Zeth K, Erbse A, Schneider-Mergener J, Chin JW, Schultz PG, Bukau B, Mogk A. Substrate recognition by the AAA+ chaperone ClpB. Nat Struct Mol Biol. 2004 Jul;11(7):607-15. Epub 2004 Jun 20.

Schlieker C, Tews I, Bukau B, Mogk A. Solubilization of aggregated proteins by ClpB/DnaK relies on the continuous extraction of unfolded polypeptides. FEBS Lett. 2004 Dec 17;578(3):351-6.

Schmid SL, Braell WA, Rothman JE. ATP catalyzes the sequestration of clathrin during enzymatic uncoating. J Biol Chem. 1985 Aug 25; 260(18):10057-62.

Schmid SL, Rothman JE. Two classes of binding sites for uncoating protein in clathrin triskelions. J Biol Chem. 1985 Aug 25; 260(18):10050-6.

Schmid SL, Rothman JE. Enzymatic dissociation of clathrin cages in a two-stage process. J Biol Chem. 1985 Aug 25; 260(18):10044-9.

Schmid SL. Biochemical requirements for the formation of clathrin- and COP-coated transport vesicles. Curr Opin Cell Biol. 1993 Aug; 5(4):621-7.

Schmid D, Baici A, Gehring H, Christen P. Kinetics of molecular chaperone action. Science. 1994 Feb 18;263(5149):971-3.

Schmitt M, Neupert W, Langer T. The molecular chaperone Hsp78 confers compartment-specific thermotolerance to mitochondria. J Cell Biol. 1996 Sep; 134(6):1375-86.

Schwikowski B, Uetz P, Fields S. A network of protein-protein interactions in yeast. Nat Biotechnol. 2000 Dec; 18(12):1257-61.

Shorter J, Lindquist S.Hsp104 catalyzes formation and elimination of self-replicating Sup35 prion conformers. Science. 2004 Jun 18;304(5678):1793-7. Epub 2004 May 20.

Singleton MR, Sawaya MR, Ellenberger T, Wigley DB. Crystal structure of T7 gene 4 ring helicase indicates a mechanism for sequential hydrolysis of nucleotides. Cell. 2000 Jun 9;101(6):589-600.

Sousa MC, Trame CB, Tsuruta H, Wilbanks SM, Reddy VS, McKay DB. Crystal and solution structures of an HslUV protease-chaperone complex. Cell. 2000 Nov 10; 103(4):633-43.

Studier FW, Moffatt BA.Use of bacteriophage T7 RNA polymerase to direct selective high-level expression of cloned genes. J Mol Biol. 1986 May 5; 189(1):113-30.

Tessarz P, Mogk A, Bukau B. Substrate threading through the central pore of the Hsp104 chaperone as a common mechanism for protein disaggregation and prion propagation. Mol Microbiol. 2008 Apr;68(1):87-97. Epub 2008 Feb 28.

Tipton KA, Verges KJ, Weissman JS. In vivo monitoring of the prion replication cycle reveals a critical role for Sis1 in delivering substrates to Hsp104. Tipton 2008 Mol Cell. 2008 Nov 21;32(4):584-91.

Tkach JM, Glover JR. Amino acid substitutions in the C-terminal AAA+ module of Hsp104 prevent substrate recognition by disrupting oligomerization and cause high temperature inactivation. J Biol Chem. 2004 Aug 20;279(34):35692-701. Epub 2004 Jun 3.

Todd MJ, Viitanen PV, Lorimer GH. Dynamics of the chaperonin ATPase cycle: implications for facilitated protein folding. Science. 1994 Jul 29;265(5172):659-66.

Tucker PA, Sallai L.The AAA+ superfamily--a myriad of motions. Curr Opin Struct Biol. 2007 Dec;17(6):641-52. Epub 2007 Nov 26.

Vacher C, Garcia-Oroz L, Rubinsztein DC. Overexpression of yeast hsp104 reduces polyglutamine aggregation and prolongs survival of a transgenic mouse model of Huntington's disease. Hum Mol Genet. 2005 Nov 15;14(22):3425-33. Epub 2005 Oct 4.

Verdon G, Albers SV, van Oosterwijk N, Dijkstra BW, Driessen AJ, Thunnissen AM. Formation of the productive ATP-Mg2+-bound dimer of GlcV, an ABC-ATPase from Sulfolobus solfataricus. J Mol Biol. 2003 Nov 21;334(2):255-67.

Walker JE, Saraste M, Runswick MJ, Gay NJ. Distantly related sequences in the alpha- and beta-subunits of ATP synthase, myosin, kinases and other ATP-requiring enzymes and a common nucleotide binding fold. EMBO J. 1982;1(8):945-51.

Wang J, Song JJ, Seong IS, Franklin MC, Kamtekar S, Eom SH, Chung CH. Nucleotide-dependent conformational changes in a protease-associated ATPase HsIU. Structure. 2001 Nov; 9(11):1107-16.

Wang Q, Song C, Yang X, Li CC. D1 ring is stable and nucleotide-independent, whereas D2 ring undergoes major conformational changes during the ATPase cycle of p97-VCP. J Biol Chem. 2003 Aug 29;278(35):32784-93. Epub 2003 Jun 13.

Wang Q, Song C, Li CC. Molecular perspectives on p97-VCP: progress in understanding its structure and diverse biological functions. J Struct Biol. 2004 Apr-May;146(1-2):44-57.

Watanabe YH, Motohashi K, Yoshida M. Roles of the two ATP binding sites of ClpB from Thermus thermophilus. J Biol Chem. 2002 Feb 22;277(8):5804-9. Epub 2001 Dec 10.

Watanabe YH, Takano M, Yoshida M. ATP binding to nucleotide binding domain (NBD)1 of the ClpB chaperone induces motion of the long coiled-coil, stabilizes the hexamer, and activates NBD2. J Biol Chem. 2005 Jul 1;280(26):24562-7. Epub 2005 Apr 4.

Watanabe YH, Nakazaki Y, Suno R, Yoshida M. Stability of the two wings of the coiled-coil domain of ClpB chaperone is critical for its disaggregation activity. Biochem J. 2009 Jun 12;421(1):71-7.

Weber-Ban EU, Reid BG, Miranker AD, Horwich AL.Global unfolding of a substrate protein by the Hsp100 chaperone ClpA. Nature. 1999 Sep 2; 401(6748):90-3.

Weibezahn J, Tessarz P, Schlieker C, Zahn R, Maglica Z, Lee S, Zentgraf H, Weber-Ban EU, Dougan DA, Tsai FT, Mogk A, Bukau B. Thermotolerance requires refolding of aggregated proteins by substrate translocation through the central pore of ClpB. Cell. 2004 Nov 24;119(5):653-65.

Weibezahn J, Bukau B, Mogk A.Unscrambling an egg: protein disaggregation by AAA+ proteins. Microb Cell Fact. 2004 Jan 16;3(1):1.

Werbeck ND, Schlee S, Reinstein J. Coupling and dynamics of subunits in the hexameric AAA+ chaperone ClpB. J Mol Biol. 2008 Apr 18;378(1):178-90. Epub 2008 Feb 21.

Whiteheart SW, Kubalek EW. SNAPs and NSF: general members of the fusion apparatus. Trends Cell Biol. 1995 Feb;5(2):64-8.

Xu Z, Yang S, Zhu D. GroE assists refolding of recombinant human pro-urokinase. J Biochem. 1997 Feb; 121(2):331-7.

Xu Z, Horwich AL, Sigler PB. The crystal structure of the asymmetric GroEL-GroES-(ADP)7 chaperonin complex. Nature. 1997 Aug 21; 388(6644):741-50.

Ye Y, Meyer HH, Rapoport TA. Function of the p97-Ufd1-Npl4 complex in retrotranslocation from the ER to the cytosol: dual recognition of nonubiquitinated polypeptide segments and polyubiquitin chains. J Cell Biol. 2003 Jul 7;162(1):71-84.

Ye Y, Shibata Y, Yun C, Ron D, Rapoport TA. A membrane protein complex mediates retro-translocation from the ER lumen into the cytosol. Nature. 2004 Jun 24;429(6994):841-7.

Yura T, Nagai H, Mori H. Regulation of the heat-shock response in bacteria. Annu Rev Microbiol. 1993; 47:321-50.

Zahn R, Perrett S, Stenberg G, Fersht AR. Catalysis of amide proton exchange by the molecular chaperones GroEL and SecB. Science. 1996 Feb 2; 271(5249):642-5.

Zolkiewski M, Kessel M, Ginsburg A, Maurizi MR. Nucleotide-dependent oligomerisation of ClpB from Escherichia coli. Protein Sci. 1999 Sep;8(9):1899-903.

Zolkiewski M. ClpB cooperates with DnaK, DnaJ, and GrpE in suppressing protein aggregation. A novel multi-chaperone system from Escherichia coli. J Biol Chem. 1999 Oct 1; 274(40):28083-6.

7. APPENDIX

A. Biphasic binding model

// Two binding sites addition of ADP to AAA2-R781C*$^{Alexa\ 532}$

IndVars: ADPo

DepVars: E, EADP1, EADP2, ADP, F

Params: Kd1, Kd2, Eo, Fo, Ampl1, Ampl2

EADP1=(E*ADP)/Kd1

EADP2=(EADP1*ADP)/Kd2

Eo=E+EADP1+EADP2

ADPo=ADP+EADP1+2*EADP2

F=Fo-Ampl1*((EADP1+EADP2)/Eo)-Ampl2*(EADP2/Eo)

// parameter values

Kd1=1

Kd2=100

Eo=0.5

Fo=5*10E+6

Ampl1=2*10E+6

Ampl2=1*10E+6

//Borders

0<E<Eo

0<EADP1<Eo

0<EADP2<Eo

0<ADP<ADPo

// Initial conditions

***

For experiments where ADP binding to AAA2-R781C*$^{Alexa\ 532}$ was studied, total enzyme concentration of 0.5 µM was used; whereas, for ADP binding to 1:1 and 1:2 stoichiometric complexes of AAA2-R781C*$^{Alexa\ 532}$ and AAA2-K601Q a total enzyme concentration of 1 and 1.5 µM was used respectively.

B. Estimation of molar mass using Laser light scattering measurements

Instrument Setup: Gel permeation chromatography coupled light scattering measurements in addition to refractive index measurements can provide accurate and continuous assessment of molar mass for proteins which is independent of calibration.

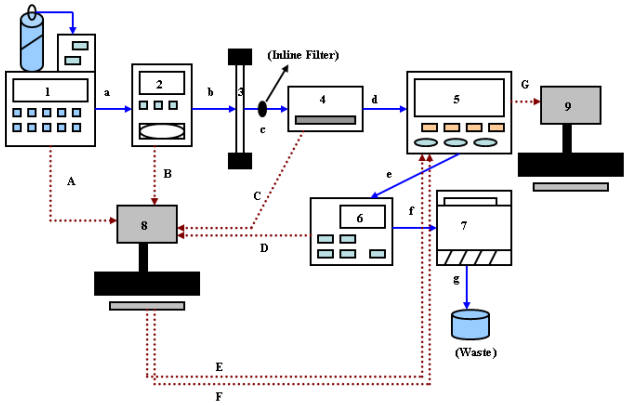

Schematic illustrating flow, network and auxiliary connections

1. Instruments: ***1****- WATERS 626 HPLC pump with WATERS 600s Controller, Buffer reservoir and Degasser;* ***2****- WATERS 717 plus Auto sampler;* ***3****- GPC column;* ***4****- WATERS 2996 Photodiode Array Detector;* ***5****- WYATT DAWN HELEOS light scattering Detector;* ***6****- WATERS 2414 RI Detector;* ***7****- WATERS Fraction Collector-III;* ***8****- Computer with EMPOWER Software;* ***9****- Computer with ASTRA Software;*

2. Dark blue lines with arrows indicate flow of the buffer through the system.

3. Doted red lines indicate Network Connections to EMPOWER Software and auxiliary channel/ analog output connections to WYATT HELEOS instrument.

Calibration: A calibration in case of DAWN HELEOS was performed by injecting pre-filtered toluene in to the flow cell as per manufacturer's protocol. Toluene has a known R_θ of 1.4059 X 10^{-5} cm^{-1} at 658 nm which is the strongest Raleigh scatterer (highest Raleigh ratio) which was measured and the instrument calibration as calculated using the following equation. This calibration constant is specific to the instrument and type of the flow cell (K5 for DAWN HELEOS).

$R_\theta\, 90^\circ = CC\, [\, (V_{90^\circ} - V_{90^\circ dark})/ (V_{laser} - V_{laser\ dark})]$

$R_\theta\, 90^\circ$- scattering at 90˚; *CC*- calibration constant; V_{90°- 90˚ detector signal voltage;

$V_{90^\circ dark}$- 90˚ detector dark offset; V_{laser}- laser monitor signal; $V_{laser\ dark}$- laser dark offset;

Appendix

The geometry of the flow cell results in a disparity in the scattering volume seen by each detector. After calibrating 90˚ angle detector, normalization coefficients for each detector were estimated in relation to the 90˚ angle detector using an isotropic scatterer.

$R_\theta 90^\circ = N^* CC\ [\ (V_{90^\circ} - V_{90^\circ dark})/\ (V_{laser} - V_{laser\ dark})]$

Where *N* is the normalization coefficient for each detector

8. ABBREVIATIONS

A	Absorption
AA	Amino acid
AAA	ATPases Associated with a variety of cellular Activities
ADP	Adenosine-5´-diphosphate
AMP PNP	Adenosine 5′-(β,γ-imido)triphosphate
ATP	Adenosine-5´-triphosphate
ATPγS	Adenosine 5'-(gamma-thiotriphosphate)
BSA	Bovine Serum Albumin
C	Celsius
Clp	Caseinolytic Protease
E. coli	Escherichia coli
EDTA	Ethylenediaminetetraaceticacid
GdmCl	Guanidinium hydrochloride
HEPES	4-(2-hydroxyethyl)-1-piperazineethanesulfonic acid
HPLC	High Performance Liquid Chromatography
Hsp	Heat Shock Protein
IPTG	Isopropyl β-D-1-thiogalactopyranoside
LDH	Lactate dehydrogenase
Mant- ADP	N-Methylanthraniloyl- Adenosine-5´-diphosphate
NADH	Nicotinamide adenine dinucleotide
NSF	N-ethylmaleimide sensitive fusion protein
PAGE	Poly Acrylamide Gel Electrophoresis
PCR	Polymerase chain reaction
PEP	Phosphoenolpyruvate
PK	Pyruvate kinase
SDS	Sodium Dodecyl Sulfate
T. thermophilus	Thermus thermophilus
TCA	TrichloroAcetic acid
TEMED	N, N, N´, N´-Tetramethylethylenediamine
Tris	Tris(hydroxymethyl)aminomethane

9. ACKNOWLEDGEMENT

I want to sincerely thank Prof. Dr. Ilme Schlichting for giving me an opportunity to work as a PhD student in her department and supporting me time and again. I also want to thank my supervisor PD. Dr. Jochen Reinstein for offering me an exciting project, help me broaden my scientific horizons and also for his continuous support in the hour of need. My utmost gratitude for both of them.

I want to thank Nico, Tatiana and Raphael for critical reading of this manuscript, and also for being such great friends. I also want to thank the other members of the chaperone group (Vinod, Thorsten, Simone and Thomas) for their generous help and friendship during my PhD work. I want to thank Sabine for her tremendous help in the lab.

I want to thank all the teachers who taught me everything I know now, through the course of my education, which helped me shape myself.

I want to thank my family and friends for their kind and continuous support, and for reminding me that there is always light at the end of the tunnel.